NASA
Technical
Paper
1849

June 1987

Three-Step Cylindrical Seal for High-Performance Turbomachines

Robert C. Hendricks

Contents

Summary

A three-step cylindrical seal configuration representing the seal for a high-performance turbopump (e.g., the space shuttle main engine fuel pump) was tested under *static* (*nonrotating*) conditions.[1] The test data included critical mass flux and pressure profiles over a wide range of inlet temperatures and pressures for fluid nitrogen and fluid hydrogen with the seal in concentric and fully eccentric positions. The critical mass flux (leakage rate) was 70 percent that of an equivalent straight cylindrical seal with a correspondingly higher pressure drop based on the same flow areas of 0.3569 cm^2 (0.05531 $in.^2$) but 85 percent that of the straight seal based on the third-step flow area of 0.3044 cm^2 (0.04718 $in.^2$). Thus 15 percent of the flow reduction was due to area change, and 15 percent was due to losses at the internal-step inlets. The mass flow rates for the three-step cylindrical seal in the fully eccentric and concentric positions were essentially the same, and the normalized flow coefficient tended to follow those for the axisymmetric Borda or orifice inlets.

The pressure profiles, however, exhibited a flat region throughout the third step of the seal for inlet stagnation temperatures less than the thermodynamic critical temperature, with the pressure magnitude dependent on the inlet stagnation temperature. Such profiles represent an extreme positive direct stiffness. The postulated choking in the maximum-clearance region engendered a crossover in the upstream pressure profile that provided a higher pressure at the maximum clearance rather than at the minimum clearance and thus resulted in a local negative stiffness. Flat and crossover pressure profiles resulting from choking within the seal are practically unknown to the seal designer. However, they are of critical importance to the stability of the turbomachine and must be assessed and integrated into any dynamic analysis of a seal of this configuration. Only direct stiffness can be assessed from the data presented herein; cross-coupling effects, damping, or added mass effects cannot be inferred. These data do illustrate how sensitive turbomachine dynamics can be to seal geometry and inlet conditions especially near an inlet, where separation and two-phase flows can occur.

Further, in seal (and bearing or damper) designs, it has been assumed that choking cannot occur within the seal if the backpressure is above the thermodynamic critical pressure. This is shown to be an invalid assumption. Choking is highly dependent on geometry, inlet-to-backpressure ratio, and inlet temperature and can occur within the seal even though the backpressure is above the thermodynamic critical pressure.

[1]Data and information contained herein were released for general use in May 1977.

Introduction

In the early phases of the space shuttle main engine program, excessive leakage and vibrations engendered catastrophic turbomachine failures that in many cases destroyed the entire apparatus. From the accident investigations it was postulated that the excessive vibrations were caused by the seals. However, the seal geometry and fluid conditions leading to such unstable operations were unknown.

In reference 1 the deficiency of information for designing seals over an extreme range of thermodynamic states is cited. The *straight cylindrical seal* of reference 1 had a continuous concentric cylindrical annulus between the solid centerbody and the housing. The shaft centerbody was 8.4244 cm (3.3167 in.) in diameter and the housing was 8.4513 cm (3.3273 in.) in diameter, providing a passage about 0.01345 cm (0.00530 in.) high and 4.13 cm (1⅝ in.) long. The flow area was 0.3569 cm^2 (0.05531 $in.^2$). The problems related to leakage and dynamics are compounded when the geometry is unconventional, such as a three-step seal. The three-step seal considered herein is essentially a concentric cylindrical annulus similar to the straight seal of reference 1 but with three distinct cylindrical pads separated by small stepped reservoirs.

Leakage rates, the response of pressure profiles to eccentric positions, applications to other fluids, and the effect of backpressure control need to be established for the three-step seal, as was done for the straight seal (ref. 1). Thus the first purpose of this sequence of tests was to determine the mass flux for a shaft seal with three stepped sealing pads in the concentric and eccentric positions. The largest pad (at the inlet) was 7.9234 cm (3.1194 in.) in diameter, the central pad was 7.8346 cm (3.0845 in.) in diameter, and the exit pad was 7.6947 cm (3.0294 in.) in diameter. The pads were nearly equal in length.

As rotor dynamics is very important to the integrity of a turbomachine system, it is important to know how the seal responds to changes in rotor position. Usually small changes

in the geometric configuration significantly alter the pressure profiles yet cause little change in the mass flux (leakage). Therefore the second purpose of this series of tests was to establish pressure profiles for the three-step seal in its concentric and fully eccentric positions.

The third purpose was to further establish the credibility of the corresponding-states approach, which could supply, if established, leakage rate data for both hydrogen and liquid oxygen. These results could then be extended to seal designs for any fluid that obeys the corresponding-states principles.

One philosophy of seal design (bearings and dampers as well) is that when the backpressure is above the thermodynamic critical pressure, two-phase flow within the seal is not possible. So in some designs the backpressure is held close to, but above, the thermodynamic critical point. This, however, is generally an incorrect assumption for stagnation entropies less than the thermodynamic critical entropy in simple geometries such as a venturi, and the thesis must be demonstrated for complex geometries such as a seal. Thus the fourth purpose of this report was to determine the influence of backpressure on choking within the three-step seal configuration when the pressure at the seal exit is controlled to pressures above the thermodynamic critical pressure of fluid hydrogen.

The eccentrically positioned centerbody results are separated into two cases, fully eccentric at 0° and fully eccentric at 180°, to facilitate comprehension and to attempt to contrive a logical presentation of the data and procedures. Results are also presented for the three-step seal in the concentric position and for backpressure control. Complementary data and results for a three-step labyrinth seal of a similar geometric configuration are given in reference 2.

Symbols

A area, cm^2 ($in.^2$)

C constant

C_f flow coefficient, $G_R/G_{R,v}$

C_1 flow reduction constant

D diameter, cm (in.)

G mass flux, g/cm^2 s ($lbm/in.^2$ s)

G_R reduced mass flux, $G/G^*(1 + \psi_Q)$

G^* flow-normalizing parameter (6010 g/cm^2 s (85.5 $lbm/in.^2$ s) for nitrogen), $\sqrt{P_c \rho_c / Z_c}$

L length, cm (in.)

P pressure, MPa (psi)

R radial position, cm (in.)

T temperature, K (°R)

$\dot{w}$ mass flow rate, g/s (lbm/s)

ω angular velocity, rad/s

ψ_Q quantum correction factor

Subscripts:

B backpressure

c thermodynamic critical value

in inlet

o stagnation

R reduced parameter based on inlet stagnation condition

S straight seal

TS three-step seal

v venturi

Apparatus and Instrumentation

Difficulties in the development of the flow system ar associated instrumentation are discussed in references 1 and and are not repeated herein.

A profile of the three-step seal is shown as figure 1. Th installed system is described in more detail in references and 3. The actual seal-housing configuration is shown figure 2. A schematic of the test installation is given figure 3; and a cross-sectional view of the backpressure contr system is illustrated in figure 4.

The seal centerbody was instrumented (fig. 1) with 1 pressure taps in both the 0° and 180° positions and taps 3.871 cm (1.524 in.) from the inlet in the 90° and 27(positions. Unfortunately the 270° tap was plugged prior the installation in our system, and no data are available f the 270° position. Note also that the line of the pressure t locations was a maximum of 17° off the true eccentric (position (ref. 1). This deviation should have had little effe on the pressure profiles but must be considered wh interpreting the pressure profile data.

In general, the flow passage was about 0.0127 c (0.0050 in.) high and had 0.038- to 0.051-cm (0.015- 0.020-in.) slot spacing to provide a small reservoir at ea step, between the shaft and housing shoulders (fig. 1). T pressure tap locations were established to give sor comparison with the straight cylindrical seal (ref. 1) and in and exit information about each stepped pad. In addition the apparatus as described in reference 1 two platinu thermometers were placed in the inlet mixing region approximately the 45° and 225° positions with a minimu immersion depth of 2.5 cm (1 in.), as shown in figure 4. F the fully eccentric tests the centerbody was moved to the position with the gap at the 180° position becoming 0.025 c (0.010 in.), as was done for the straight seal of reference

To control the backpressure (the pressure at the seal exi the system geometry had to be modified without altering t seal configuration. The flow system was modified in two way A backpressure control valve was added at the exit plane the conical exit flange, and high-pressure gas injection w used for the unique pressure control required for th

configuration (figs. 3 and 4). The three-step seal was then reinstalled into the flow system. Operations with nitrogen and hydrogen indicated (1) that independent gas supply systems were required to handle the flow system and the backpressure control (fig. 4) and (2) that the plug diameter of the valve in the conical exit flange had to be increased from 2.54 to 2.86 cm (1 to 1.125 in.), with the seat diameter at 3.3 cm (1.3 in.). With these system modifications the backpressure was controlled by using gaseous hydrogen injection when the working fluid was cryogenic hydrogen; otherwise gaseous nitrogen was used.

Operation

One significant departure from the operations outlined in reference 1 occurred in the initial phases of operation: one hydrogen run and one nitrogen run were monitored by using a parallel system consisting of the central automatic digital data encoder (CADDE), the Escort minicomputer, and a television monitor. Although this system was difficult to control and the limitations of the supply dewar hampered data acquistion, the television display with 1.5-sec update greatly aided data acquistion. Such a system also points out the need for efficient, fast, and low-core-storage thermophysical properties routines.

Results and Discussion

Results are presented for the three-step cylindrical seal in the concentric position, simulating normal operations, and in the fully eccentric position, simulating rotor dynamics to the point of rub; for flow similarities; and for the effects of backpressure on flow and pressure profiles. Comparisons are made with the straight cylindrical seal data (ref. 1) and extended instrumentation and operations methods are discussed as required. (See table I.) The data for the three-step cylindrical seal are given in tables II to V.

Concentric Position—Simulating Normal Operations

Flow rate.—The mass flux (leakage) data for gaseous hydrogen flowing through the three-step seal (fig. 5), taken on two different dates, were in good agreement. The reduced inlet stagnation temperature ($T_{R,o} = T_o/T_c$) varied between 8.2 and 8.8.

The mass flux (leakage) data for liquid hydrogen, also for two different dates (fig. 5), generally agreed with those for the straight seal (ref. 1) when related as

$$G_{R,TS} \approx C_1 G_{R,S} \tag{1}$$

where $C_1 \sim 0.7$ when the data were compared on the flow area equal to that of the *straight* seal, A=0.3569 cm^2 (0.05531 in.^{2}) (ref. 1). When the data were compared on the smallest flow area of the *three-step* seal ($A_{\text{step 1}}$=0.3166 cm^2 (0.04907 in.^{2}), $A_{\text{step 2}} = 0.3131$ cm^2 (0.04853 in.^{2}), $A_{\text{step 3}} = 0.3044$ cm^2 (0.04718 in.^{2})), C_1 equaled 0.85. Thus the reduction in mass flux due to flow area changes of the offset-stepped passages was at most 15 percent, with the remaining 15 percent reduction due to the inlet geometry losses of the internal steps.

With gaseous and fluid nitrogen flowing through the three-step seal the mass flux data over a range of reduced inlet stagnation temperatures (fig. 6) were again about 30 percent less than those for the straight seal (ref. 1). The values assigned to C_1 (eq. (1)), were similar to those assigned for fluid hydrogen (i.e., 0.70 or 0.85 depending on the area used). The gaseous nitrogen data were taken on three different dates. One set was taken immediately prior to a hydrogen run, and consequently no fluid nitrogen data were acquired on that date.

Pressure profiles—Immediately apparent in the pressure profiles for gaseous hydrogen (fig. 7) is the lack of symmetry between the 0° and 180° positions, as noted also for the straight seal (ref. 1). Although care was taken to center the seal within the housing, the lack of symmetry of the pressure profiles shows that the seal centerbody was not precisely centered. This may suggest that simple geometries be designed and fabricated in order to maintain proper tolerances and adequate dynamics, but the problem here is to determine the validity of these profiles. One of the major problems with these profiles occurred 4.496 cm (1.77 in.) from the inlet plane (adjacent to the exit), where the pressure transducers were the most unreliable. The discrepancy between the signal and the recorded data has not been resolved. These concentric profiles look more like the eccentric straight seal profiles of reference 1.

Similar features were noted for the fluid hydrogen profiles in figure 8. However, the sharp dip in the 180° profile at the inlet to the third step is absent in the 0° profile. Although the instrumentation could be the cause, the amplitude diminished with pressure and, as shown later, with temperature. Similar behavior with nitrogen virtually ruled out the thermal expansion effects caused by ambient heat input, and the independence of fluid or run date essentially ruled out partially plugged pressure taps. Further, these results appeared to vindicate the suspect pressure transducers. However, the shaft and housing geometry was not ruled out and of course, being common to all tests, will as indicated earlier substantially influence the results.

The pressure profiles for gaseous nitrogen (figs. 9 and 10) are quite similar to those for hydrogen (fig. 7). The pressure profiles for fluid nitrogen (fig. 11) are quite similar to those for fluid hydrogen except that the drop in pressure at the inlet to the third step is even more pronounced. At a reduced inlet stagnation temperature $T_{R,o} = 0.67$ (fig. 12) the amplitude of the coincident dip (location of sudden pressure change) appeared to be related to the stagnation pressure level. At $T_{R,o} = 0.78$ the pattern of the coincident dip changed somewhat, but at $T_{R,o} = 0.9$ the dip virtually disappeared. At $T_{R,o}$ of 1.01 and 1.04 the coincident dip changed to a

coincident bump quite similar to that noted in the gaseous profiles. These coincident bumps and dips appear to be density related, and perhaps the two-phase model discussed in appendix C of reference 1 can be applied. However, the circumferential distribution of flow, which was not considered in the model, appears to be of significant importance in these results.

The bumps and dips in the hydrogen pressure profiles (fig. 13) show a similar dependence on reduced temperature. Thus the evidence tends to rule out thermal contraction of the seal surfaces and again points to seal geometry and fluid modeling.

Summary for concentric position.—Reduced critical mass flux (leakage) and pressure profiles for nitrogen and hydrogen flowing through the concentric annulus of a three-step cylindrical seal have been assessed. In general

$$G_{R,TS} \approx C_1 G_{R,S} \tag{1}$$

where $C_1 \sim 0.7$ when the flow area was equal to that of the straight seal (ref. 1) (0.3569 cm^2; 0.05531 $in.^2$) and $C_1 = 0.85$ when the smallest flow area (0.3044 cm^2; 0.04718 $in.^2$) of the three-step seal was used.

Although the centerbody was thought to be concentrically placed in the housing, the pressure profiles at 0° and 180° indicated some misalignment. Note that small position changes resulted in large differences in the pressure distribution but had virtually no affect on the mass flux (leakage). A coincident dip in pressure at the inlet of the third step was found to be temperature dependent. The dip changed to a bump as inlet stagnation temperature was increased above $T_{R,o} = 1$. The dip was most predominant for $T_{R,o} < 1$.

Fully Eccentric Position—Simulating Rotor Dynamics to Point of Rub

The discussion of the three-step cylindrical seal in the fully eccentric position centers primarily around the unusual third-step pressure profile noted at 180° and the attempts to demonstrate its validity. For that reason the flow rates are discussed first. The data for this configuration are presented in table III.

Flow rate.—As was true for the concentric and fully eccentric positions of the straight seal (ref. 1), the mass fluxes for the three-step seal were virtually the same in both positions at corresponding values of $T_{R,o}$ and $P_{R,o}$. The $T_{R,o} = 1.12$ reduced mass flux isotherm for fluid nitrogen (fig. 14) was taken in part by using the television monitor to rapidly establish the proper temperature, pressure, and mass flux relations.

The mass flux data for fluid hydrogen in the three-step seal (fig. 15) extended to a reduced pressure of approximately 4.8. The results are 6 percent lower than those for both the three-step and straight cylindrical seals in figure 16 and appear to be more closely aligned with the classic-venturi-times-0.35 locus. These results only further point out the need to return to the classic venturi and acquire critical flow data at elevated pressures (up to $P_{R,o} = 10$ in the current facility). The isotherm $T_{R,o} = 1.2$ was acquired with the aid of the television monitor; producing the $T_{R,o} = 1.0$ isotherm required more precise control. The $T_{R,o} = 0.8$ isotherm is limited because of adiabatic fluid compression in the inlet reservoir.

Pressure profiles.—The pressure profiles for gaseous nitrogen (fig. 17) show increased asymmetry over that noted for the concentric configuration. The magnitude of the separation appeared similar to that encountered with the straight cylindrical seal (ref. 1) in the fully eccentric position. The exception was the bump near the inlet to the third step. The bump represents a profile crossover region and thus a region of negative stiffness, which is undesirable. As will shown this crossover of the pressure profile persisted and appeared similar to the exit region of the straight cylindrical seal (ref. 1).

The coincident dip noted in the previous section for the three-step seal in the concentric position was more pronounced for fluid nitrogen flowing through the three-step seal in the eccentric position (fig. 18). The amplitude of this coincident dip was sensitive to inlet stagnation temperature (fig. 19) as was true for the concentric position. For both positions the coincident dip at $T_{R,o} < 1$ changed to a bump at $T_{R,o} \sim 1.12$. Profile crossover prior to the third step can also be noted.

The pressure profiles for fluid hydrogen (fig. 20), discussed later, also show a coincident dip as well as profile crossover in the second step. The representative gaseous hydrogen pressure profile in figure 20 is of course quite similar to the gaseous nitrogen profile in figure 17.

The inlet pressures for the three-step cylindrical seal were considerably higher than those for the straight cylindrical seal (ref. 1) for two reasons:

(1) The flow decreased by a factor of 1.4. This decrease implies that the inlet pressure must be doubled to achieve equivalent flow rates.

(2) Adiabatic compression of the fluid in the dewar to 10.54 MPa (1515 psia) increased the $T_{R,o}$ to 0.92. This increase implies a reduction in flow rate of about 20 percent.

I requested, and was granted, permission from the NASA Lewis Research Center Saftey Committee, to operate at the elevated pressures, which were still within the pressure limits of the facility. The reasons for limiting the inlet pressure to 10.54 MPa (1515 psia) were as follows:

(1) The makeup gas supply for the facility was simply too small to keep up with the high flow rates.

(2) The pressure drops were large at the high flow rates.

(3) Flows through the hydraulic control valve and inlet mixing chamber (fig. 4) at these high flow rates were nearly critical (choked). (See ref. 1 for a facility description.) For this facility further increases in pressure could only be useful at lower flow rates; that is, they could be accomplished in part by increasing the inlet temperatures.

Further, to illustrate the dependence of the coincident dip in pressure profile on inlet stagnation temperature as well as

the dependence of the inlet stagnation temperature on adiabatic compression, the dewar was brought to equilibrium at ambient conditions of about 0.121 MPa (17.5 psia) prior to pressurization. The dewar was then pressurized to the operating pressure and data were taken; four such representative profiles are given in figure 20. Values of $T_{R,o}$ and the corresponding pressures are shown in table IV. See table III of reference 1 for other critical parameters.

To illustrate the nature of the pressure profiles for $T_{R,o} \sim 1.2$, which represents the temperature level of the third stage of the hydrogen pump in the space shuttle main engine, three representative runs were plotted in figure 21. In these profiles the coincident dip has disappeared: if anything, a small bump appears in its place. There is some question as to the validity of the 180° pressure values at the 4.364-cm (1.718-in.) position, and this must be investigated further.

Instrumentation modification.—To determine whether the measured coincident dip in the pressure profile was dependent on the instrumentation or the recording system or was a function of geometry and fluid phase, several instrumentation lines were rearranged. The four pressure lines used to define the pressure profile at the first step were interchanged with the four lines used to define the profile at the third step for both the 0° and 180° sets of pressure taps.

The results of these modifications further defined the pressure profiles as shown for typical fluid nitrogen pressure profiles (fig. 22). These profiles do not differ substantially from those in figures 18 and 19. However, figure 22 offers greater detail as to how inlet temperature and pressure affect the coincident dip and the profile for the third step of the seal in particular. These effects are summarized as figure 23, where the pressure profiles along the 180° plane for the third step have been replotted. At high pressure the effect of inlet temperature is clearly delineated, but note that the inlet pressure was not the same for all profiles. At low pressure the different inlet pressures and the proximity to the thermodynamic critical point make the results difficult to interpret. Clearly a temperature effect similar to that at high pressure does exist. For $T_{R,o} < 0.9$ the 180° profile is independent of pressure level. This effect tends to reinforce the two-phase flow model given in appendix C of reference 1 and implies that the measurements are dependent on the system and the fluid phase. The mass flow rates associated with the pressure profiles of figure 22 are given in figure 24. For more detail of mass flow as a function of pressure see reference 1.

The pressure profiles of figures 17 to 22 represent an extreme stiffness[2] *with an inclusive region of negative stiffness and have a pronounced influence on rotor dynamics.* This phenomenon is inexplicable: it can be related to flow separation and is exacerbated by two-phase flows. It is therefore dependent on geometric and thermophysical properties and must be properly accounted for in any dynamic seal analysis, where the fluid can be two-phase or flow separation can occur.

Flow similarities and extrapolation of results.—Through the use of similarity parameters a data base or theory can be extrapolated. Extrapolation of the results became desirable because the SSME-turbopump operating pressures were as high as 34.5 MPa (5000 psia) and the test facility was limited to 12 MPa (1750 psia).

Similarities: Subsequent work on inlet effects for Borda and 90°-sharp-edge inlets (refs. 4 to 7) revealed several features of the flow similar to those described herein:

(1) Very strong separation can and does occur for sharp-edge inlets or wherever streamlines suffer a discontinuity.

(2) Strong separation can lead to fluid jetting to a length of over 105 tube diameters, and recompression can occur within the tube.

(3) Separation effects are strongly dependent on inlet stagnation temperature and are significantly reduced at $T_{R,o} > 1$.

(4) Flow rates are independent of the flow separation details, but pressure profiles are strongly affected.

(5) Differences between Borda and 90°-sharp-edge inlets are small, perhaps 5 to 10 percent at most.

(6) For strongly separated flows control appears to be at the inlet, not at the exit.

Using these results at elevated pressures characteristic of the space shuttle main engine required extrapolation.

Extrapolation of mass flux data: The projected inlet stagnation pressure-temperature characteristics for a three-stage turbopump are $T_{R,o} \sim 1.2$ and $P_{R,o} \sim 16$ at the first pump stage; $T_{R,o} \sim 1$ and $P_{R,o} \sim 9$ at the second pump stage; and $T_{R,o} \sim 0.85$ and $P_{R,o} \sim 1.1$ at the third pump stage. These will most likely lead to the following results:

(1) In all cases the flow rates will be less than the maximum noted for $T_{R,o} \sim 0.7$ for nitrogen and hydrogen (figs. 5 and 6) when extrapolated to the proper pressure (fig. 16).

(2) Thermophysical properties will change rapidly.

(3) The pressure profiles will be dependent on temperature and hence on stage.

(4) Rotation, absent in these simulations, will be an important variable. (One velocity boundary condition is ωR, and therefore rotation must be of importance.)

(5) Inlet and exit conditions (geometry, pressure, and temperature), coupled with items 1 to 4, will be crucial to dynamic stability.

As noted in reference 1 the facility is limited to a hydrogen dumping rate of about 300 g/s (2/3 lbm/s), and this eliminates operation at elevated reduced pressures. Extrapolation is necessary to obtain some idea of the flow rates through the pump seals at elevated pressure. Taking the data at $T_{R,o} = 0.8$ from the straight seal (ref. 1) and those herein, an extrapolation

[2]In rotating systems the stiffness matrix has terms involving direct and cross-coupled stiffness. Direct stiffness results from a force and a displacement along the same coordinate, and cross-coupled stiffness results from a force and a displacement at 90° to each other. Because the facility used in these tests was static (not rotating), only one component, the direct stiffness, could be assessed. Seal dynamics are discussed in reference 1.

can be made based on results from two-phase choked flow in a classic venturi. (See fig. 16 and ref. 1.) Hydrogen flow rate data[3] based on the flow area of the straight seal (0.3569 cm^2; 0.05531 $in.^2$) were plotted as a function of reduced pressure for the straight and three-step seals. Lines drawn through these points are nearly parallel in each case, and the slopes are in reasonable agreement with that for the classic venturi.

Note (fig. 16) that the classic venturi flow rate times 0.47 (eq.(18) of ref. 1) nearly represented the straight seal data (ref. 1) and that the classic venturi flow rate times 0.35 nearly represented the three-step seal data when these data were based on an area of 0.3569 cm^2 (0.05531 $in.^2$). These extrapolations indicate that for a seal with a reduced inlet stagnation pressure of $P_{R,o} = 20$ (25.85 MPa; 3750 psia) and exit pressure near atmospheric conditions the flow rates for hydrogen at $T_{R,o} = 0.8$ (26.4 K) would be 1250 and 905 g/s (2.76 and 1.99 lbm/s) for the straight seal and the three-step seal, respectively. It is immediately obvious that higher pressure data are needed. These data could have been acquired with a venturi at equivalent flow rates in another facility but were not.

When the ratio of the smallest area of the three-step seal to the straight seal area ($A_{TS}/A_S = 0.3044/0.3569 = 0.85$) is considered and 15 percent of the leakage is attributed to inlet losses at the two extra seal steps and to surfaces in the three-step seal, the flow rates for the straight seal and the three-step seal merge. However, the pressure profiles for the two seals remain significantly different for $T_{R,o} < 1$. Flow rate affects leakage, and pressure profile affects dynamic stability.

Summary for fully eccentric position.—Reduced critical mass flux (leakage) and pressure profiles for nitrogen and hydrogen flowing through a three-step cylindrical seal in the fully eccentric position, with a clearance of 0.0254 cm (0.0100 in.) at the 180° position, have been assessed:

(1) The mass fluxes did not differ substantially from those recorded for the three-step cylindrical seal set in its concentric position. A similar relation was found for the straight seal in the concentric and eccentric positions (ref. 1).

(2) The pressure profiles for both fluid nitrogen and fluid hydrogen exhibited a coincident dip at the inlet to the third step. The amplitude of the dip depended on the inlet temperature and to a lesser extent on the inlet pressure. In general, the dip occurred for $T_{R,o} < 1$; for $T_{R,o} > 1$ it tended to disappear or become a bump. The gaseous hydrogen and nitrogen profiles were quite similar with a slight bump at the inlet of the third step; the bump persisted for the fluid data within the second step. For $T_{R,o} < 1$ the bump represents a region where the pressure profiles cross over and thus a region of negative stiffness. Such *profile* crossovers were noted near the exit of the straight cylindrical seal and were related to changes in the choking phenomenon. It is assumed that the choking phenomenon varies circumferentially and thus engenders the crossover.

Instrumentation modifications, measurements, and time of recording had little effect on these results. Consequently the results are dependent on the geometry and the fluid phase, represent an extreme stiffness, and must be properly introduced into any dynamic analysis.

(3) The similarities between the mass flux and pressure profile results of these tests and subsequent inlet flow studies for Borda and 90°-sharp-edge inlets were pronounced. It was assumed that flows through the inlet to the third step can be separated, with subsequent fluid jetting.

(4) The differences in the 0° and 180° pressure profiles was a measure of the direct stiffness coefficient of the seal or the ability of the turbomachine to recover from a perturbed state. As a flat portion of a pressure profile represents a region near the saturation pressure, the differences in the 0° and 180° pressure profiles had reached a maximum. Thus this condition represents an extreme value of the seal's direct stiffness coefficient. This is further verified in the next section.

(5) Extrapolation of mass flux based on limited data appeared to give reasonable values for both the straight and three-step cylindrical seals when compared with the classic venturi. It is apparent that high-pressure hydrogen (or helium) data taken with the classic venturi are needed to benchmark (increase the valid range of) the theoretical calculations.

More data near $T_{R,o}$ of 0.85, 1.0, and 1.2 should be acquired at high pressures since such conditions more nearly coincide with projected turbopump operating conditions. Also required is information on the effects of rotation especially when thermophysical properties are not constant, as will be the case for these listed values of $T_{R,o}$.

Backpressure Control

As most seals operate against a nominal backpressure, it was necessary to determine mass flux and pressure profiles for the three-step seal with controlled backpressure over a range of inlet stagnation temperatures and pressures. In view of the anomalous profiles at the third step of the seal, the results were divided into fully eccentric at the 180° position and fully eccentric at the 0° position, followed by those of the concentric position. Since reduced critical mass flow rates (leakage) are not significantly altered by increasing the backpressure, the emphasis is on the pressure profiles. Data for backpressure control are presented in table V.

Case 1—fully eccentric seal with 0.0254-cm (0.0100-in.) clearance at 180°.—Typical gaseous nitrogen pressure profiles (fig. 25) indicate some departures from symmetry and a profile crossover (bump) near the entry to the third step. The bump is significantly affected by fluid conditions (figs. 26 and 27) and is assumed to follow the circumferential distribution of the choke. By holding the inlet stagnation

[3]Estimated from data at $T_{R,o}$ from 0.7 to 0.9; only a few actual points were available at $T_{R,o} = 0.8$.

pressure nearly constant and increasing the backpressure, the significant flat region of the third step was eliminated. Although the elimination should have been anticipated, the flat pressure profile appeared to be unique[4] for two reasons:

(1) The cross-sectional area of each seal step *decreased* in the direction of flow.

(2) The passage area downstream of the choke was constant.

Although a multiplicity of shock front positions could be found, interest centered on the backpressure required to eliminate the choke at the exit of the second step and the inlet to the third step of the three-step seal. For fluid nitrogen the choke was eliminated at a reduced backpressure above $P_B/P_c \sim 1/3$ at reduced inlet pressures $P_{in}/P_c \sim 1.15$.

Hydrogen profiles were quite similar to those for nitrogen except that eliminating the choke at the inlet of the third step now required $P_B/P_c \sim 1$ at $P_{in}/P_c \sim 4.2$ (fig. 28). Higher values of P_{in}/P_c had a pronounced influence on the choke and are explored later in this section.

The position of the shock was strongly dependent on backpressure (figs. 29 and 30). Only the second- and third-step profiles are presented in these figures because the first-step profile was monotonic and reflected profiles of previous sections where the backpressure was not controlled. The movement of the shock, which could be easily followed on the television monitor of the real-time display system, was readily controlled by the backpressure system.[5]

The shock moved into the passage as backpressure was increased (fig. 29). Once the critical pressure ratio was attained, the shock was swallowed up and gaslike behavior became evident. However, a substantial pressure difference between the 0° and 180° positions still existed. Note that only the 180° profile was plotted since the 0° data resembled those of figure 28 and interest centered on delineating the flat-profile behavior. The lower limit of the pressure drop is probably the triple point (refs. 4 to 7). In an application, however, the lower limit is closer to the saturation pressure based on inlet stagnation conditions. Flat pressure profiles are related to extreme values of the seal's direct stiffness and are of great interest to the seal designer,[6] as are profile crossovers since they represent regions of negative stiffness.

As the shuttle main engine pump inlet pressure, which is the seal backpressure, is proposed to be approximately 1.4 MPa (200 psig), a series of runs were taken at that backpressure (fig. 30). At first it was concluded that backpressure greater than the thermodynamic critical pressure of the fluid was sufficient to preclude the extreme pressure differences noted at lower backpressures when the seal was choked at the inlet of the third step; however, this conclusion is shown in the next section to be invalid. The inlet pressures were simply too low to sustain the shock, which was swallowed, resulting in the profiles of figure 30. (Only the 180° position profiles are shown in fig. 30. A more complete profile set is given in fig. 31. That also illustrates a region of negative stiffness in the second step.)

Case 2—fully eccentric seal with 0.0254-cm (0.0100-in.) clearance at 0°.—The unusual nature of the profiles described for case 1 and the apparently unique characteristics of the flat profiles left me in a state of disbelief. I attempted to discredit or reaffirm the results by moving the centerbody from touching the 0° position to touching the 180° position. In general the results of case 2 confirmed the findings of case 1. Again the mass flow rates, although given, were not significantly different from those for case 1 (except in extreme cases such as unchoking) and I concentrated on the pressure profiles.

With backpressure greater than the thermodynamic critical pressure the extreme pressure differences for the third step (fig. 32) again *appeared* to have been eliminated. The 0° profiles (fig. 33) were similar to the 180° profiles (fig. 29). This suggested that the profiles of figures 25 to 31 were indeed valid and that pressure profiles, while virtually unknown to the designer, represented a new phenomenon to be contended with. Further, the circumferential distribution of the choke engenders an upstream profile crossover that represents a region of negative stiffness included between two regions of positive stiffness.

The hydrogen[7] profiles of figures 33 and 34 gave the first evidence that the flat profile for the third step could exist when the backpressure was above the thermodynamic critical pressure. Again the position of the shock was quite sensitive to P_{in}/P_B at a fixed value of $T_{R,o}$. Subsequent testing then focused on the following two questions:

(1) Can the flat profile for the third step exist for $P_B/P_c > 1$, and if so, what is the relation to P_{in}?

(2) Does a shock hysteresis exist such that applying

[4]See also results for tubes with Borda and 90°-sharp-edge inlets in the section *Flow similarities and extrapolation of results.*

[5]See also refs. 4 to 7 on Borda and 90°-sharp-edge inlet geometries.

[6]As an illustration, if the inlet stagnation pressure at the third step is 6.9 MPa (1000 psi), the average restoring force on the shaft surface nearly touching the housing (fully eccentric case) becomes $(P_{0°} - P_{180°}) \times D \times L = (4.62 - 0.14) \times 7.69 \times 1.14 = 3930$ N, or $(670 - 20) \times 3.0294 \times 0.45 = 886$ lbf. This restoring force represents a very stiff spring, analogous to a very large sledgehammer.

[7]At the time these data were taken, it was believed that corresponding-states principles would not apply. Consequently all data for case 2 are for hydrogen. At first glance, these data did not appear to follow the corresponding-states principles; however, subsequent data reinforced the notion that

$$\left.\frac{P_B/P_c}{P_{in}/P_c}T_{R,o}\right|_{N_2} \sim \left(\frac{1/3}{1.15}\times 0.7\right)\Bigg|_{N_2} \sim \left.\frac{P_B/P_c}{P_{in}/P_c}T_{R,o}\right|_{H_2} \sim \left(\frac{1}{4.2}\times 0.8\right)\Bigg|_{H_2}$$

backpressure after the flow is established results in different profiles than when the backpressure is applied before the flow is established?

In general, the answers were yes and no, respectively.

It is clear from figure 35 that a "flat region" can occur for backpressure considerably beyond P_c. But determining exactly how extensive the flat region will be is beyond the capability of the present flow system for both pressure and temperature. Applying backpressure before or after flow was established resulted in different transient shock behavior, but the steady results appeared to be unaffected.

To note the effect of increased inlet pressure on the flat pressure profile in the third step, with backpressure fixed, compare runs 423 and 420 of figure 35 and runs 413 and 410 of figure 34. These runs are typical and conclusively demonstrate the dependence of the profile on P_{in}/P_B. Figures 34, 35, and 29 (in retrospect) give some idea as to the point of neutral stability,[8] which can be obtained at $T_{R,o} \sim 0.88$:

$$\left.\frac{P_{in}}{P_B T_{R,o}}\right|_{\substack{\text{Neutral}\\ \text{stability}}} \sim \left.\frac{8.17}{1.89 \times 0.89}\right|_{\text{Run 423}} = 4.9$$

$$\left.\frac{P_{in}}{P_B T_{R,o}}\right|_{\substack{\text{Neutral}\\ \text{stability}}} = \left.\frac{6.14}{1.57 \times 0.85}\right|_{\text{Run 413}} = 4.8$$

$$\left.\frac{P_{in}}{P_B T_{R,o}}\right|_{\substack{\text{Above}\\ \text{neutral}\\ \text{stability}}} = \left.\frac{7.64}{1.954 \times 0.88}\right|_{\text{Run 420}} = 4.4$$

$$\left.\frac{P_{in}}{P_B T_{R,o}}\right|_{\substack{\text{Above}\\ \text{neutral}\\ \text{stability}}} = \left.\frac{6.81}{1.7 \times 0.86}\right|_{\text{Run 410}} = 4.7$$

This indicates that for fluid hydrogen, when the ratio $(P_{in}/P_B)/T_{R,o} > 4.8$ at this value of $T_{R,o}$ (~ 0.88), the pressure profile will become flat in the third step of the seal. For $(P_{in}/P_B)/T_{R,o} < 4.8$ the profile, while still showing a pressure difference, will be more conventional (i.e., gaslike).

Previous nitrogen data indicated that $T_{R,o}$ also has a strong effect and that the proper neutral stability curves should be modified by $T_{R,o}$ as indicated previously (recall footnote 7). Some effects of increased $T_{R,o}$ are illustrated in figure 36. Although the data are very limited, there is a distinct indication that the flattened profiles in the third step are not limited to low $T_{R,o}$. These results represent a departure from the profiles of figure 23, where the flat profile became gaslike at elevated inlet temperatures. At this time I cannot offer an explanation that will resolve these difficulties.[9]

One reason for emphasizing and defining these unusual conditions is how they affect dynamics. These data and some preliminary numerical work indicate the significant role played by inlet boundary conditions. It is true that the passage plays an important role, but it is secondary. In all cases investigated (refs. 1 and 2) the stiffness in the inlet region is positive but rapidly degrades with axial position and becomes negative toward the outlet (crossover). This should have been anticipated from the fluid mechanics. For the three-step labyrinth seal the crossover occurs within each step (ref. 2); for the cylindrical seal the crossover occurs close to two-thirds of the axial length (ref. 1); for the data herein it occurs in the second step ahead of the third step, where the flow separates, and for the eccentric case a flat region ensues.

Case 3—concentric position with backpressure control.—The system was the same as the eccentric position system except that the seal was positioned to provide a concentric annulus and the backpressure was controlled.

The gaseous hydrogen pressure profiles for the concentric position with backpressure control (figs. 37 and 38) do not appear significantly different from those for the concentric position without backpressure control (figs. 7, 8, and 13), even to the point of having profile crossover that may represent some transducer error. However, the fluid hydrogen profiles do differ. At a fixed backpressure changes in inlet stagnation pressure provide an increase in the entire profile. The same profile can be almost duplicated by fixing the inlet stagnation pressure and increasing the backpressure.

The fluid hydrogen pressure profiles for the concentric position with backpressure control (figs. 37 and 38) did not have the flat region in the third step that was noted in reference 1 and explored in detail in the section Fully Eccentric Position. This does not imply that they cannot exist, but for the conditions of these tests and within instrumentation limitations they did not occur.

Typically the fluid data behaved like those for a gas, independent of the backpressure. However, the 0° and 180° profiles were somewhat closer together than those for the concentric configuration without backpressure. This indicated better centerbody alignment here and suggests that small departures in alignment can produce substantial changes in the pressure profile.

Summary for backpressure control.—To summarize, the effects of backpressure control on reduced critical mass flux (leakage) and pressure profile data for fluid nitrogen or fluid hydrogen flowing through a three-step cylindrical seal are as follows:

[8]The point where the shock holds at the inlet to the third step just prior to unchoking.

[9]Joule Thomson effects, flash cooling, or large density differences at elevated pressures may be sufficient to "trigger" jetting.

(1) With the centerbody in its fully eccentric position at 0° measurements for fluid hydrogen, with the backpressure at or above the thermodynamic critical pressure, indicated a flat pressure profile in the third step of the seal. The data obtained with the centerbody in the fully eccentric position at 180°, under equivalent backpressure conditions, corroborated the previous results. These results demonstrated that flat pressure profiles can occur in the third step of this three-step seal even when the backpressure is well above the thermodynamic critical pressure. Further, the circumferential choking phenomenon engendered upstream pressure profile crossover that resulted in a region of negative stiffness between regions of positive stiffness[10]. These new phenomena represent another factor with which seal designers must contend.

(2) The flat pressure profiles were not found for the seal in the concentric position with elevated backpressure. Further, the data indicated a better alignment of the centerbody than reported in the section Concentric Position and suggested that small changes in the position of the centerbody strongly affect the pressure profile of the three-step seal.

(3) Extrapolation of mass flux (leakage) based on limited data appeared to give reasonable values for both the straight and three-step cylindrical seals when compared with the classic venturi. Clearly high-pressure hydrogen (or helium) data (to $P_{R,o} = 30$) must be taken with the classic venturi to increase the valid range of the theoretical calculations. More seal data near $T_{R,o}$ of 0.85, 1.0, and 1.2 should be acquired at these pressures since such conditions more nearly coincide with projected turbopump operating conditions. Also necessary is information on the effects of rotation especially when thermophysical properties are not constant, as will be the case for these values of $T_{R,o}$.

Flow Coefficient Analogy

A most convenient way to display mass flux for complex geometries is to relate these flows to those calculated and measured for the classic venturi. In references 4 to 7 the two-phase choked flows in a venturi were calculated and ratioed to experimental data for the Borda inlet. The single orifice also followed trends established for the Borda but at a lower level, more equivalent to the trends for the three-step cylindrical seal. These results provided a baseline variation of $C_f = G_R/G_{R,v}$ as a function of reduced inlet stagnation temperature. The Borda data were weak functions of pressure except near $T_{R,o} = 1$. Unfortunately the seal data were more dependent on pressure, as indicated by the deviation bars in figure 39. Here the flow-coefficient–$T_{R,o}$ locus for the Borda inlet is reproduced along with data for the three-step cylindrical seal in the concentric and fully eccentric positions. Although there appeared to be little difference in C_f for the concentric and fully eccentric cases, the deviation bars were large. These data, for a complex geometry, tended to mimic those for the simple axisymmetric Borda inlet but were lower by a factor of $C_{f,TS} \sim 0.65\ C_{f,\text{Borda}}$. Thus another similarity in flow arose but no such similitude existed for the pressure profiles.

[10]For the fully eccentric case there is some evidence that at sufficiently high inlet pressures the flat profile can occur for $T_{R,o} > 1$.

Summary of Results

This report summarizes the analysis and testing of a three-step cylindrical seal for high-performance turbomachines (e.g., the space shuttle main engine fuel pump).

Critical mass flux (leakage rate) and pressure profile data were taken over a wide range of inlet temperatures and pressures with fluid nitrogen and fluid hydrogen flowing through a simulated *static* (*nonrotating*) three-step seal configuration set in the concentric and fully eccentric positions. The flow areas decreased from the inlet to the exit. The areas for steps 1 to 3 were 0.3166 cm^2 (0.04907 $in.^2$), 0.3131 cm^2 (0.04853 $in.^2$), and 0.3044 cm^2 (0.04718 $in.^2$), respectively. The mass flux (leakage rate) was 70 percent that of an equivalent cylindrical seal with a correspondingly higher pressure drop based on the flow area of 0.03569 cm^2 (0.05531 $in.^2$) but 85 percent that of the straight seal based on the third-step, or minimum, flow area of 0.3044 cm^2 (0.04718 $in.^2$). Thus 15 percent of the flow reduction was assumed to be due to flow area change, and 15 percent was assumed to be due to losses at the internal step inlets. The mass flow rates for the three-step cylindrical seal in the fully eccentric and concentric positions were essentially the same, and the normalized flow coefficient tended to follow those for the axisymmetric Borda or orifice inlets as a function of inlet stagnation temperature. However, the dependency on pressure was more pronounced and cannot be neglected.

For inlet entropy less than the thermodynamic critical entropy the pressure profiles sometimes exhibited a flat region throughout the maximum clearance of the third step of the seal. This flat region occurred for inlet stagnation temperatures less than the thermodynamic critical temperature, with the pressure level within the seal dependent on the inlet stagnation temperature and to a lesser extent on the inlet stagnation pressure.[10] Such profiles represent an extreme positive direct stiffness.

It was postulated that choking occurred at the inlet to the third step with the effect diminishing circumferentially to unchoked in the minimum-clearance region. It was further postulated that choking engendered a crossover in the upstream pressure profile, with a higher pressure at the maximum-clearance region rather than at the minimum-clearance region. This resulted in a local negative stiffness between regions of positive stiffness.

Flat and crossover pressure profiles resulting from choking, postulated to occur within the seal, are practically unknown

to seal designers but are of critical importance to the stability of turbomachines.

It must be remembered, however, that these tests were *static*. The shaft was *not rotating* and one boundary condition in an actual application was not satisfied. Consequently the effects could be mitigated or enhanced by rotation. Further, the effects of added mass, damping, and cross coupling of stiffness and damping were not assessed, nor can they be inferred. However, these effects are very important to dynamics and should be determined in a future analytical/experimental program. These data do illustrate how sensitive turbomachine dynamics can be to seal geometry and inlet conditions especially near an inlet, where separation and two-phase flows can occur.

Further, in seal and bearing or damper designs, it has been assumed that choking cannot occur within the seal if the backpressure is above the thermodynamic critical pressure. This was shown to be an invalid assumption. Choking, which effects direct stiffness, is highly dependent on geometry, inlet-to-backpressure ratio, and inlet temperature and can occur within the seal even though the backpressure is above the thermodynamic critical pressure.

It is recommended that this program be extended to include rotation, inlet and outlet geometric variations, fluid injection, and different seal designs with measurements and analyses that provide direct and cross-coupled coefficients for dynamic analysis.

Lewis Research Center
National Aeronautics and Space Administration
Cleveland, Ohio, October 8, 1986

References

1. Hendricks, R.C.: Straight Cylindrical Seal for High-Performance Turbomachines. NASA TP-1850, 1987.
2. Hendricks, R.C.: Three-Step Labyrinth Seal for High-Performance Turbomachines, NASA TP-1848, 1987.
3. Hendricks, R.C., et al.: Experimental Heat-Transfer Results for Cryogenic Hydrogen Flowing in Tubes at Subcritical and Supercritical Pressures to 800 Pounds Per Square Inch Absolute. NASA TN D-3095, 1966.
4. Hendricks, R.C.; and Simoneau, R.J.: Some Flow Phenomena in a Constant Area Duct with a Borda Type Inlet Including the Critical Region. ASME Paper 78-WA/HT-37, Dec. 1978.
5. Hendricks, R.C.: Some Aspects of a Free Jet Phenomena to 105 *L/D* in a Constant Area Duct. XV International Congress of Refrigeration, International Institute of Refrigeration, Paper B1-78, 1979.
6. Hendricks, R.C.: Some Observations of a Free Jet Phenomena in a 90°-Sharp-Edge Inlet Geometry. Advances in Cryogenic Engineering, Vol. 25, K.D. Timmerhaus and H.A. Snyder, eds., Plenum, 1980, pp. 506-520.
7. Hendricks, R.C.; and Poolos, N.P.: Critical Mass Flux Through Short Borda Type Inlets of Various Cross Sections. XV International Congress of Refrigeration, International Institute of Refrigeration, Paper B1-77, 1979.

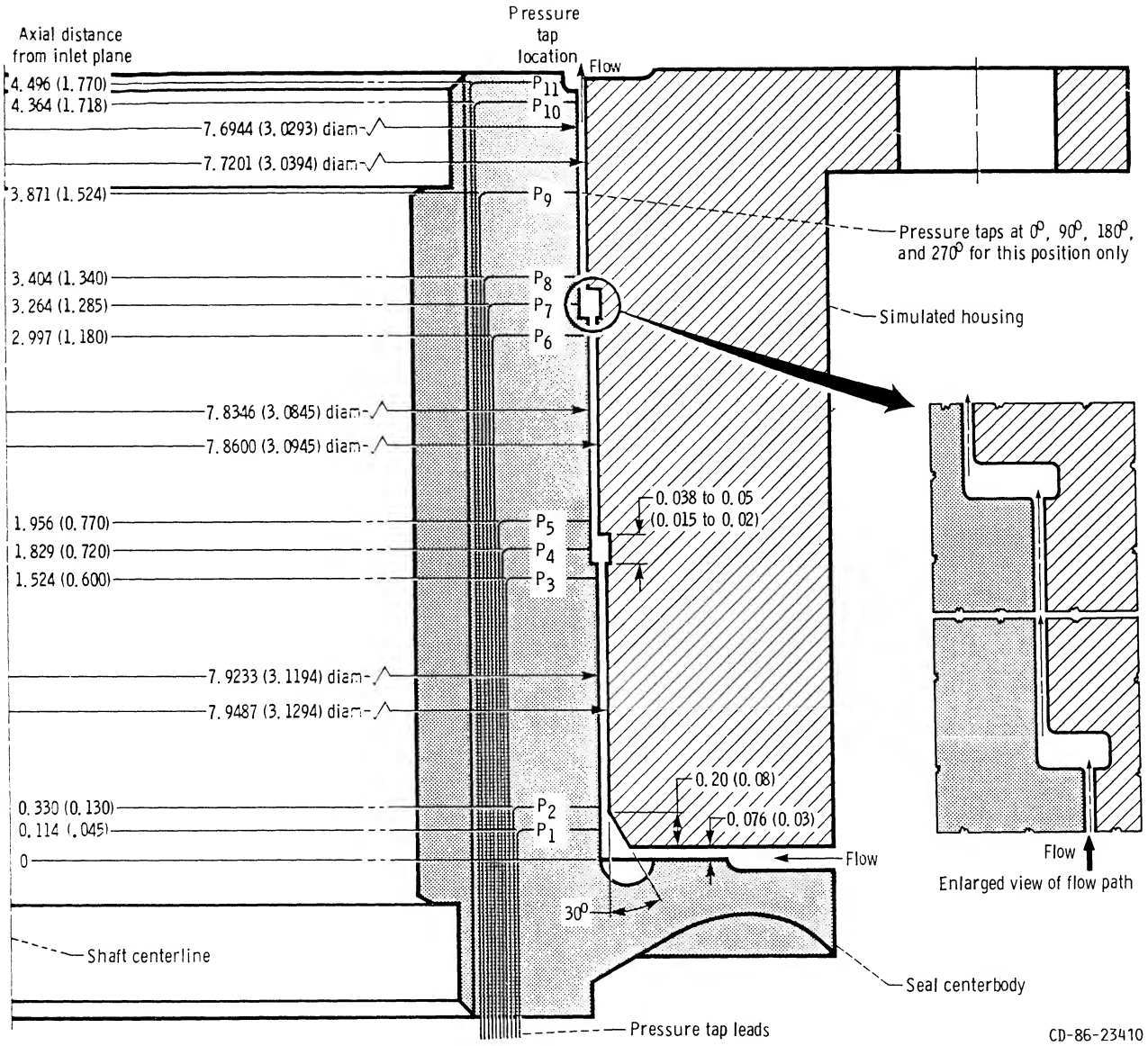

(a) Pressure taps.
(b) Step geometry.

Figure 1.—Schematic of three-step flow path and pressure tap locations. (Linear dimensions are in centimeters (inches).)

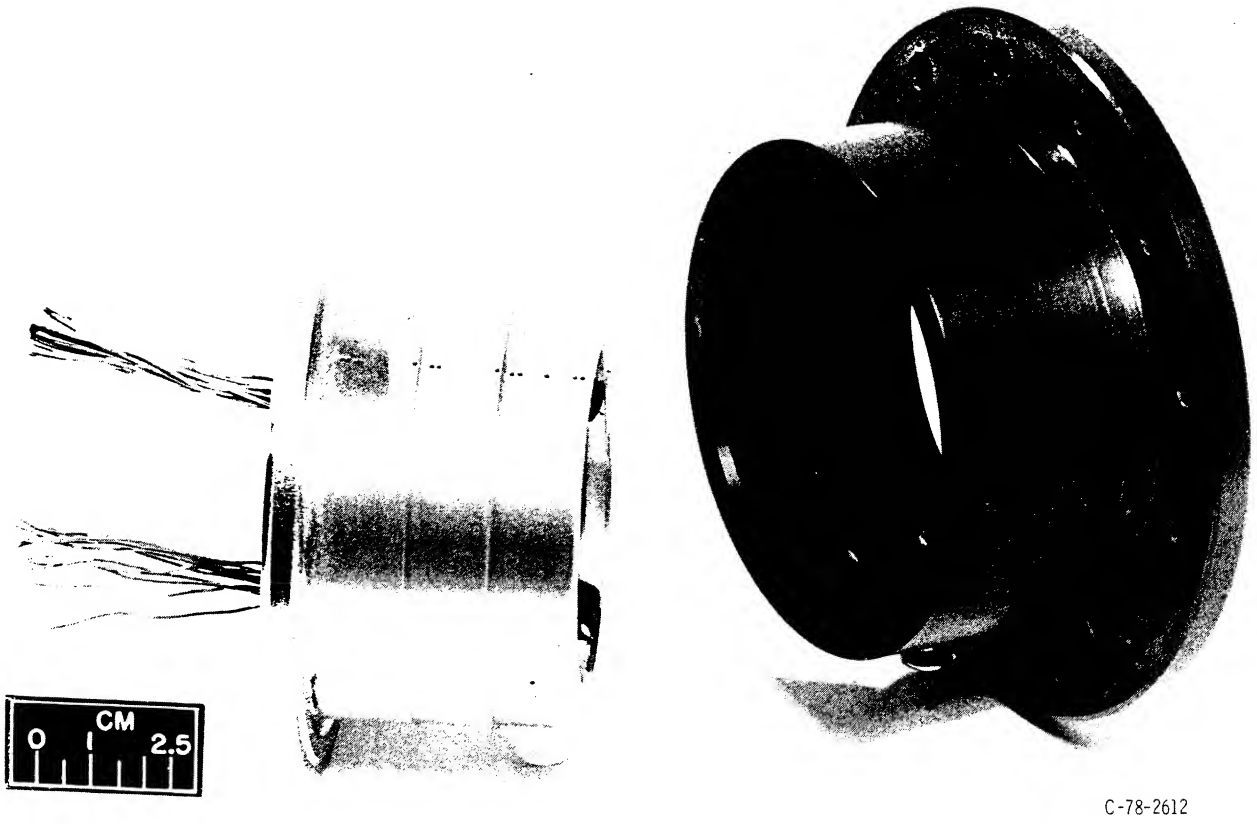

Figure 2.—Three-step seal (simulated shaft, centerbody, and housing).

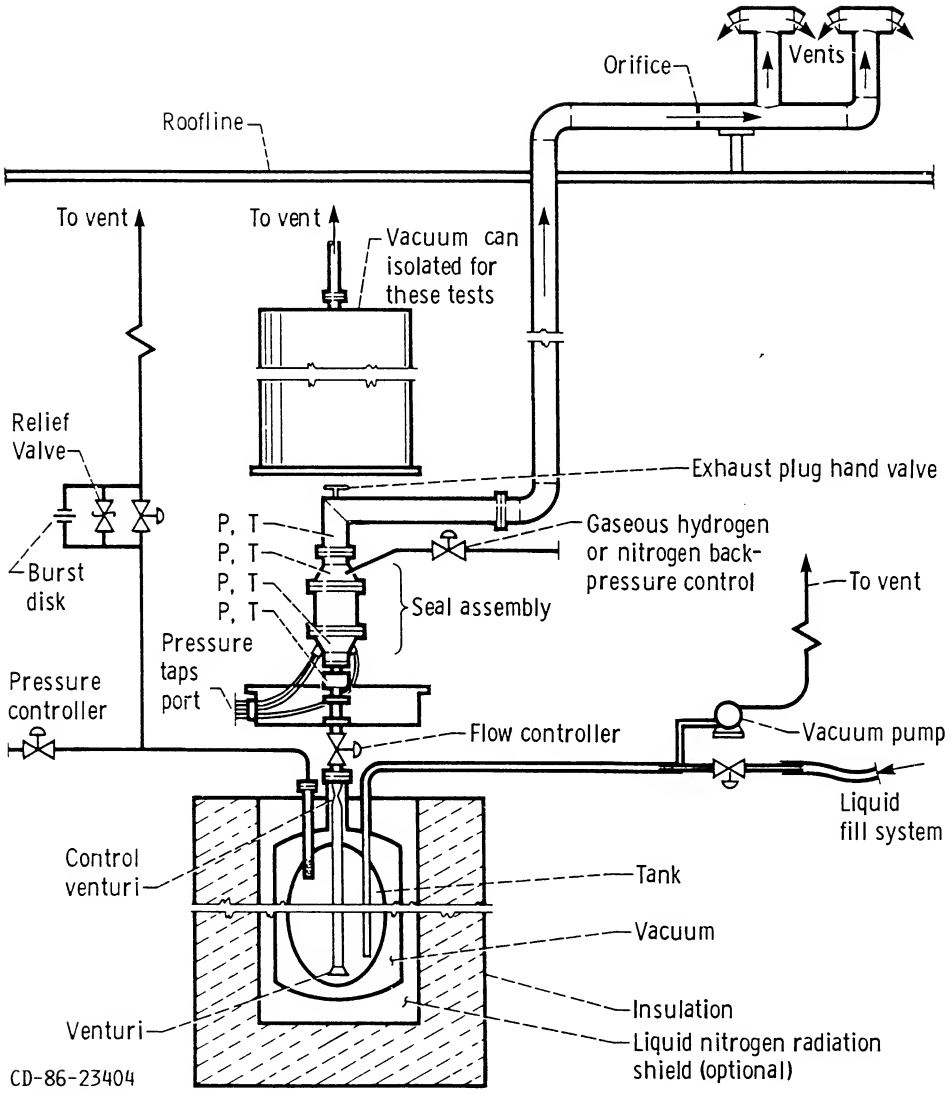

Figure 3.—Schematic of test installation modified for backpressure control.

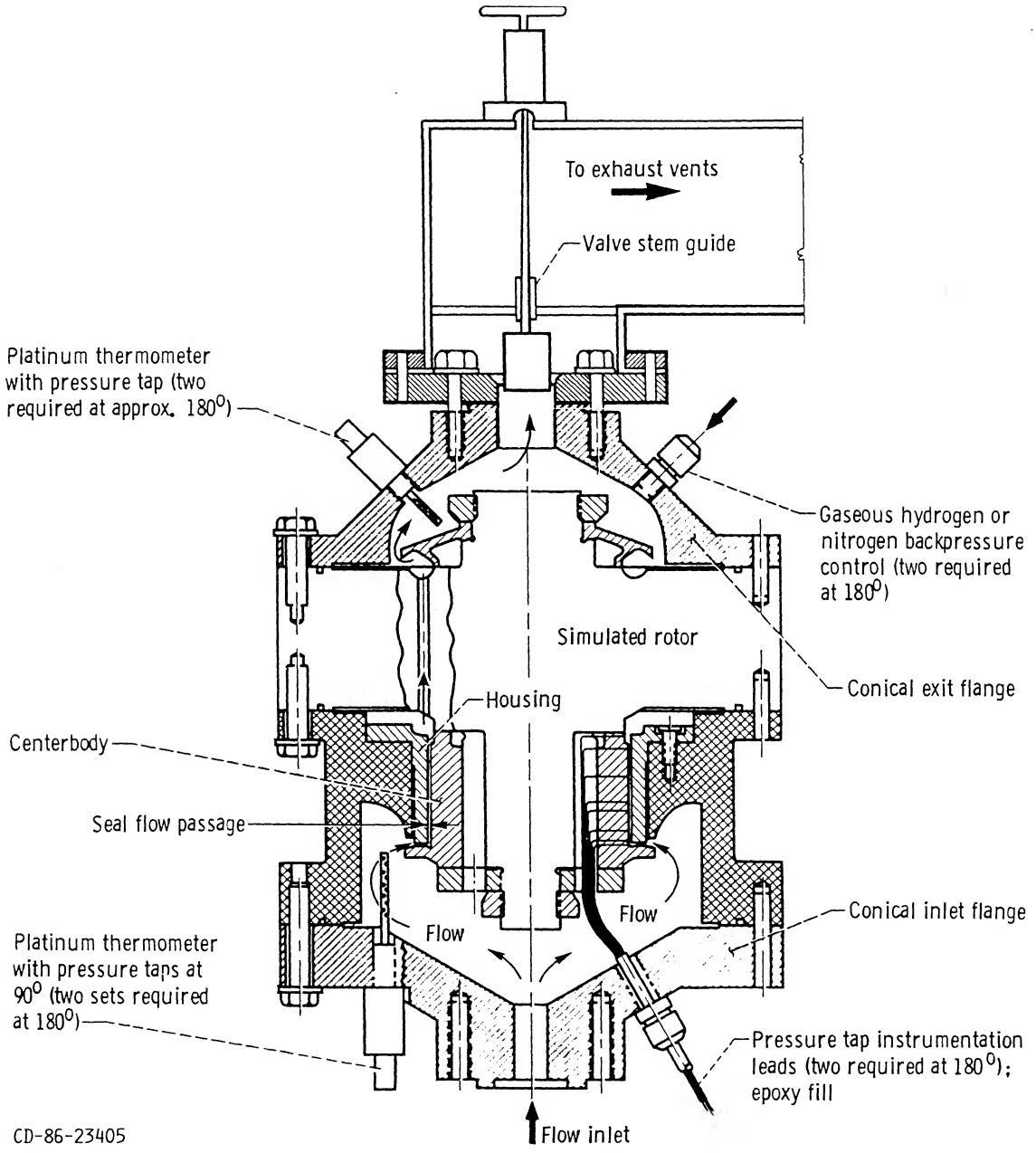

Figure 4.—Cross-sectional view of simulated seal configuration modified for backpressure control.

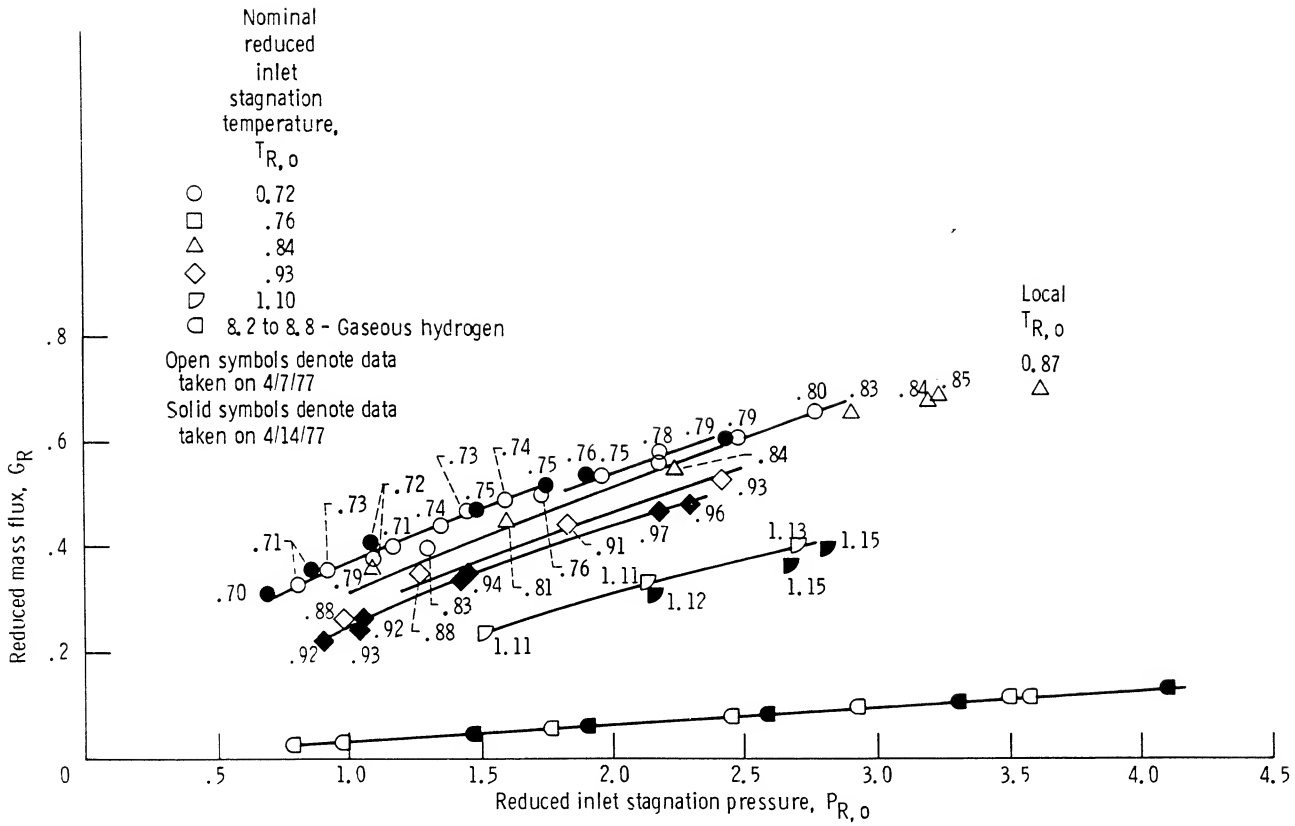

Figure 5.—Reduced mass flux of fluid hydrogen through three-step cylindrical seal in concentric position, as function of reduced inlet stagnation pressure.

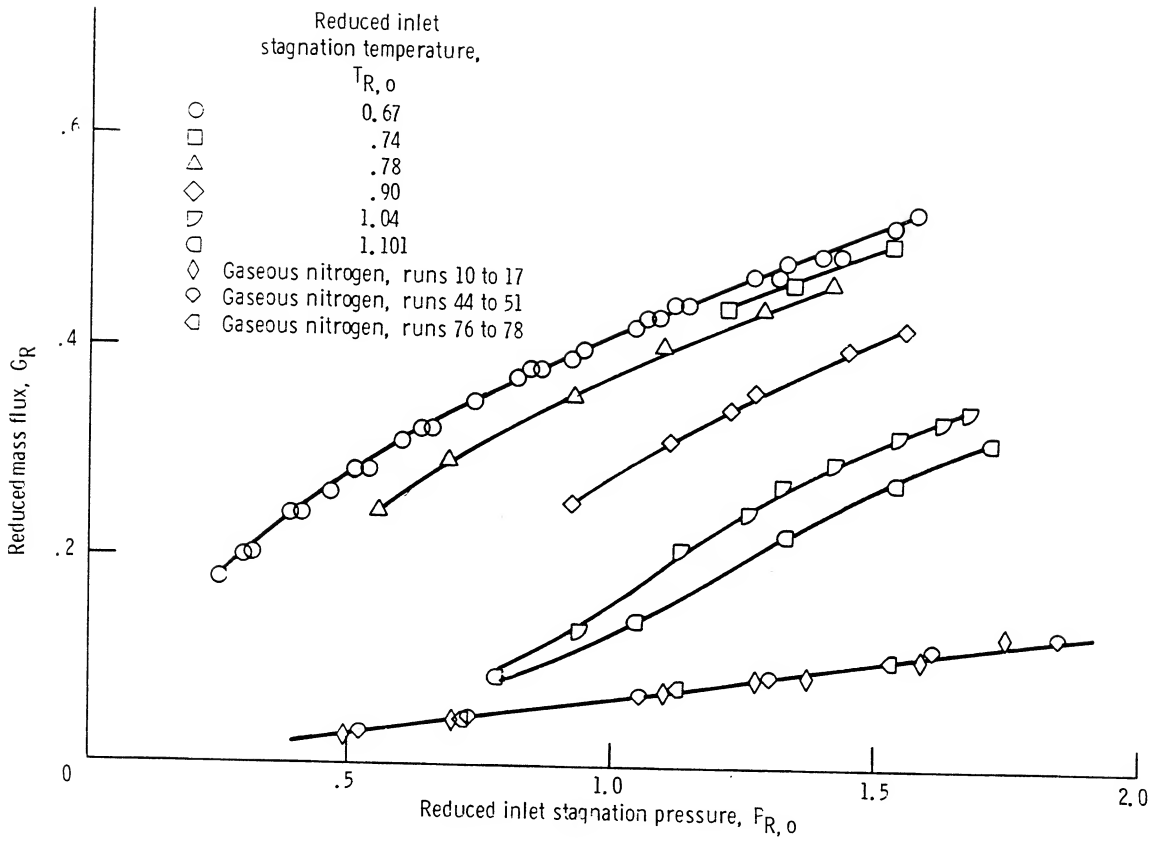

Figure 6.—Reduced mass flux of gaseous nitrogen through three-step cylindrical seal in concentric position, as function of reduced inlet stagnation pressure.

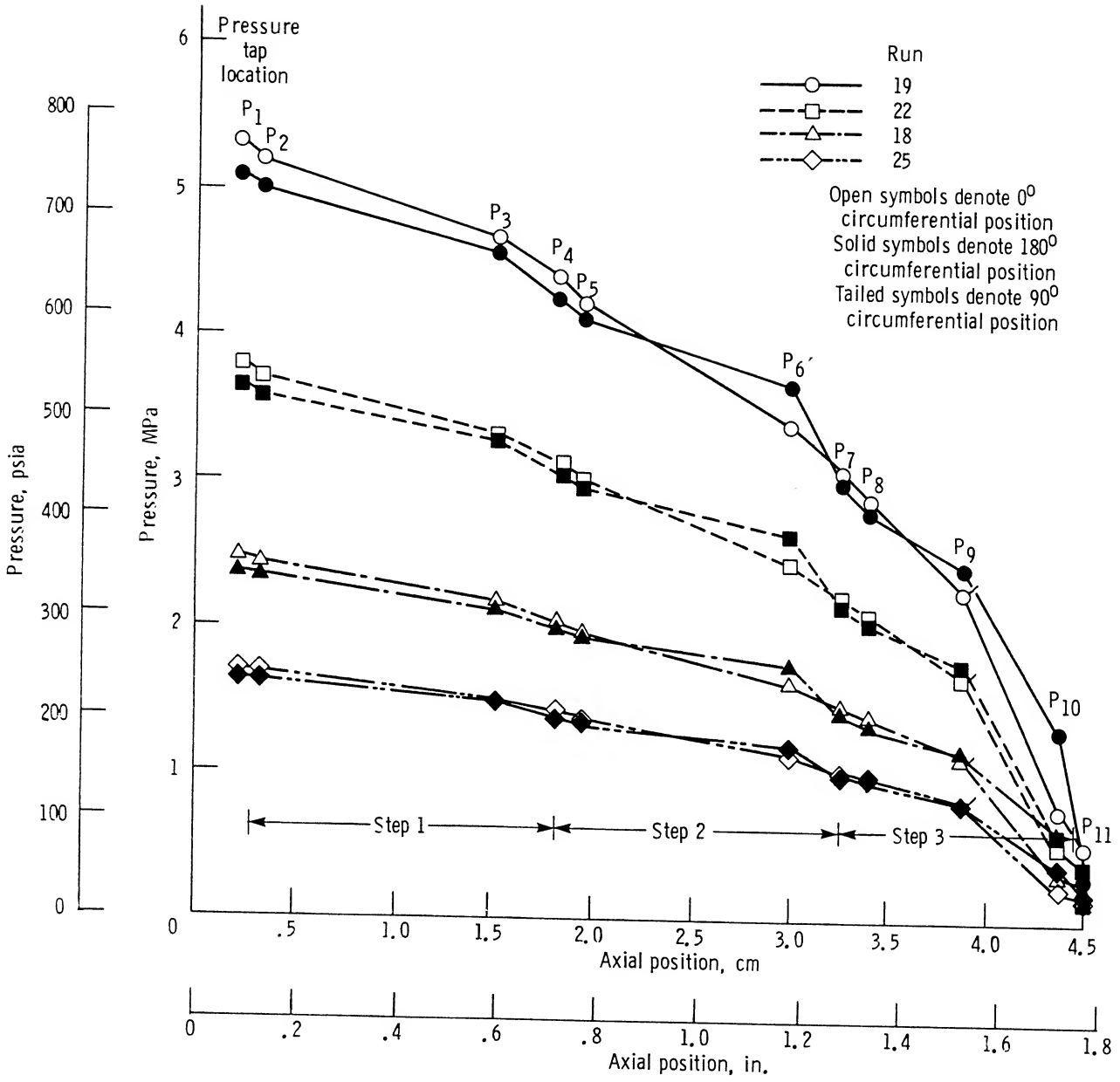

Figure 7.—Axial pressure distribution of gaseous hydrogen flow through three-step cylindrical seal in concentric position.

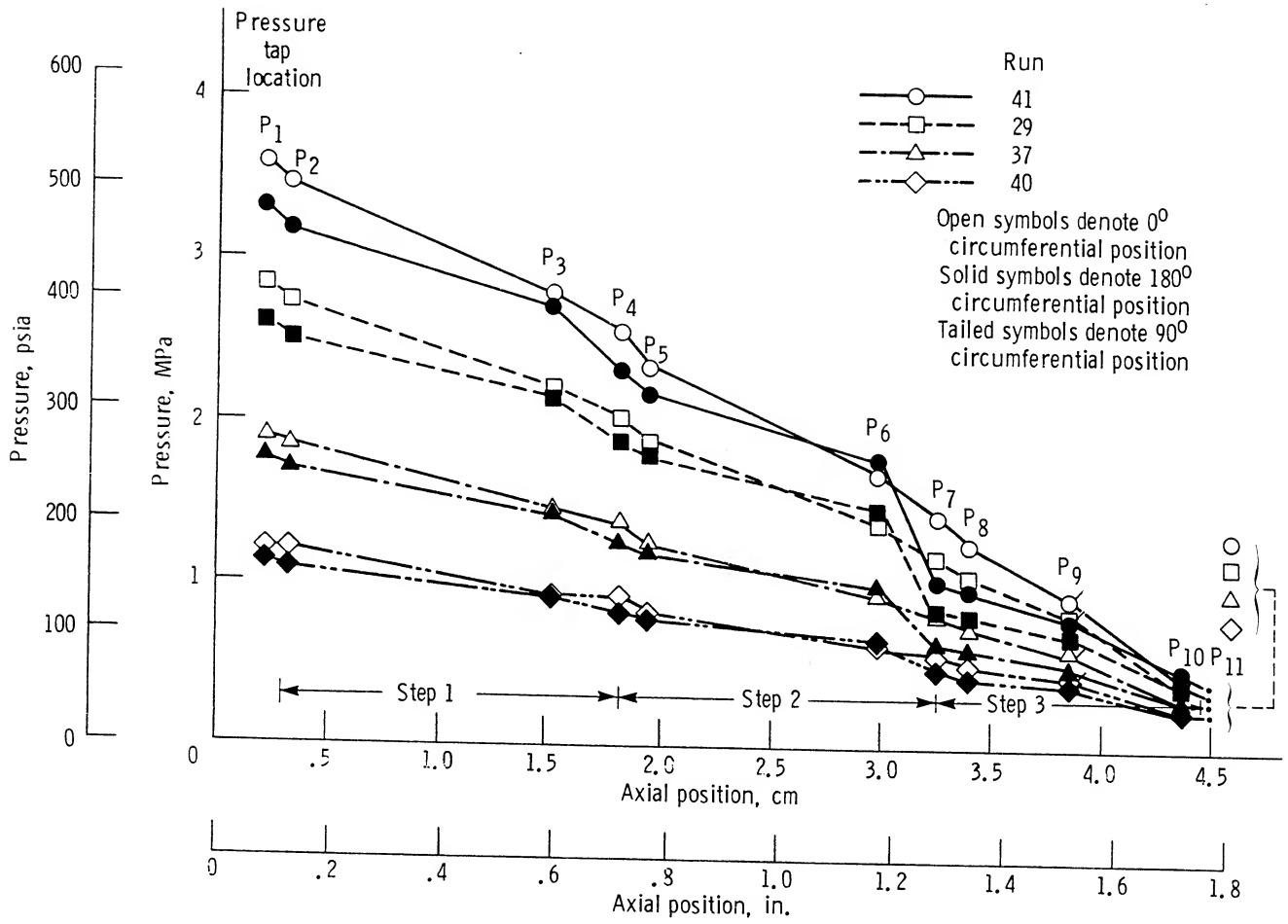

Figure 8.—Axial pressure distribution of fluid hydrogen flow through three-step cylindrical seal in concentric position.

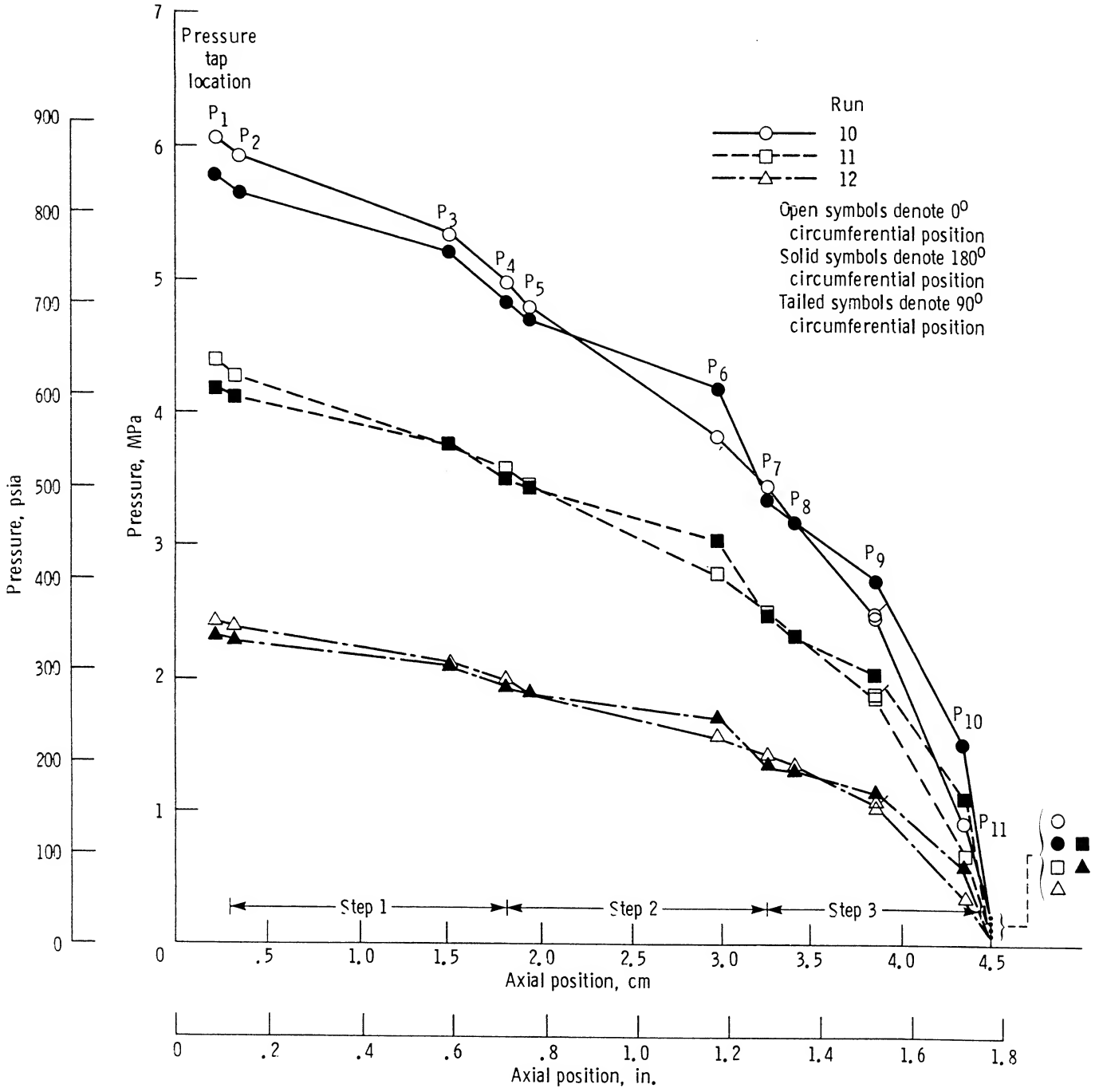

Figure 9.—Axial pressure distribution of gaseous nitrogen flow through three-step cylindrical seal in concentric position for runs 10 to 12.

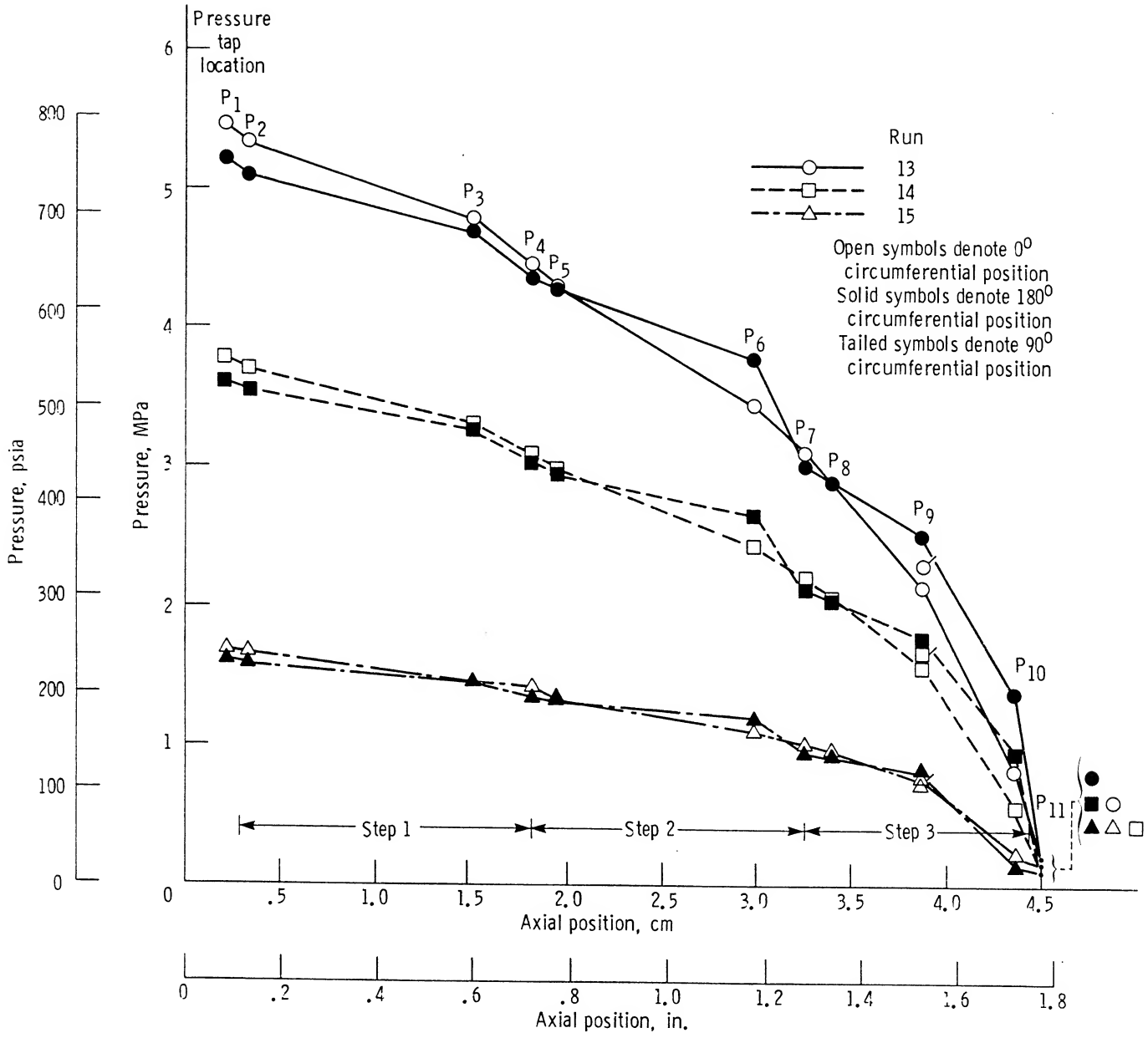

Figure 10.—Axial pressure distribution of gaseous nitrogen flow through three-step cylindrical seal in concentric position for runs 13 to 15.

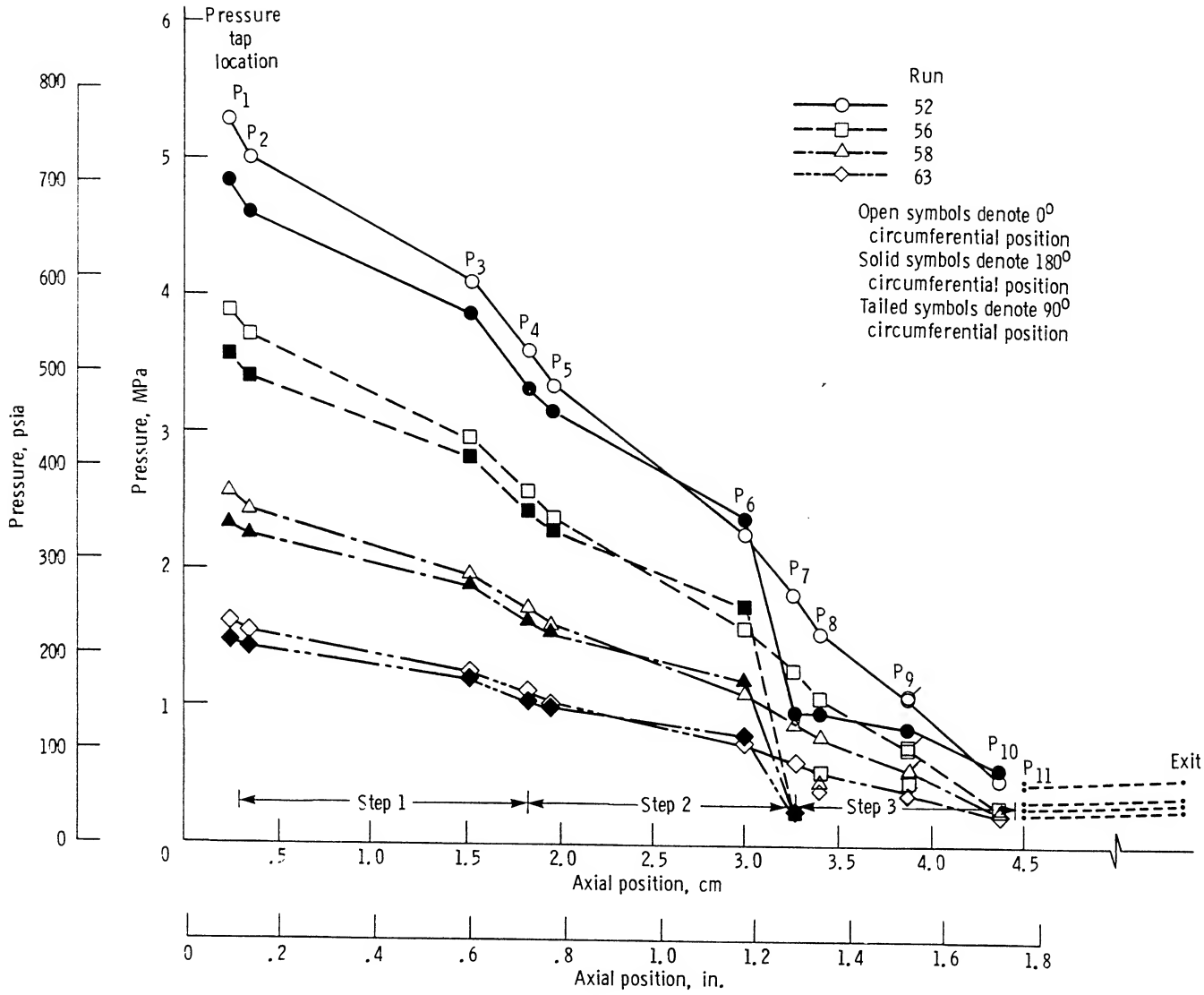

Figure 11.—Axial pressure distribution of fluid nitrogen flow through three-step cylindrical seal in concentric position for runs 52, 56, 58, and 63.

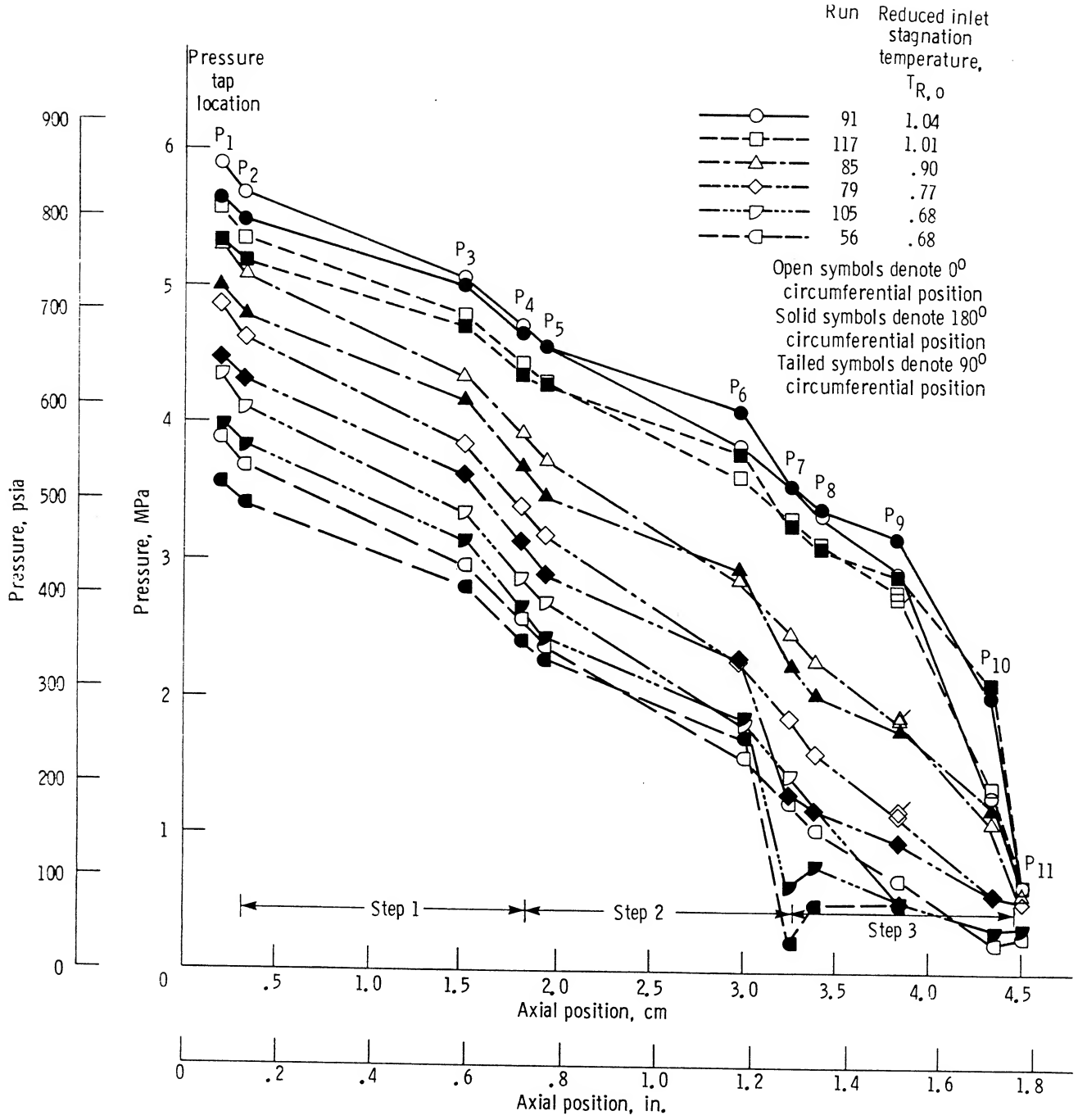

Figure 12.—Axial pressure distribution of fluid nitrogen flow through three-step cylindrical seal in concentric position for runs 56, 79, 85, 91, 105, and 116.

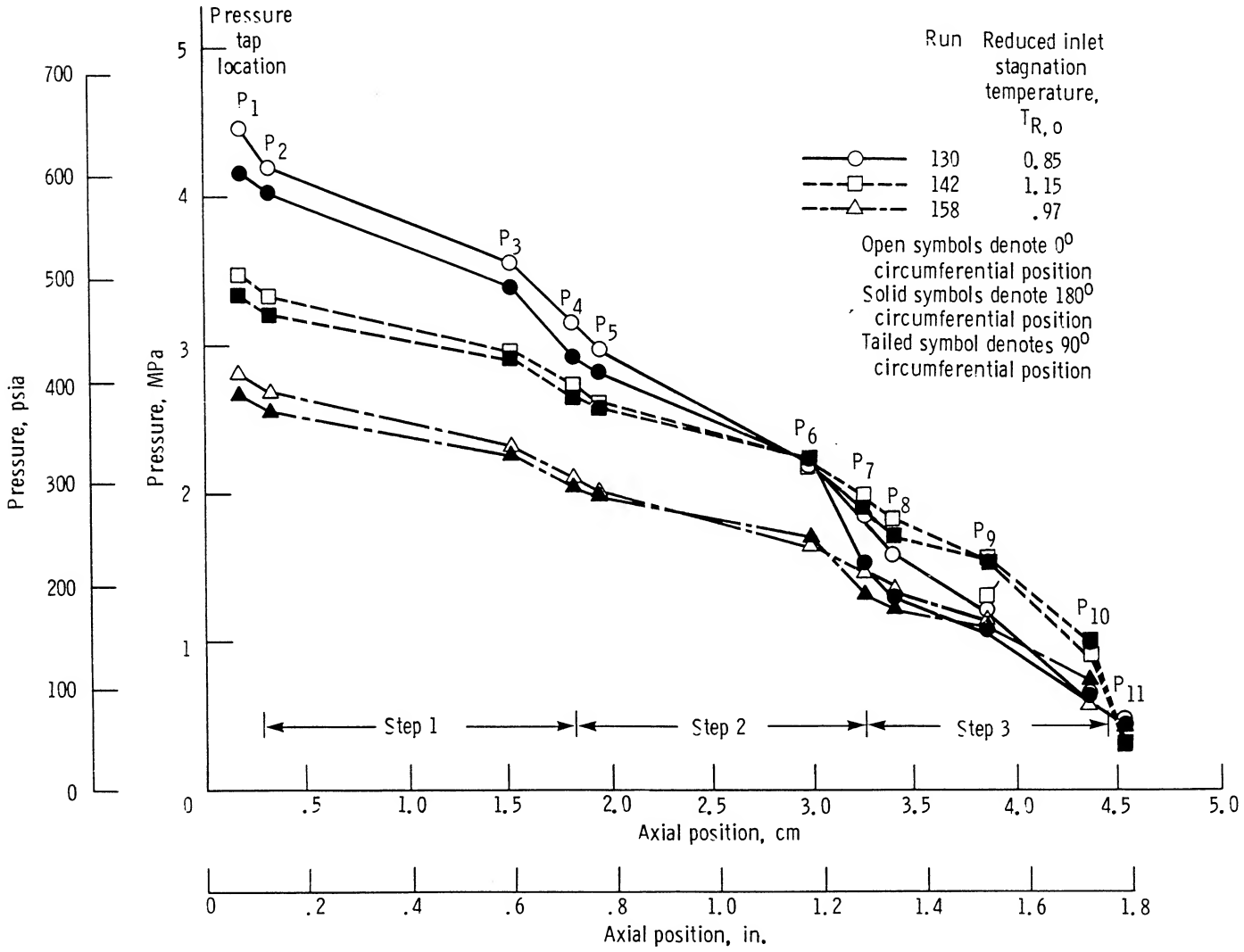

Figure 13.—Axial pressure distribution of fluid hydrogen flow through three-step cylindrical seal in concentric position.

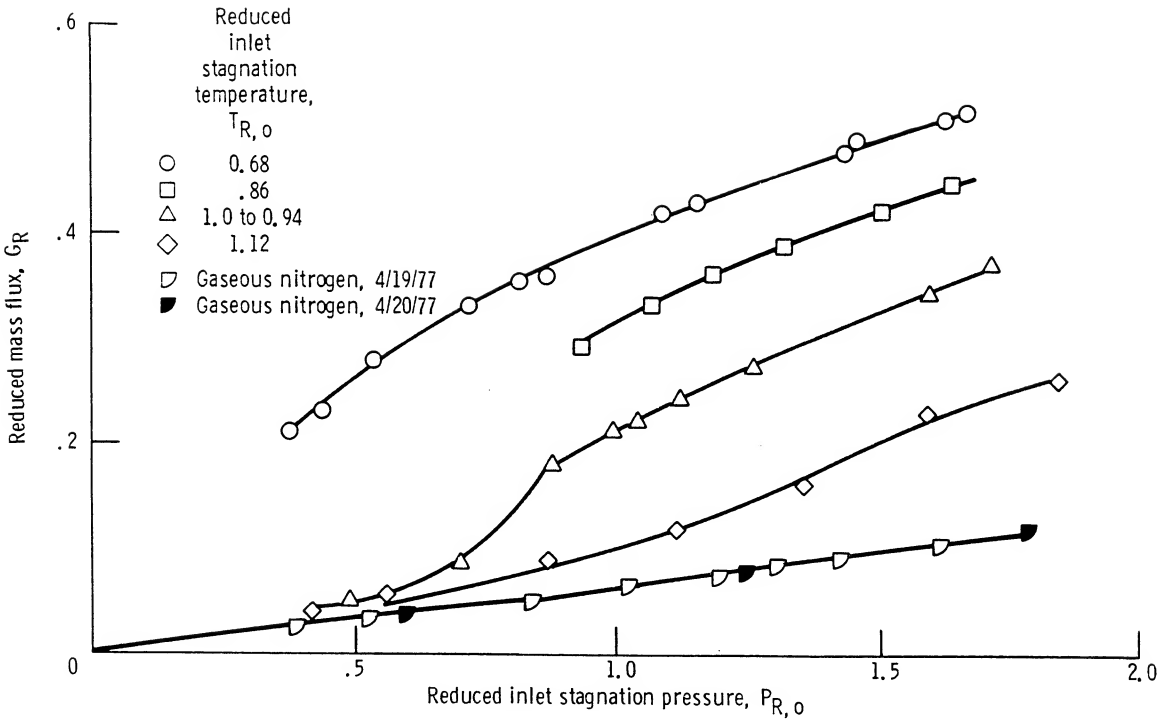

Figure 14.—Reduced mass flux of fluid nitrogen through three-step cylindrical seal in fully eccentric position, as function of reduced inlet stagnation pressure.

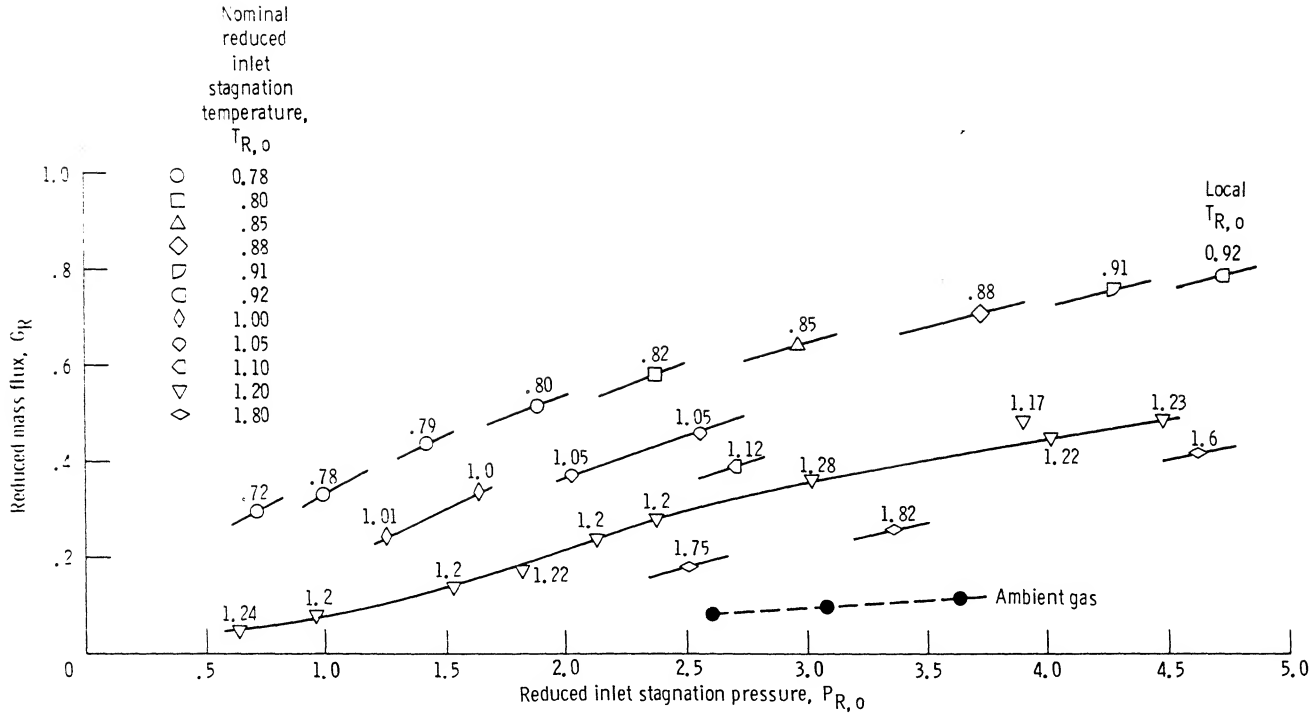

Figure 15.—Reduced mass flux of fluid hydrogen through three-step cylindrical seal in fully eccentric position, as function of reduced inlet stagnation pressure.

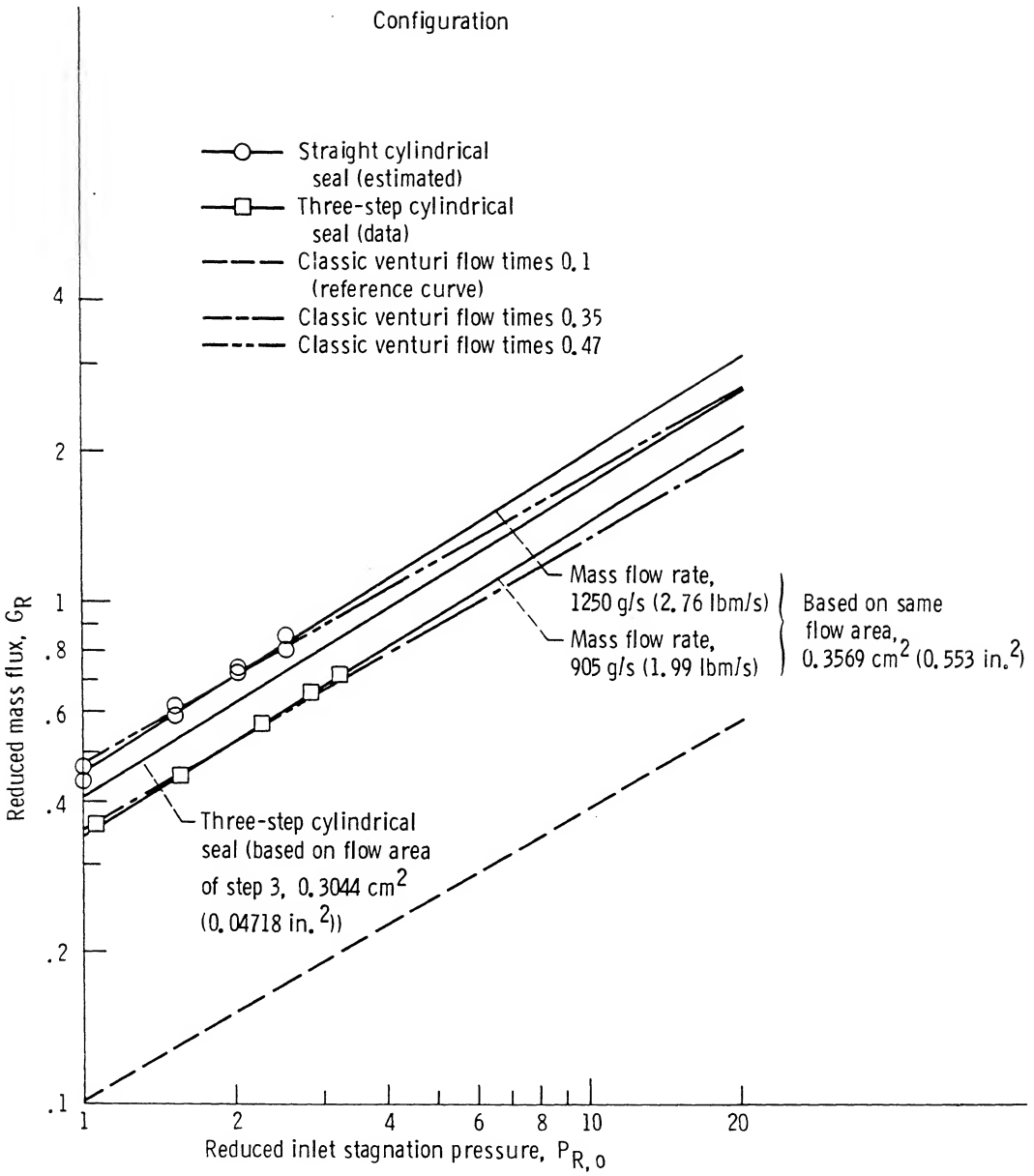

Figure 16.—Extrapolated reduced mass flux of liquid hydrogen for straight and three-step seal configurations, as function of reduced inlet stagnation pressure. (G^* = 1158 g/cm^2 s (16.44 lbm/in.^{2} s); T_c ~ 33 K (59.4 °R); ψ_Q = − 0.04 at $T_{R,o}$; P_c ~ 1.29 MPa (187.5 psia); $T_{R,o}$ = 0.8.)

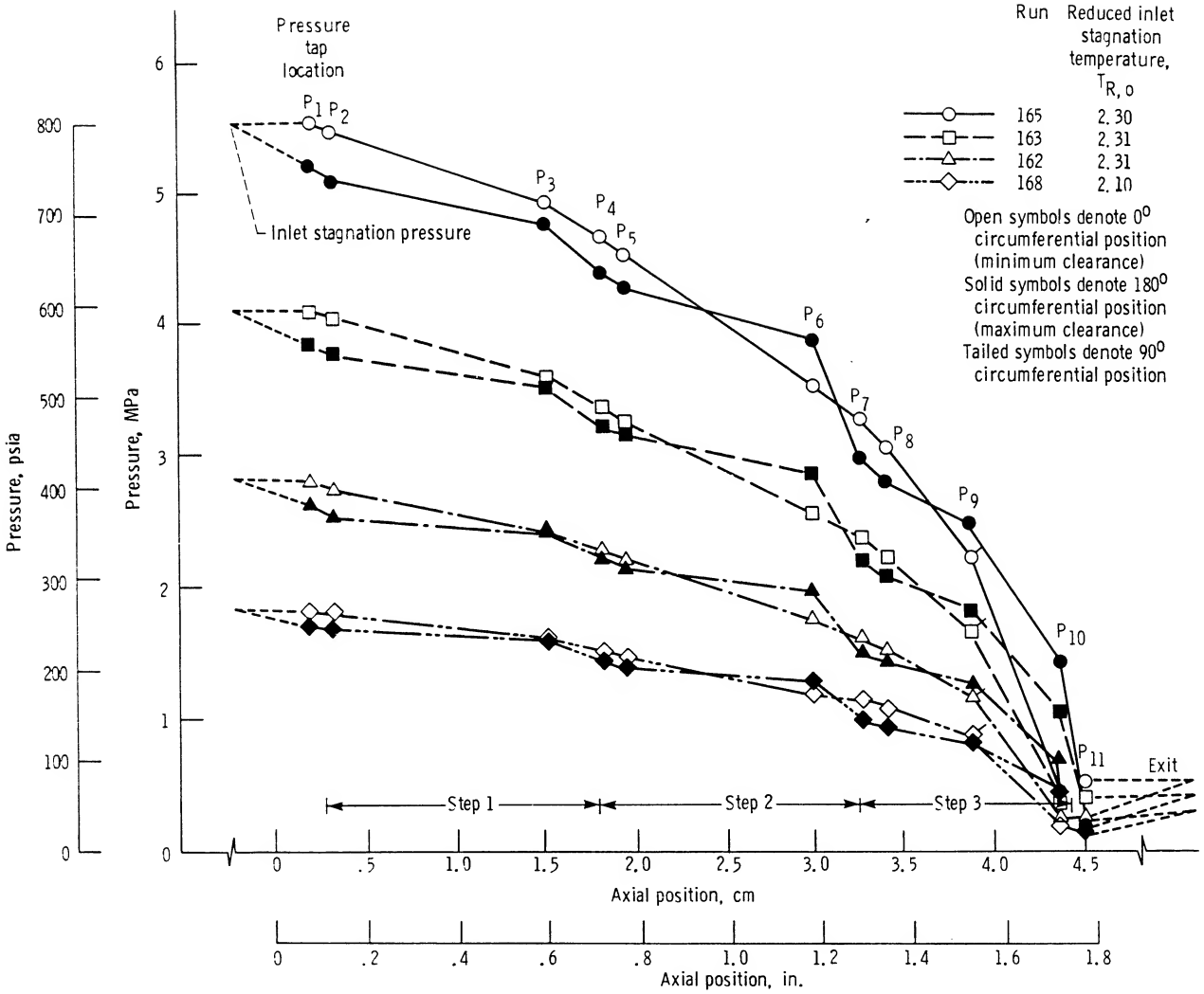

Figure 17.—Axial pressure distribution of gaseous nitrogen flow through three-step cylindrical seal in fully eccentric position.

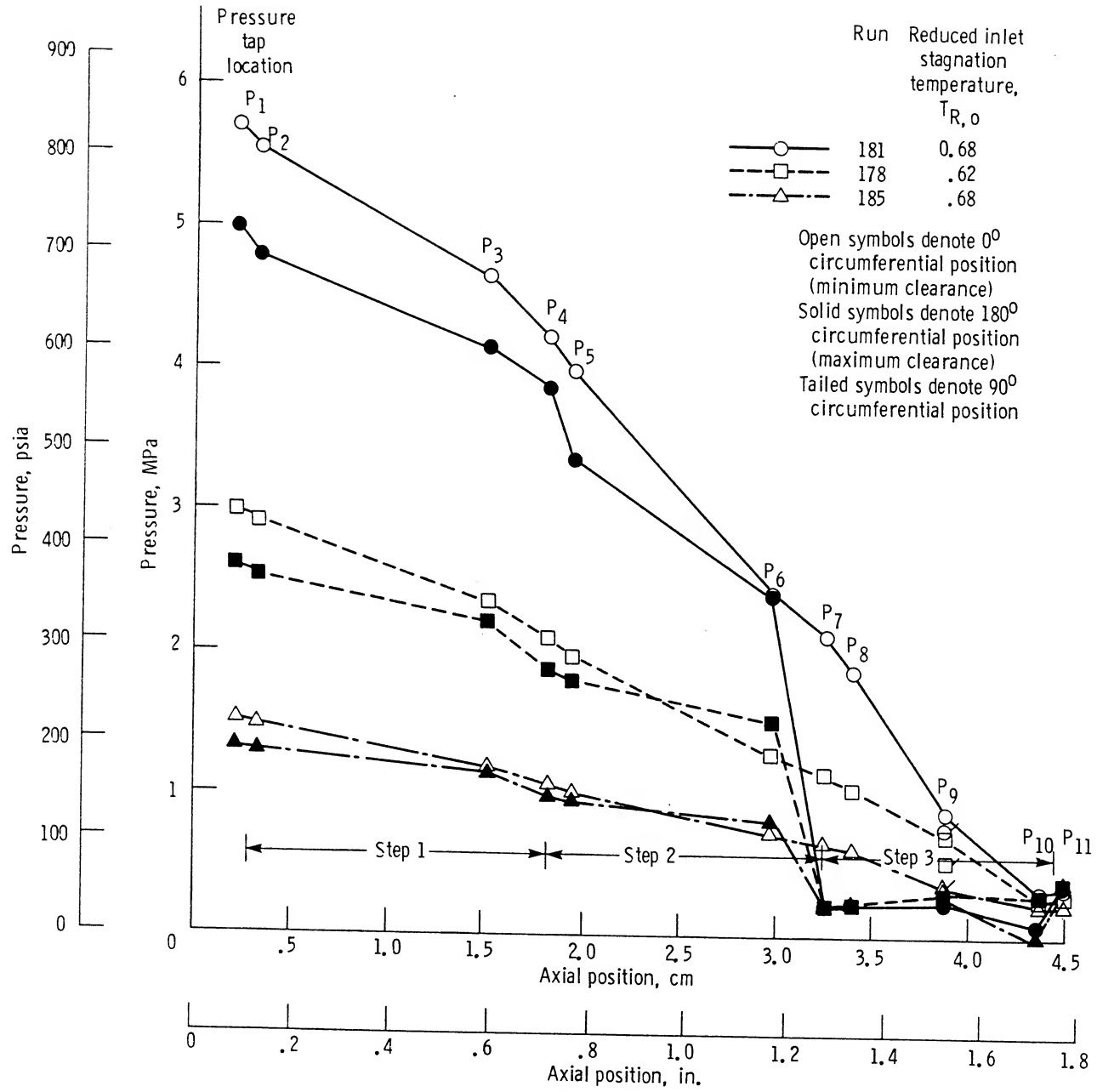

Figure 18.—Axial pressure distribution of fluid nitrogen flow through three-step cylindrical seal in fully eccentric position for runs 178, 181, and 185.

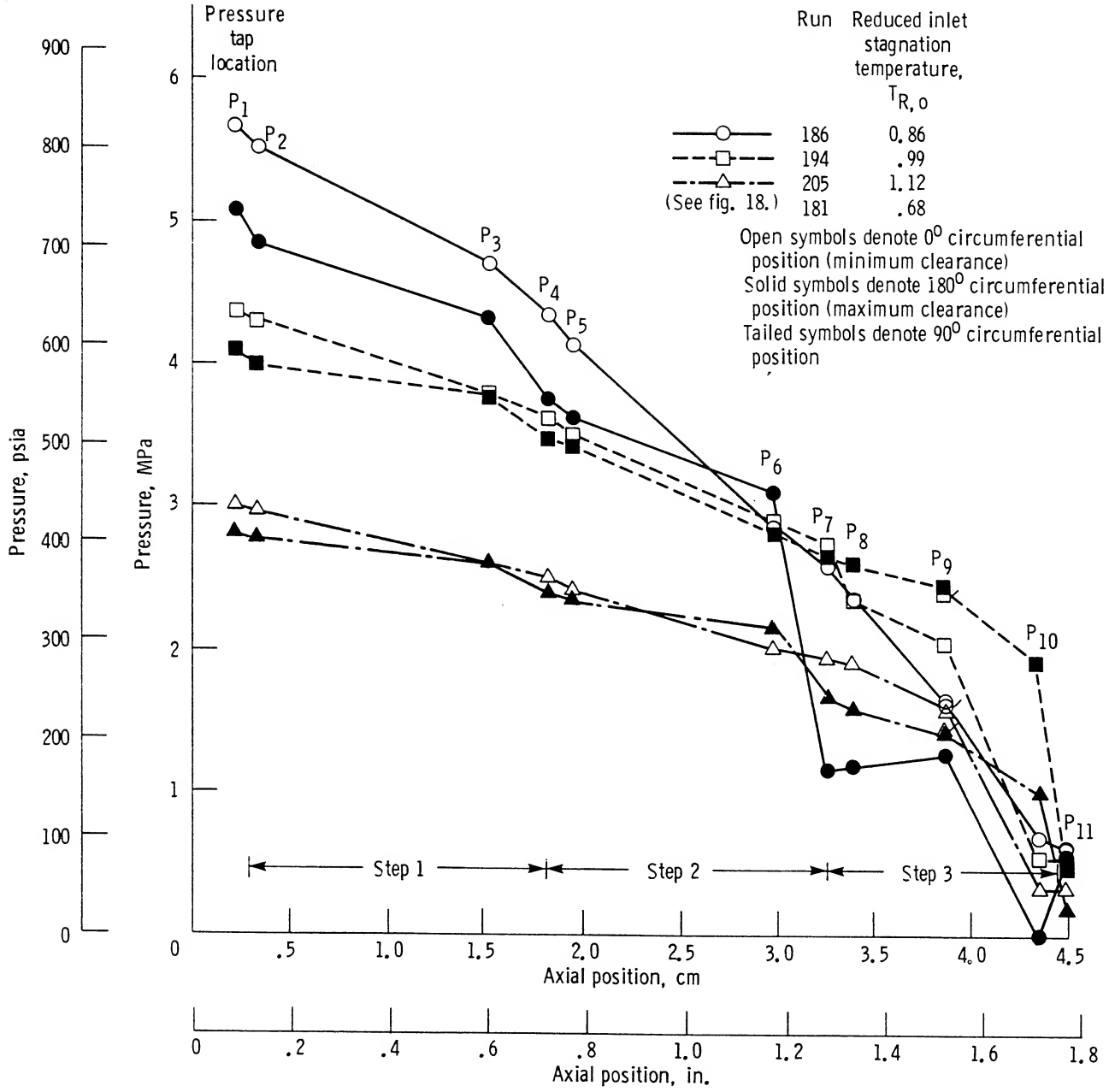

Figure 19.—Axial pressure distribution of fluid nitrogen flow through three-step cylindrical seal in fully eccentric position for runs 186, 194, and 205.

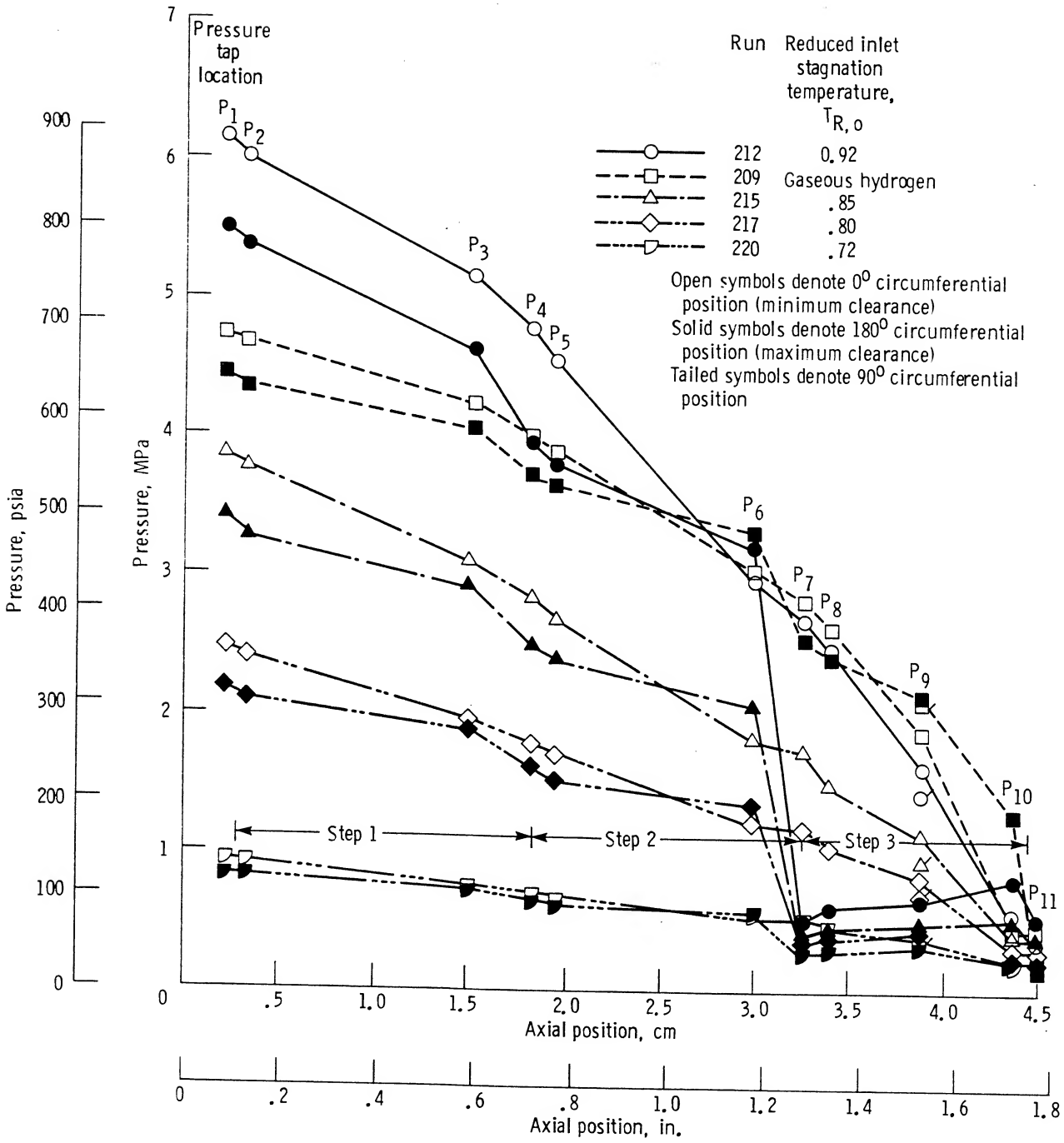

Figure 20.—Axial pressure distribution of fluid hydrogen flow through three-step cylindrical seal in fully eccentric position for runs 209, 212, 215, 217, and 220.

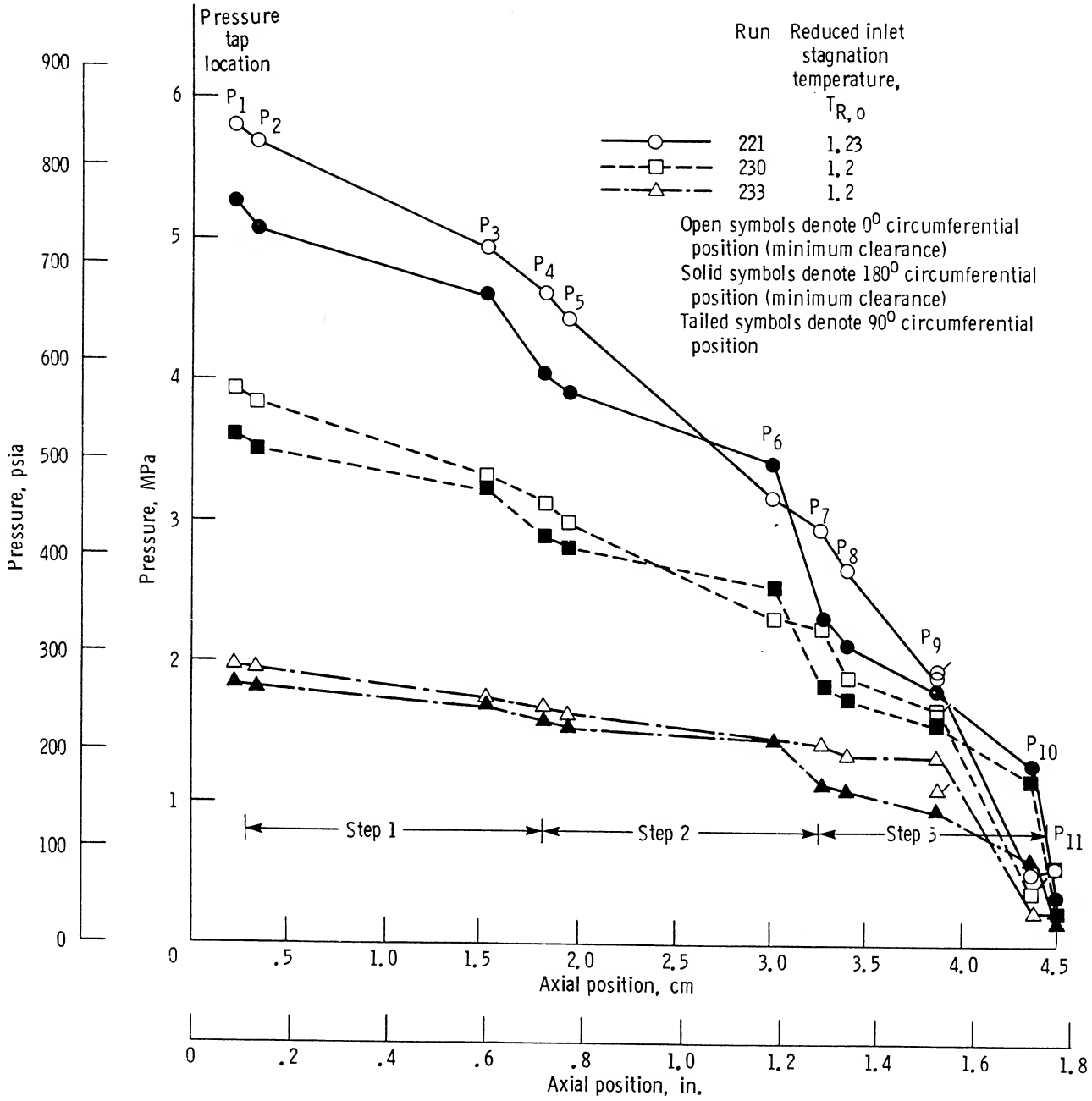

Figure 21.—Axial pressure distribution of fluid hydrogen flow through three-step cylindrical seal in fully eccentric position for runs 221, 230, and 233.

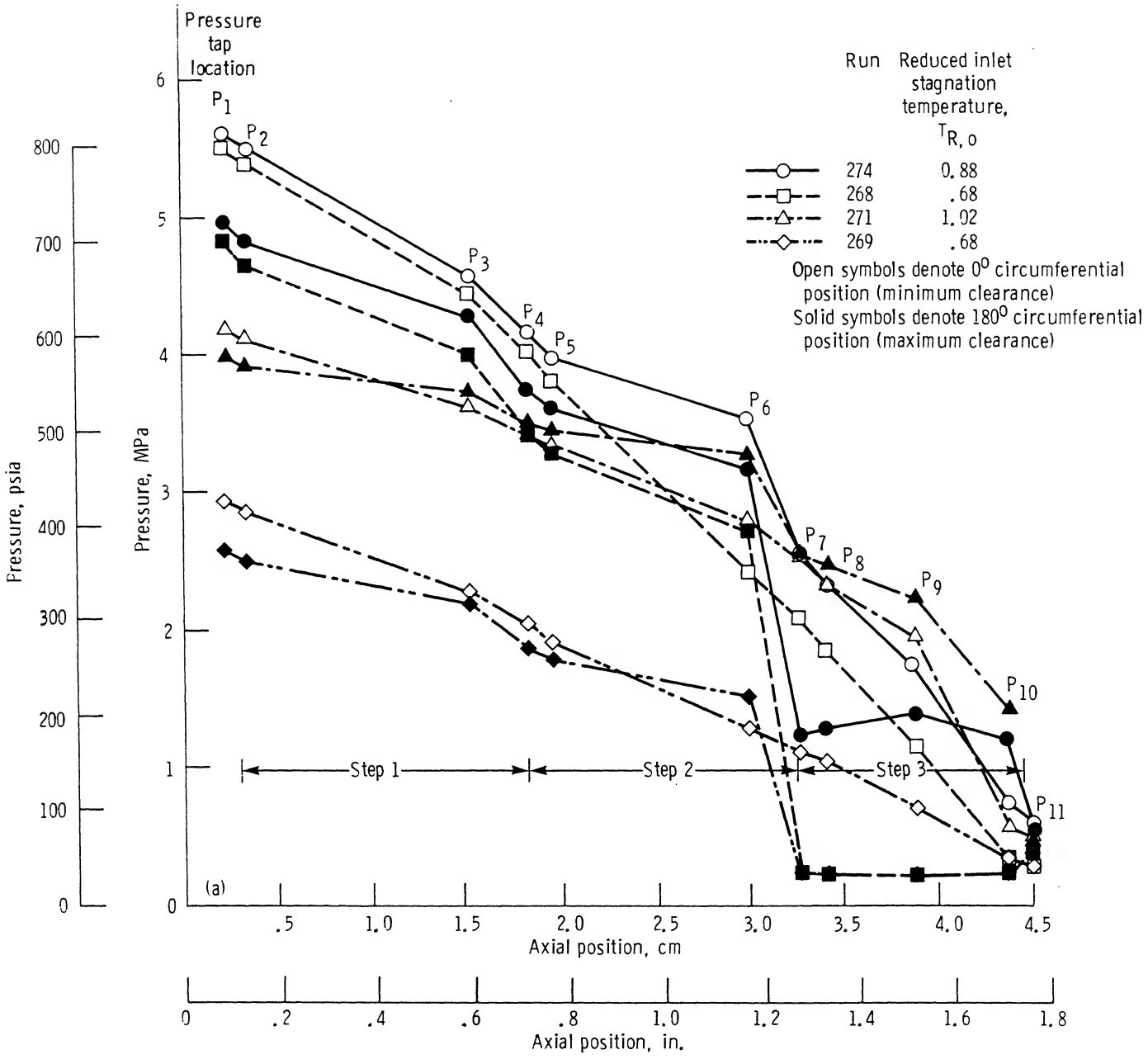

(a) Runs 268, 269, 271, 274.

Figure 22.—Axial pressure distribution of fluid nitrogen flow through three-step cylindrical seal in fully eccentric position for runs.

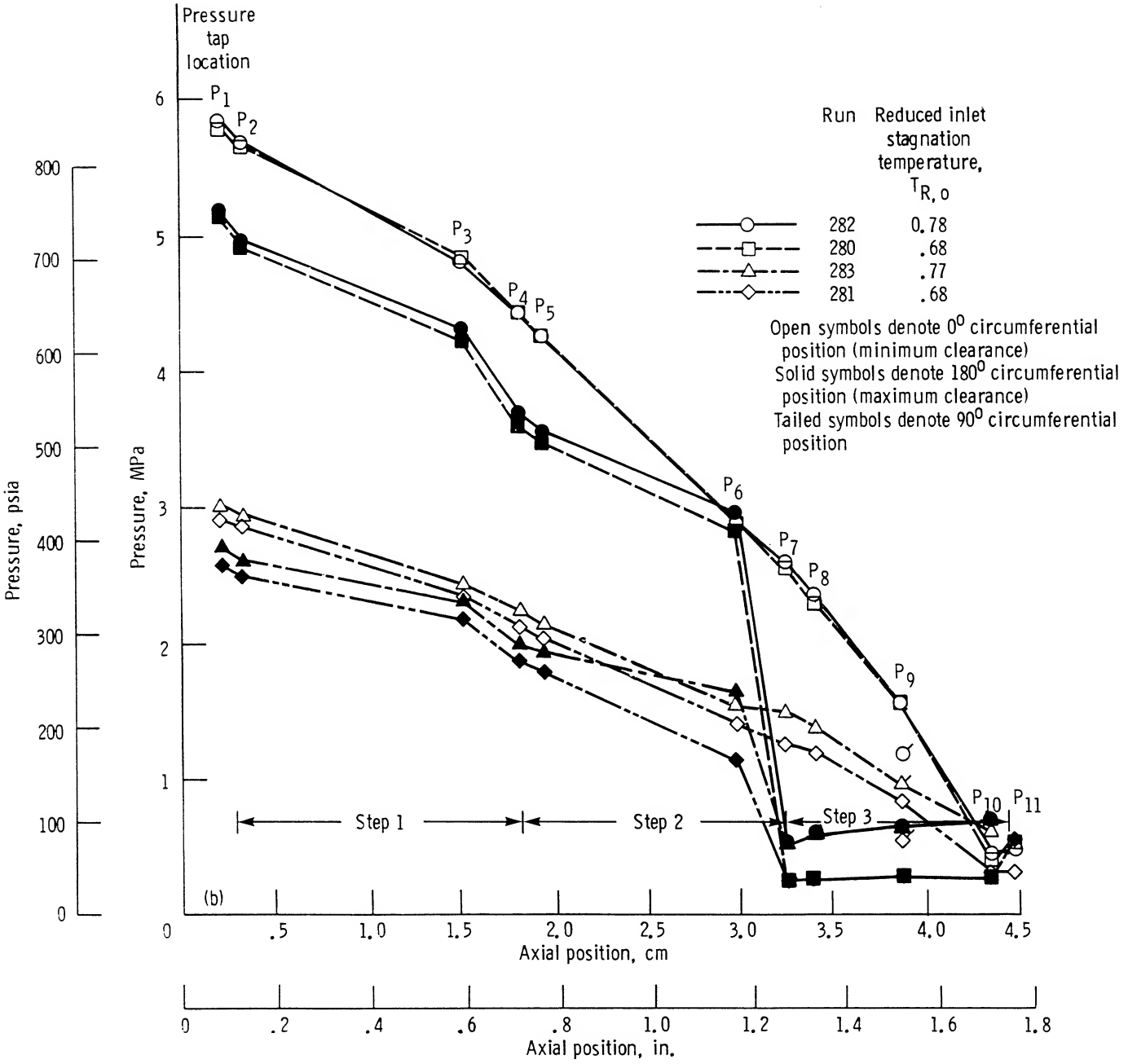

(b) Runs 280 to 283.

Figure 22.—Continued.

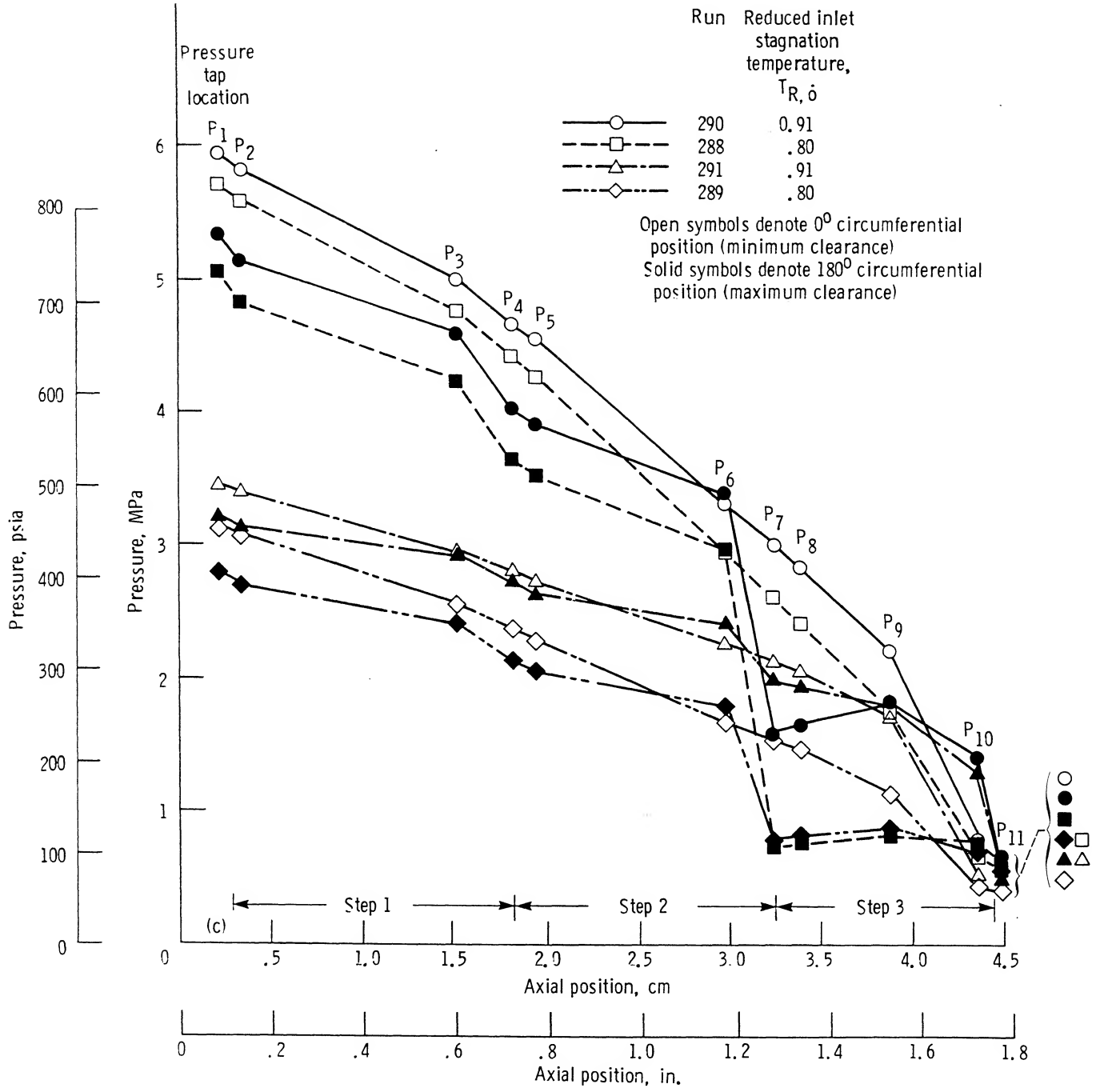

(c) Runs 288 to 291.

Figure 22.—Continued.

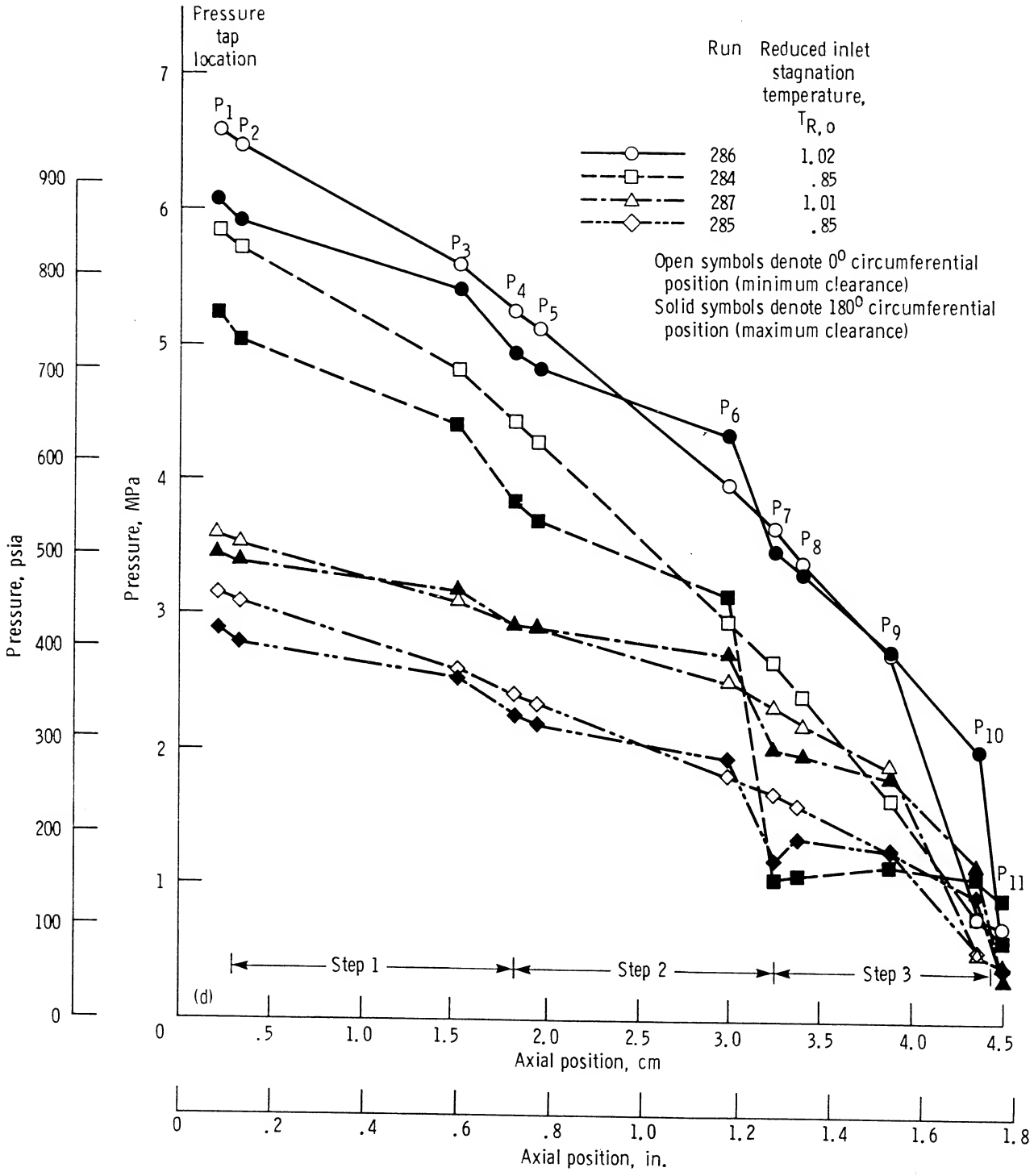

(d) Runs 284 to 287.

Figure 22.—Continued.

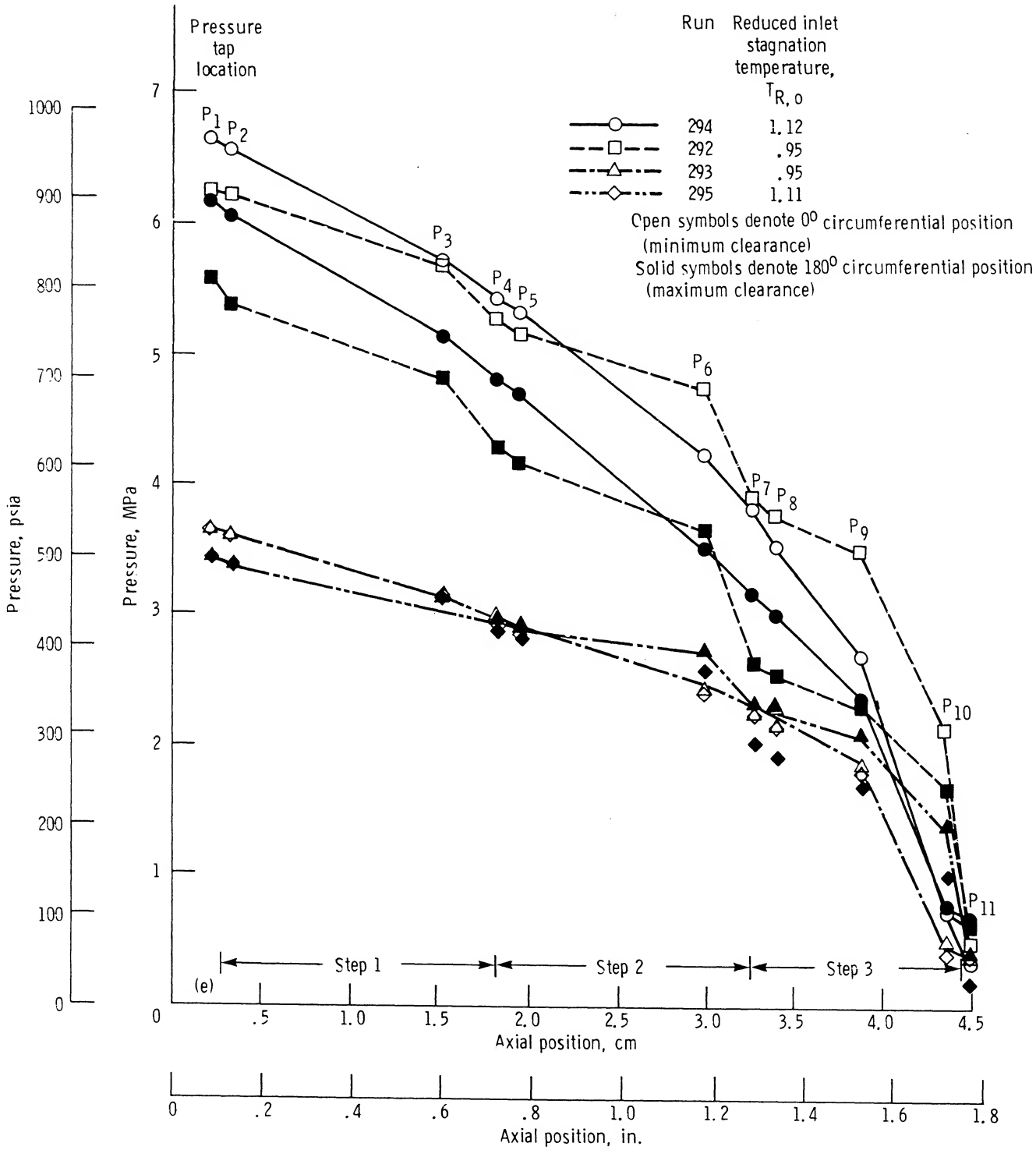

(e) Runs 292 to 295.

Figure 22.—Concluded.

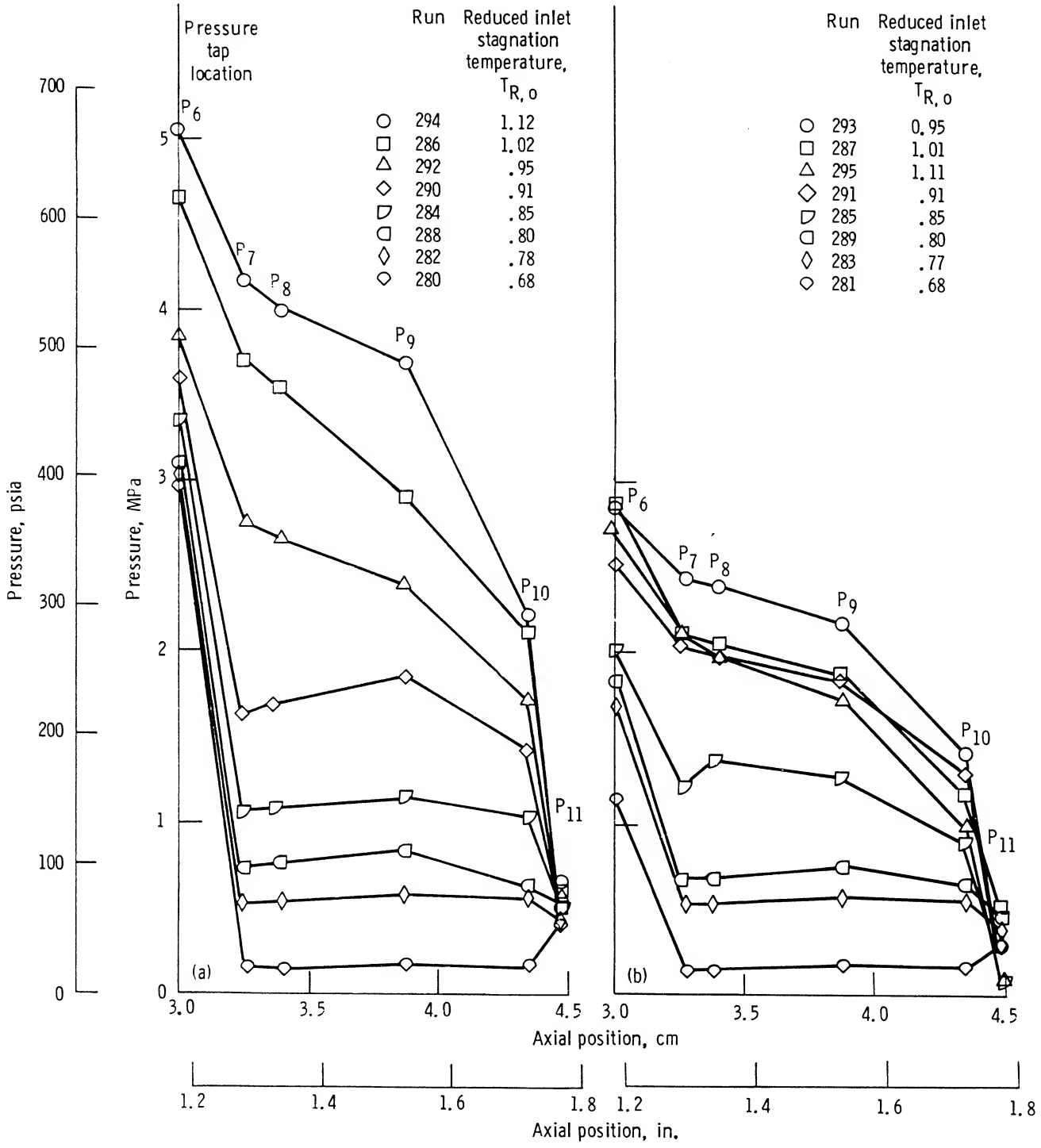

(a) High inlet pressure. (b) Low inlet pressure.

Figure 23.—Axial pressure distribution of fluid nitrogen flow through third step of three-step cylindrical seal, illustrating effect of reduced inlet pressure and temperature.

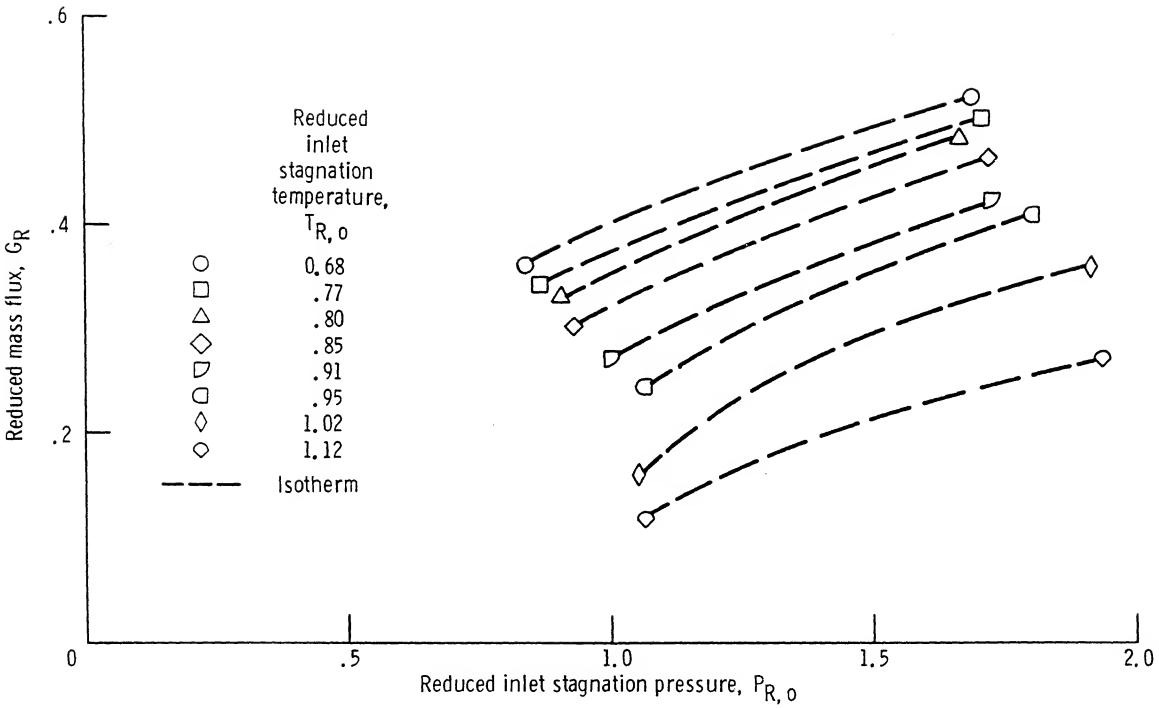

Figure 24.—Reduced mass flux of fluid nitrogen through three-step cylindrical seal in fully eccentric position, as function of reduced inlet stagnation pressure.

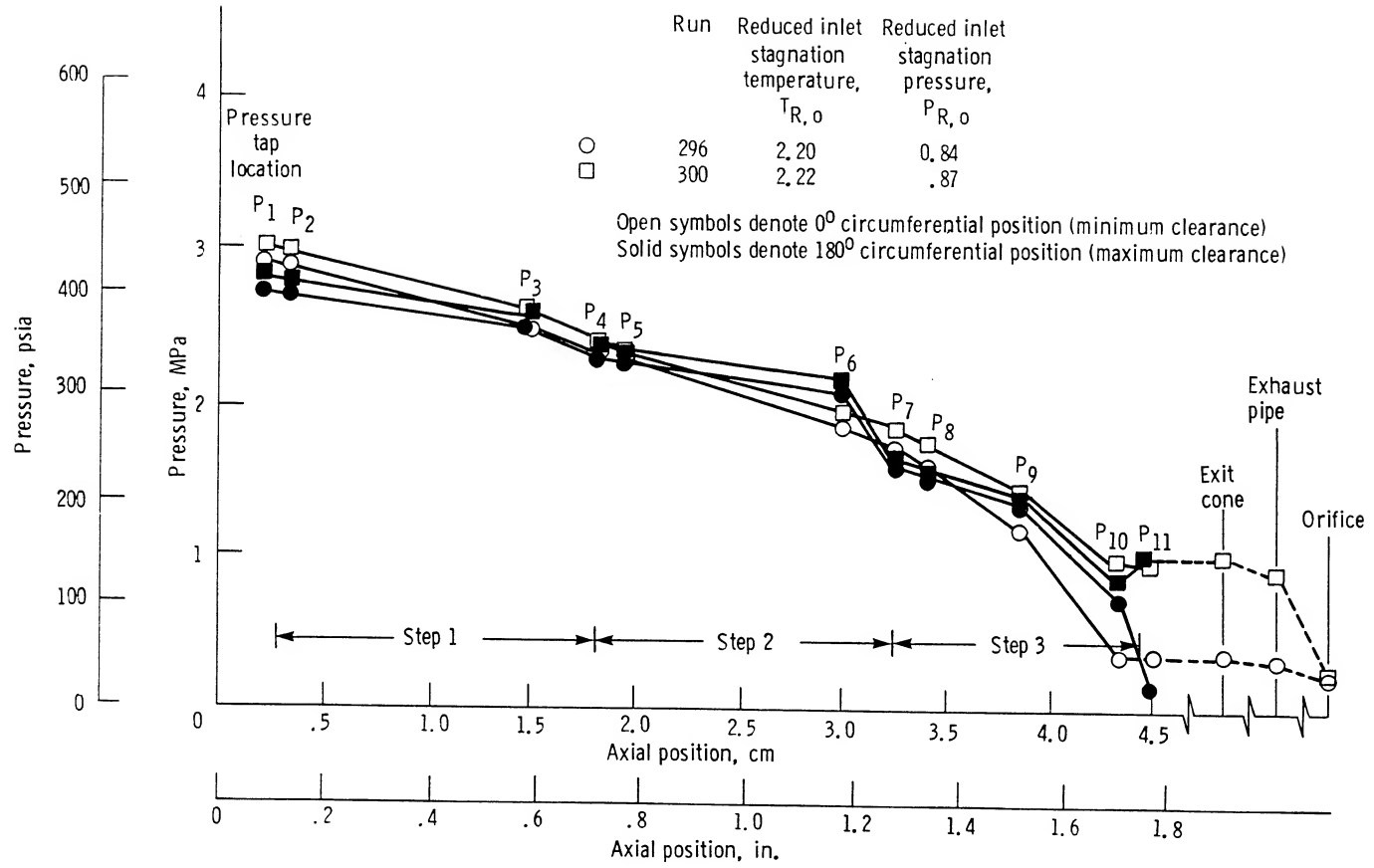

Figure 25.—Axial pressure distribution of gaseous nitrogen flow through three-step cylindrical seal in fully eccentric position with backpressure control for runs 296 and 300. Reduced mass flux, G_R, 0.056.

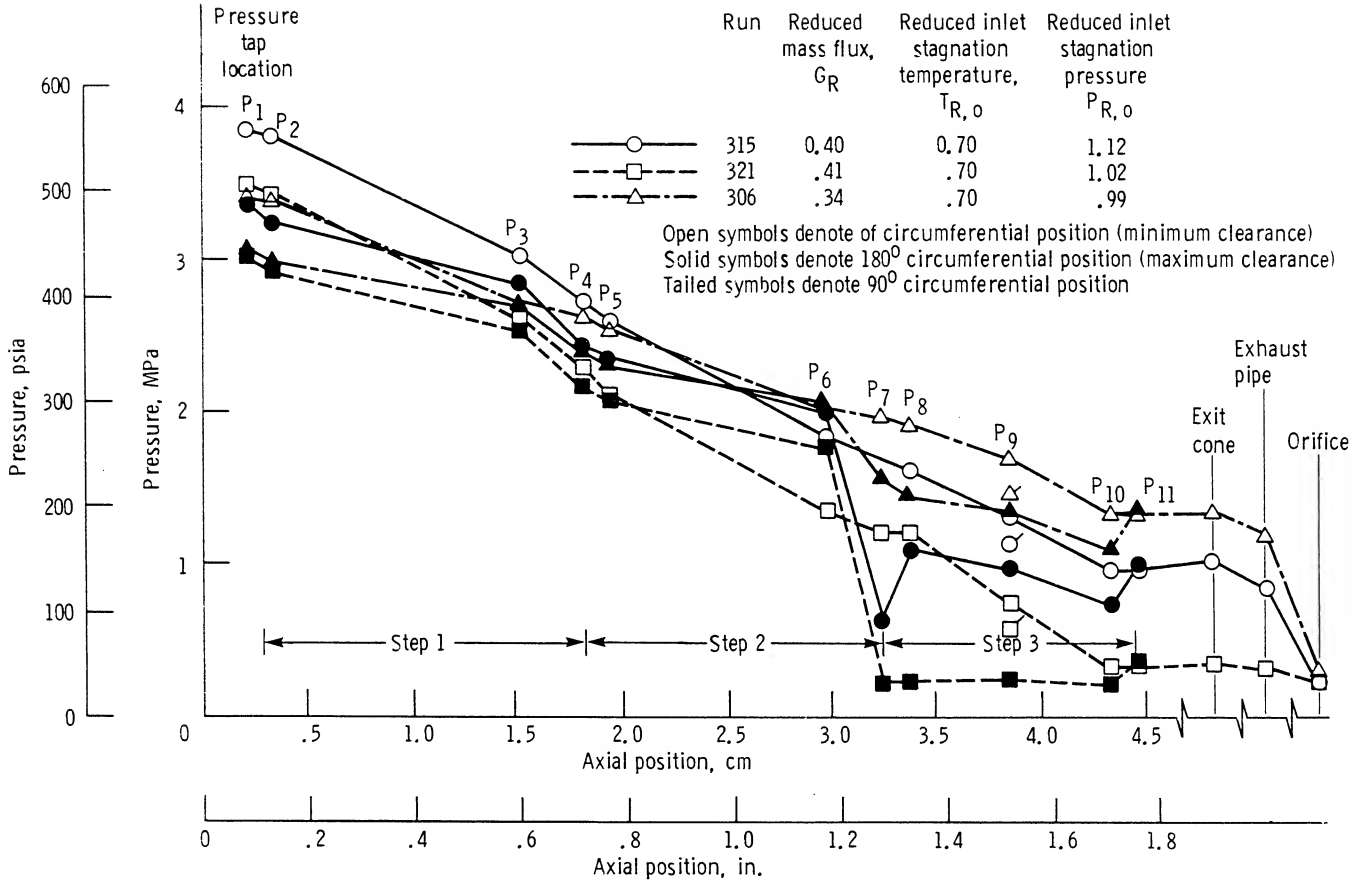

Figure 26.—Axial pressure distribution of fluid nitrogen flow through three-step cylindrical seal in fully eccentric position with backpressure control for runs 306, 315, and 321.

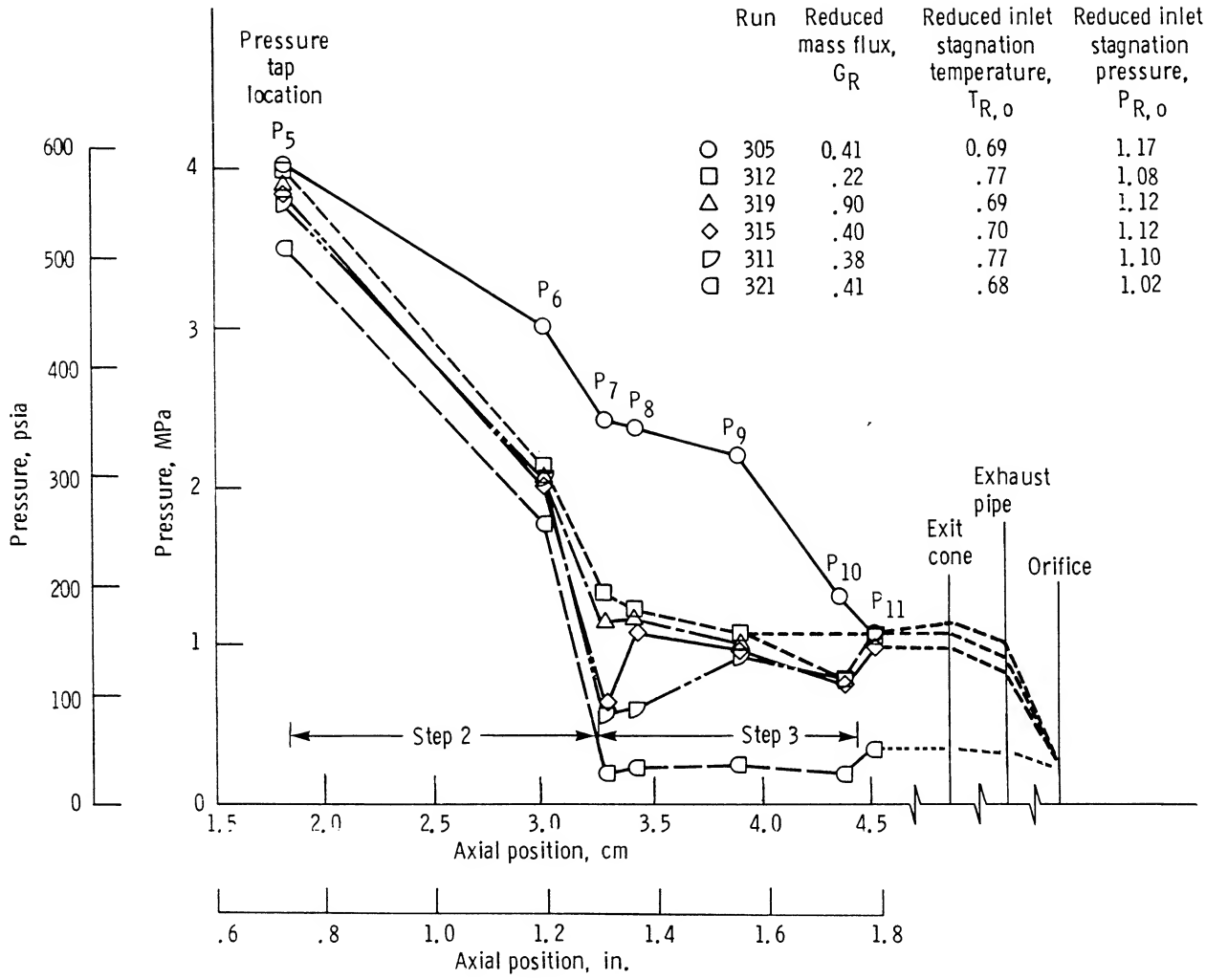

Figure 27.—Axial pressure distribution of fluid nitrogen flow through second and third steps of a three-step cylindrical seal in fully eccentric position with backpressure control (pressure profile at 180° circumferential position).

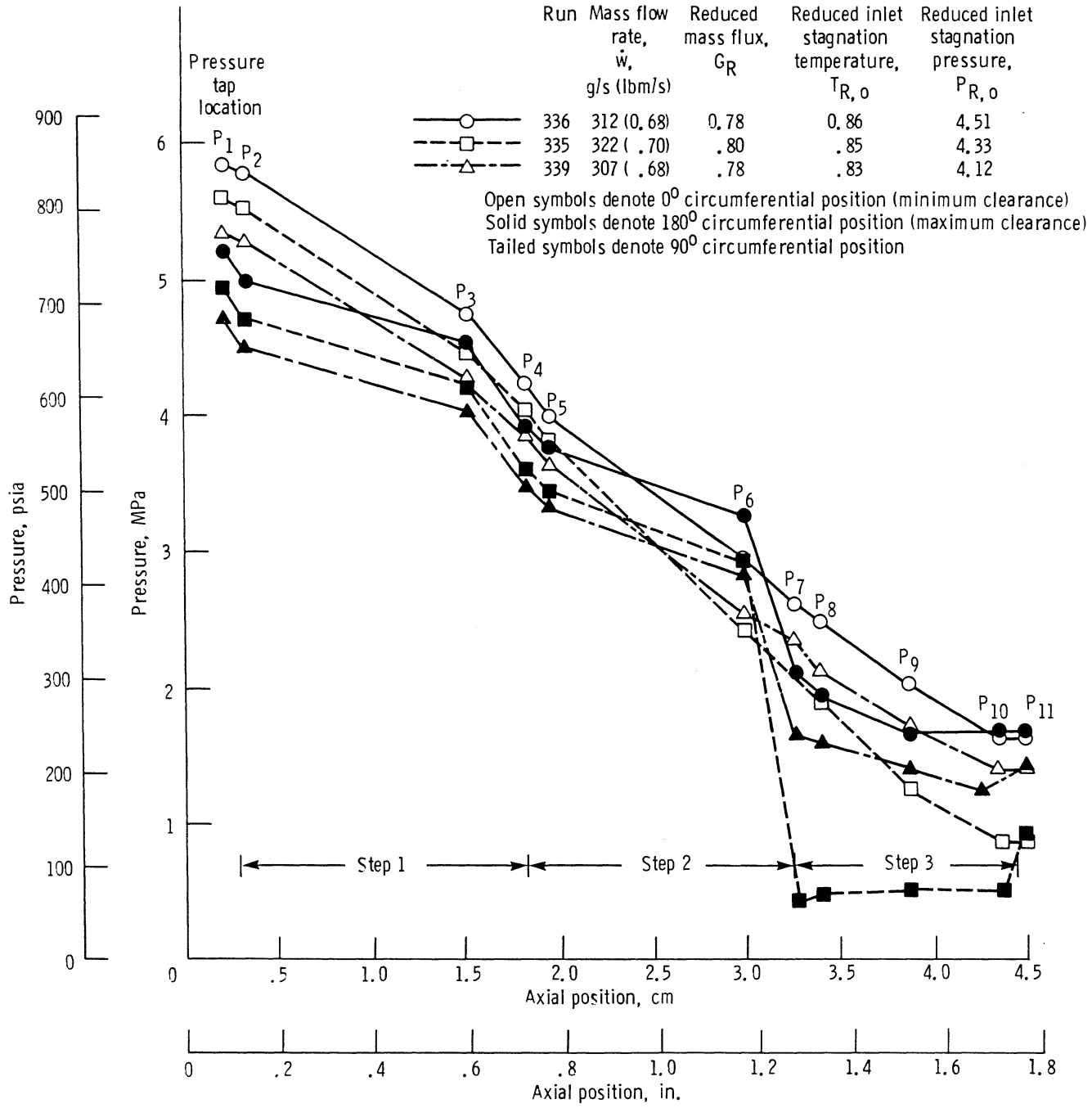

Figure 28.—Axial pressure distribution of fluid hydrogen flow through three-step cylindrical seal in fully eccentric position with backpressure control.

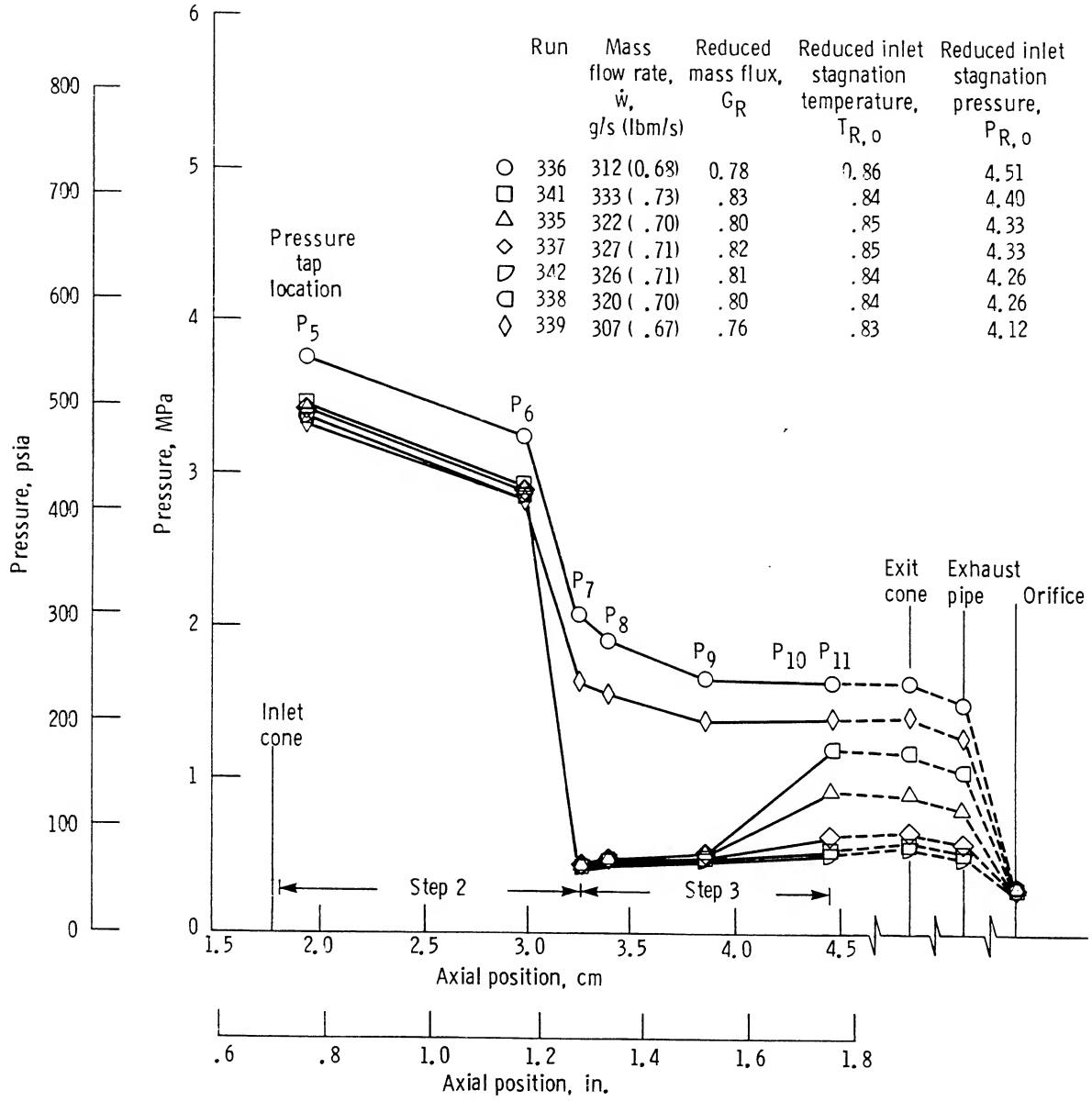

Figure 29.—Axial pressure distribution of fluid hydrogen flow through second and third steps of a three-step cylindrical seal in fully eccentric position with backpressure control (pressure profile at 180° circumferential position); runs 335 to 339, 341, and 342.

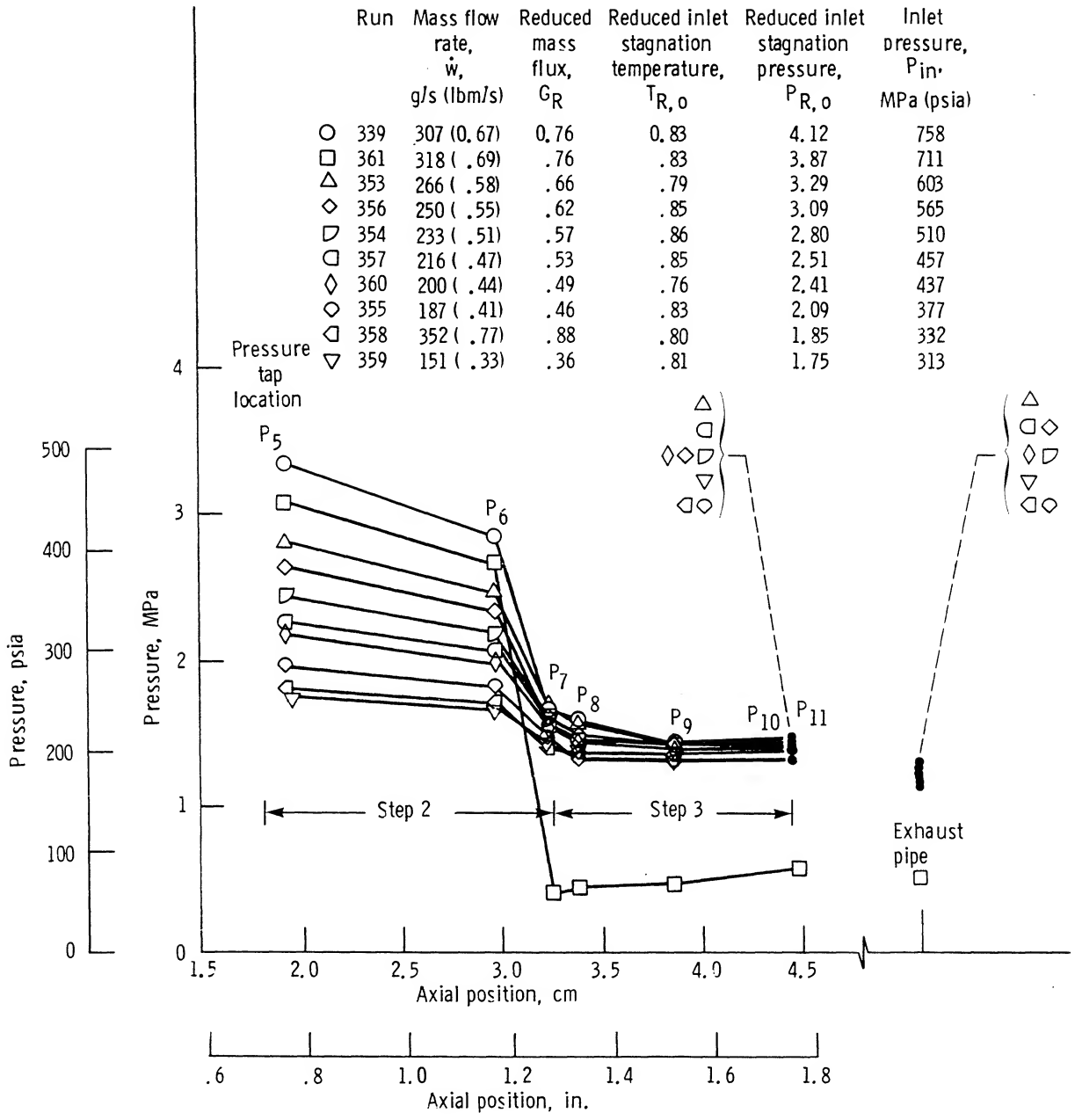

Figure 30.—Axial pressure distribution of fluid hydrogen flow through second and third step of a three-step cylindrical seal in fully eccentric position with backpressure control (pressure profile at 180° circumferential position); runs 339 and 353 to 361.

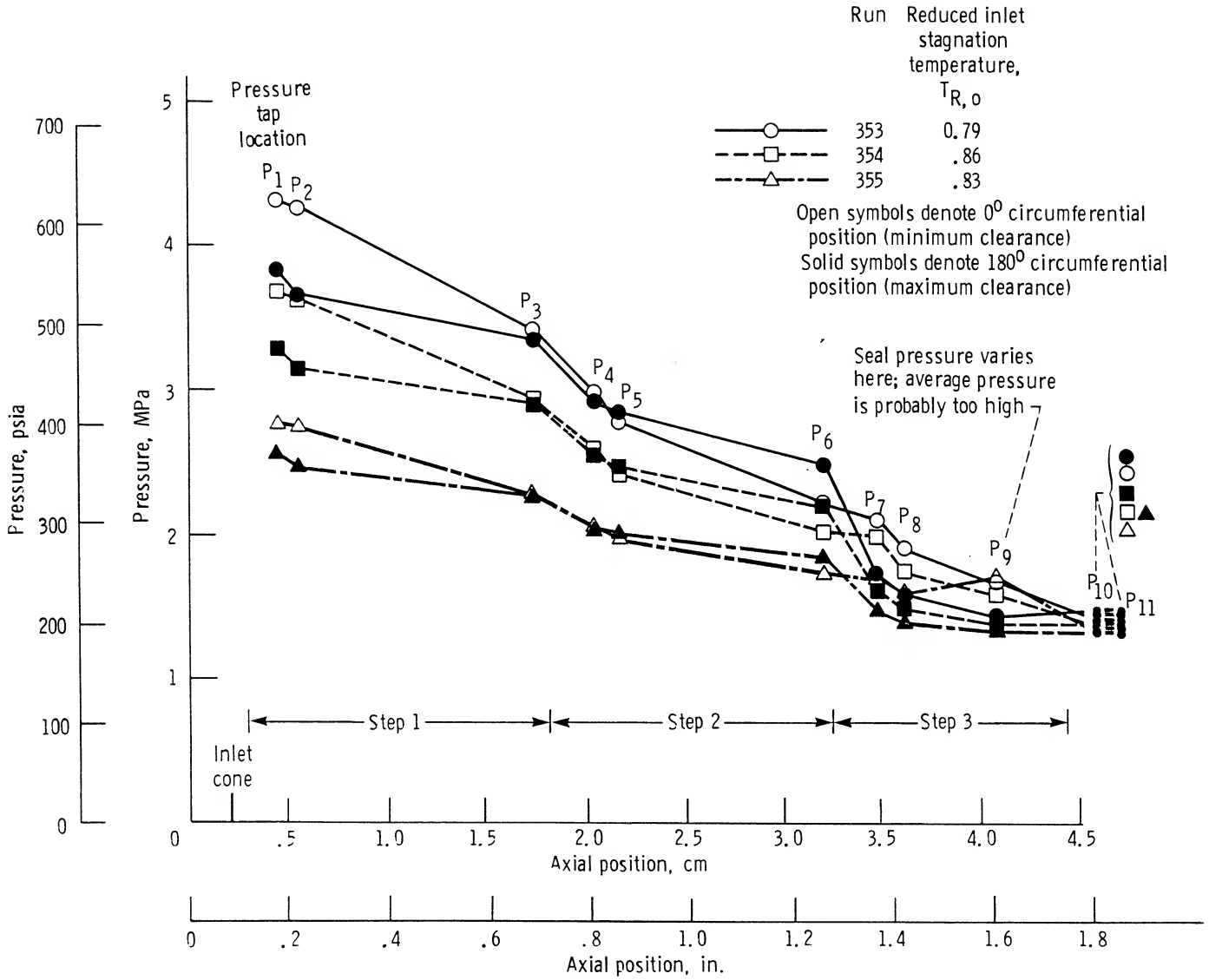

Figure 31.—Axial pressure distribution of fluid hydrogen flow through three-step cylindrical seal in fully eccentric position with backpressure control for runs .

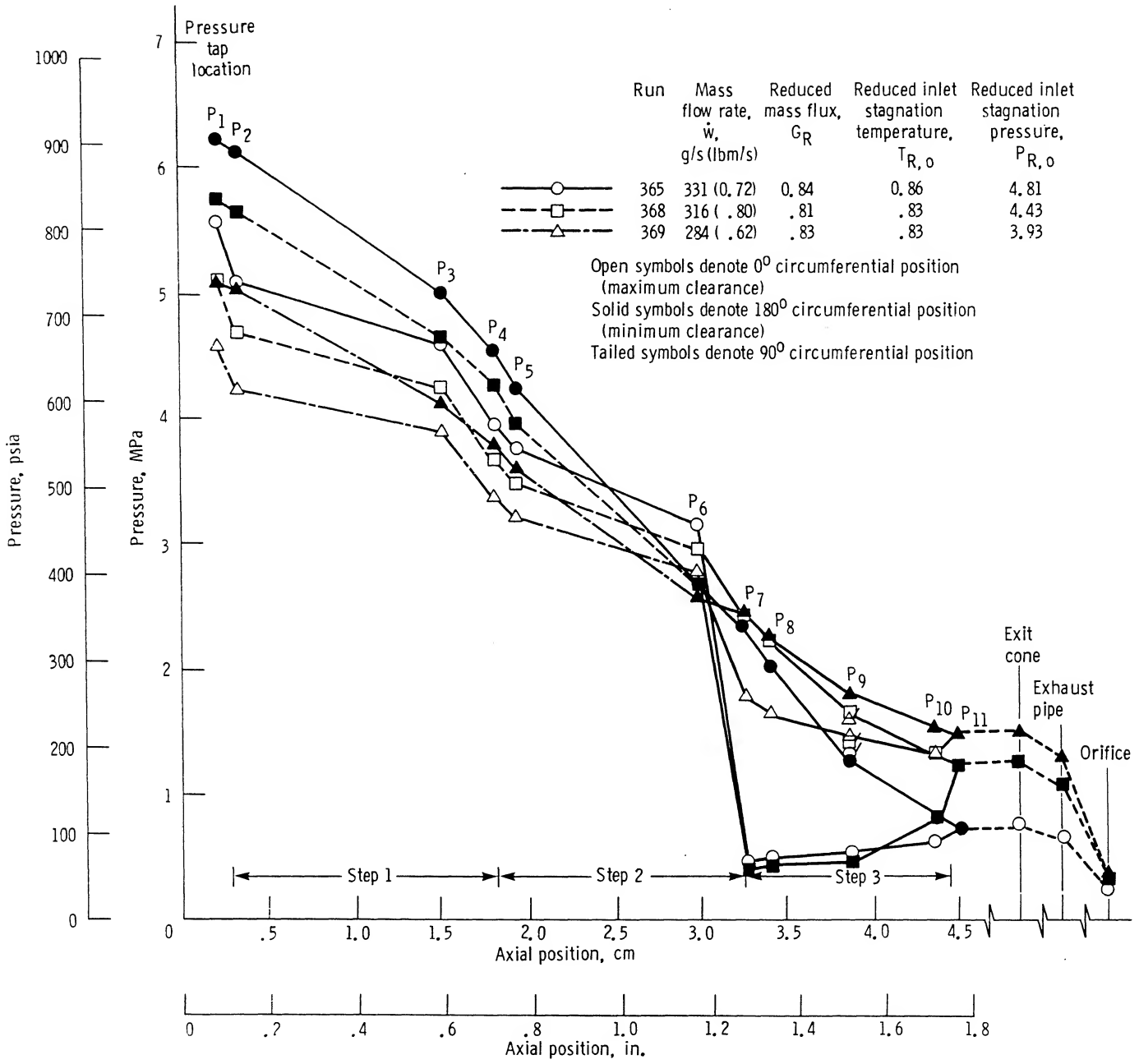

Figure 32.—Axial pressure distribution of fluid hydrogen flow through three-step cylindrical seal in fully eccentric position with backpressure control and centerbody shifted from previous figures (clearance of 0.025 cm (0.010 in.) at no clearance at 180°).

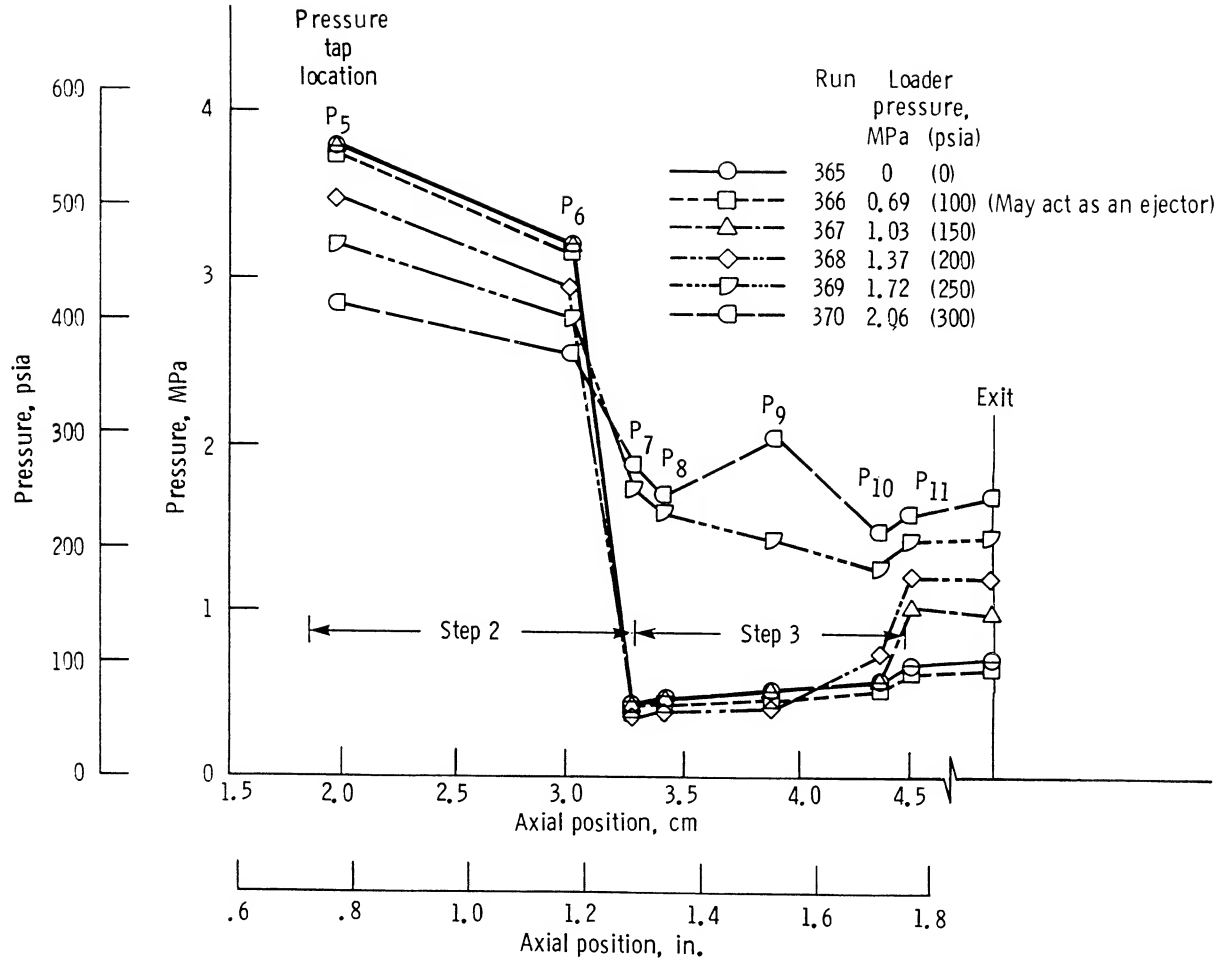

Figure 33.—Axial pressure distribution of fluid hydrogen flow through three-step cylindrical seal in fully eccentric position with backpressure control and rub point at 180° position.

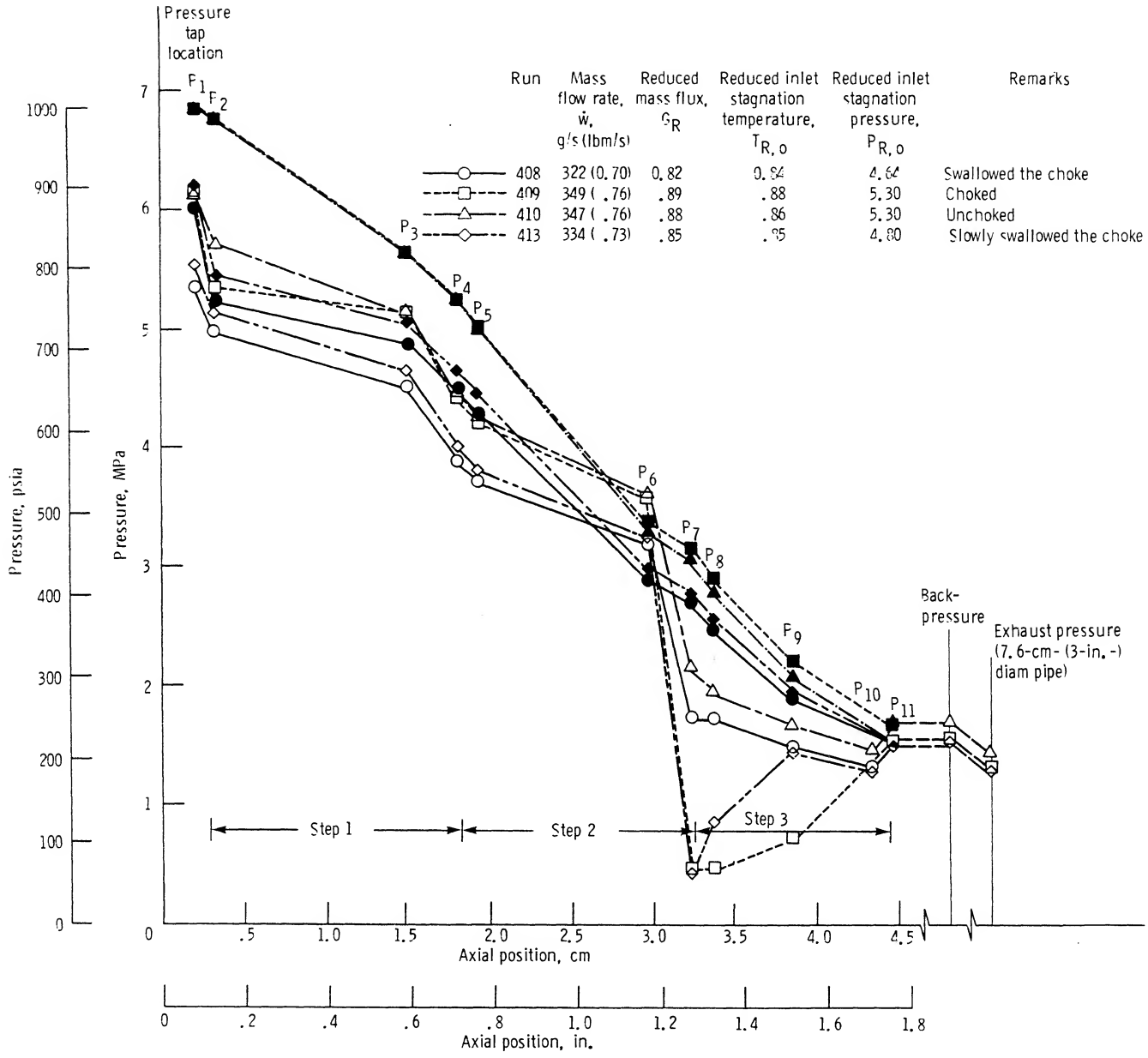

Figure 34.—Axial pressure distribution of fluid hydrogen flow through three-step cylindrical seal in fully eccentric position with backpressure control for runs 408 to 410 and 413.

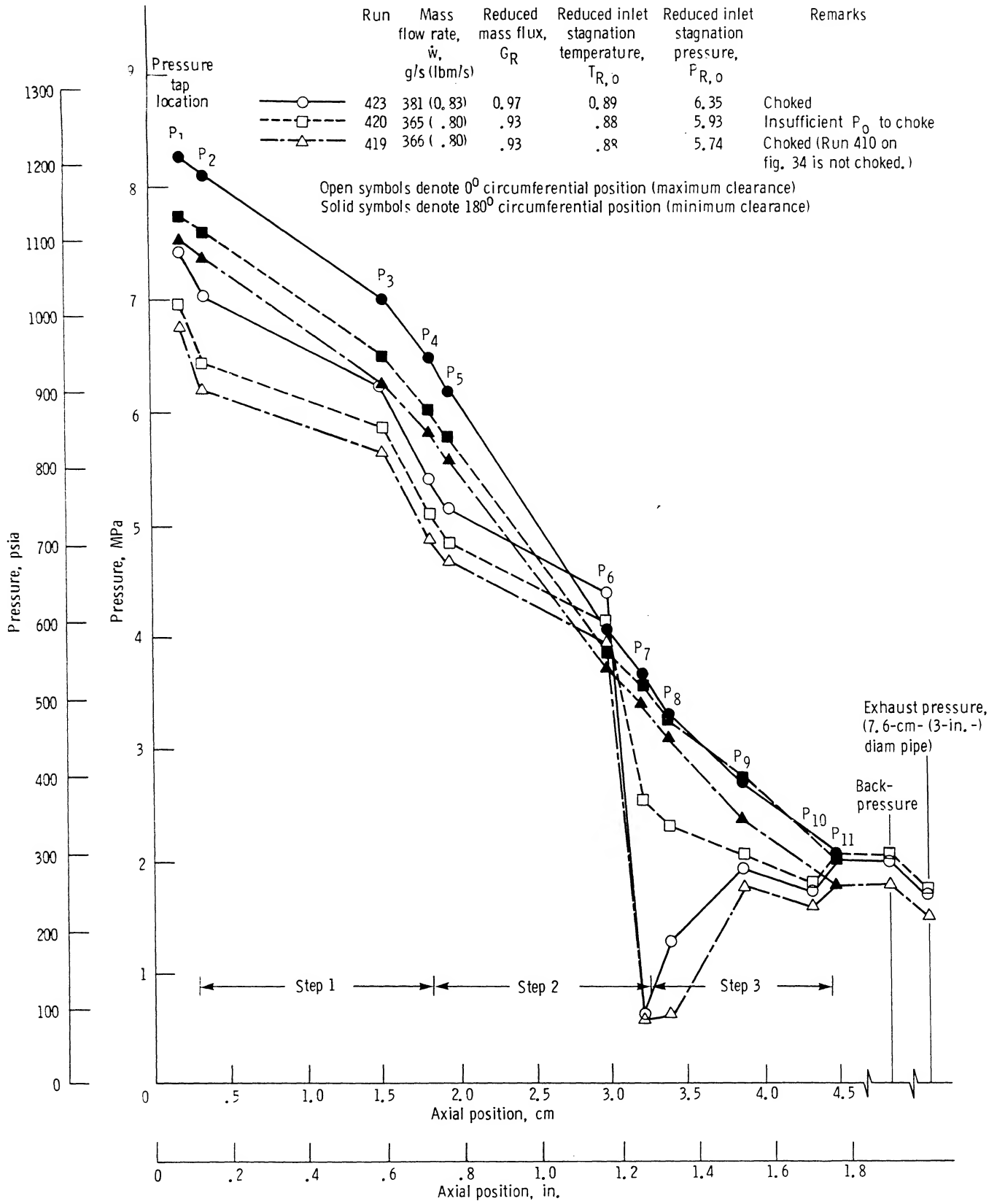

Figure 35.—Axial pressure distribution of fluid hydrogen flow through three-step cylindrical seal in fully eccentric position with backpressure control, illustrating effects of choking in third stage.

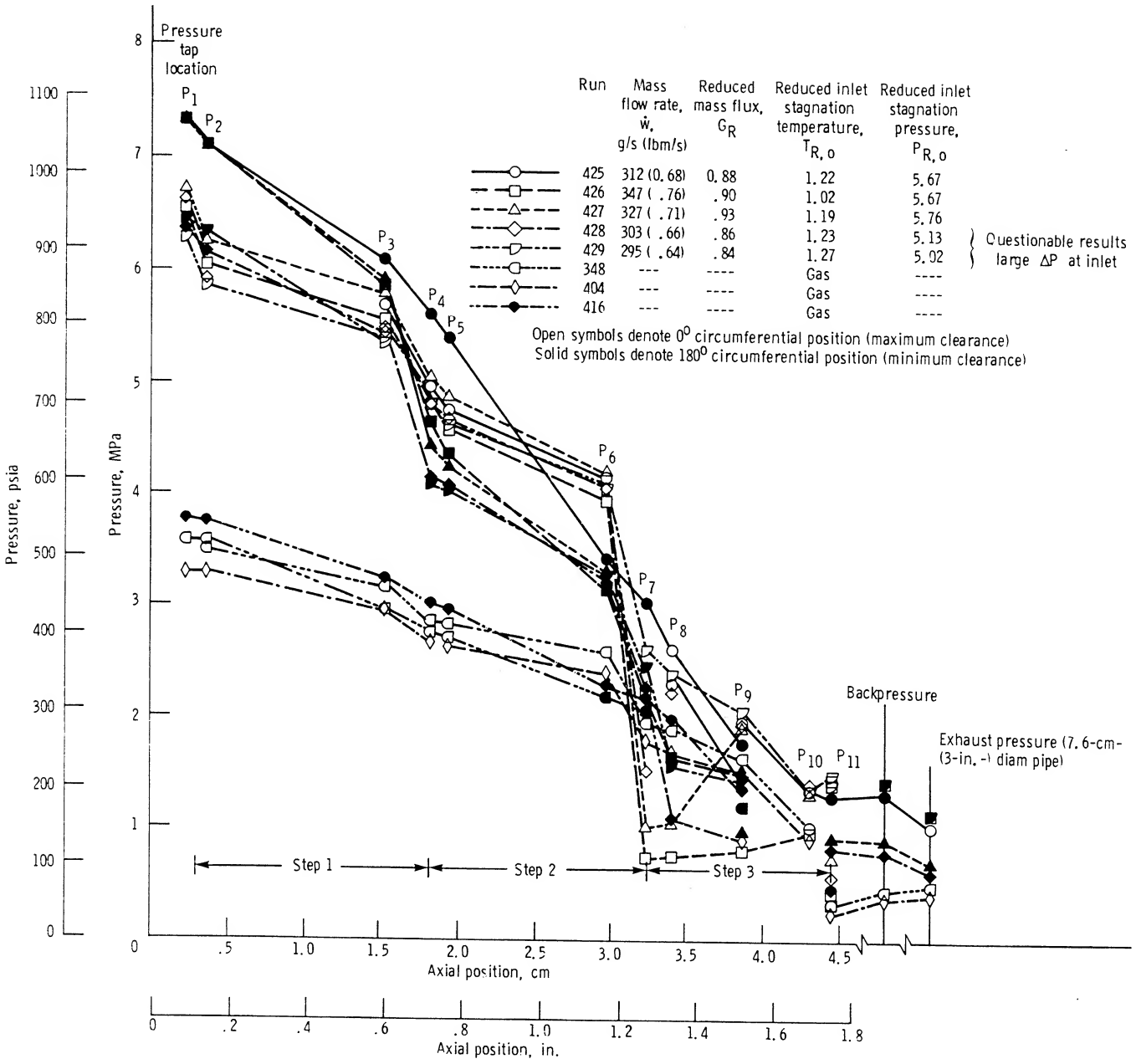

Figure 36.—Axial pressure distribution of fluid hydrogen flow through three-step cylindrical seal in fully eccentric position with backpressure control for runs 425 to 429.

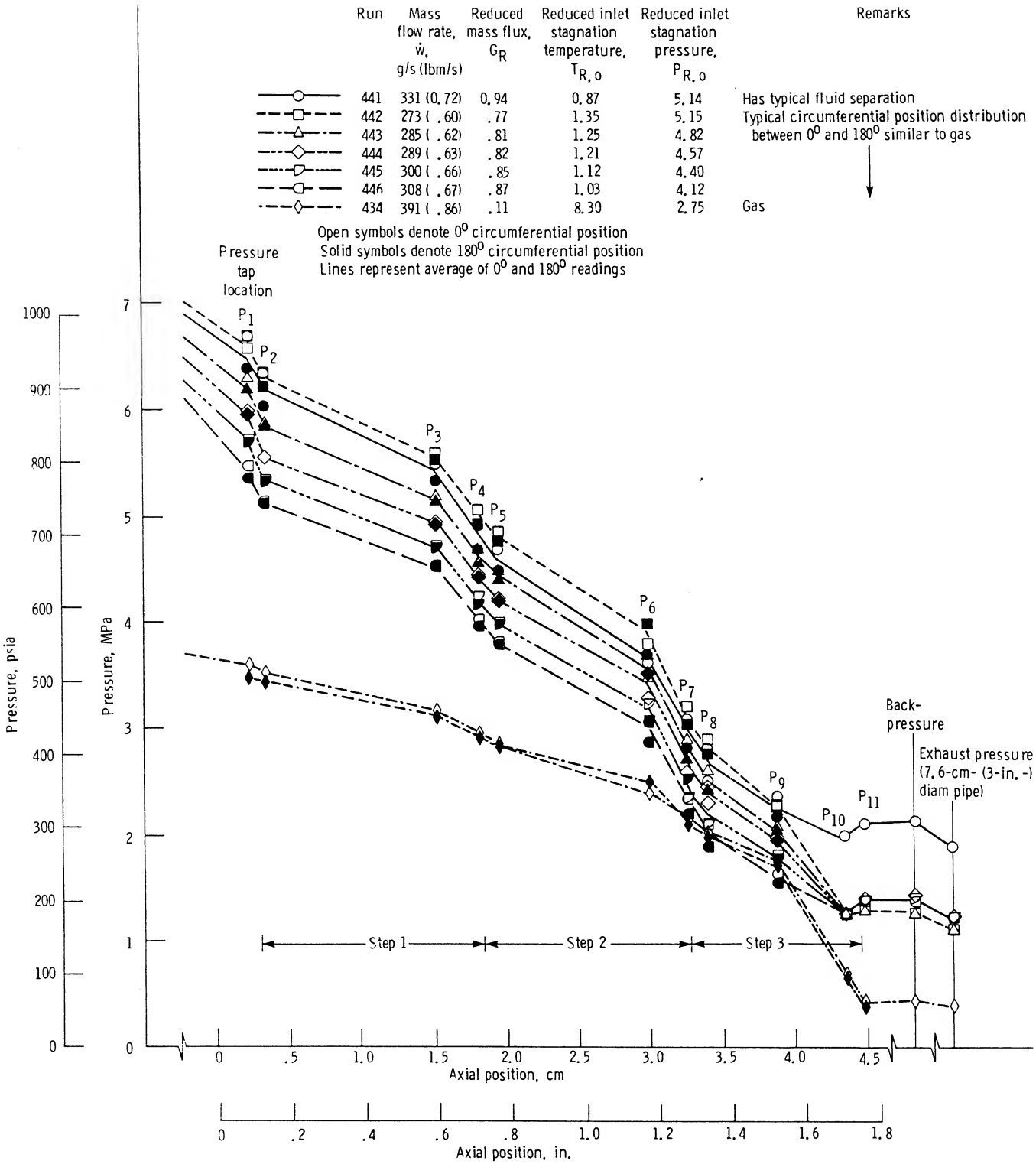

Figure 37.—Axial pressure distribution of fluid and gaseous hydrogen flow through three-step cylindrical seal in concentric position with and without backpressure control for runs 434 and 441 to 446.

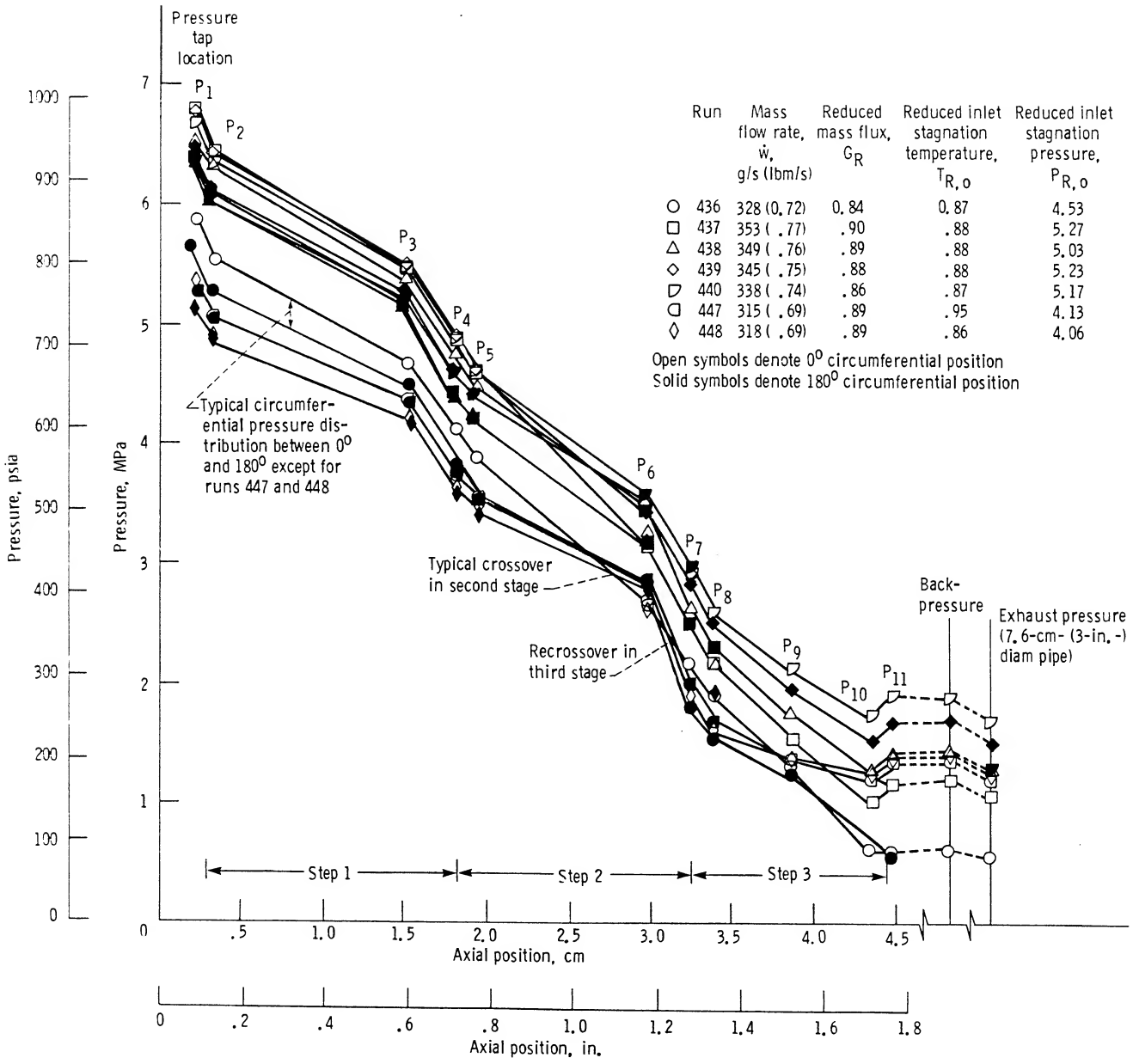

Figure 38.—Axial pressure distribution of fluid and gaseous hydrogen flow through three-step cylindrical seal in near-concentric position with and without backpressure control for runs 436 to 440, 447, and 448 (0° and 180° profiles show only for run 436).

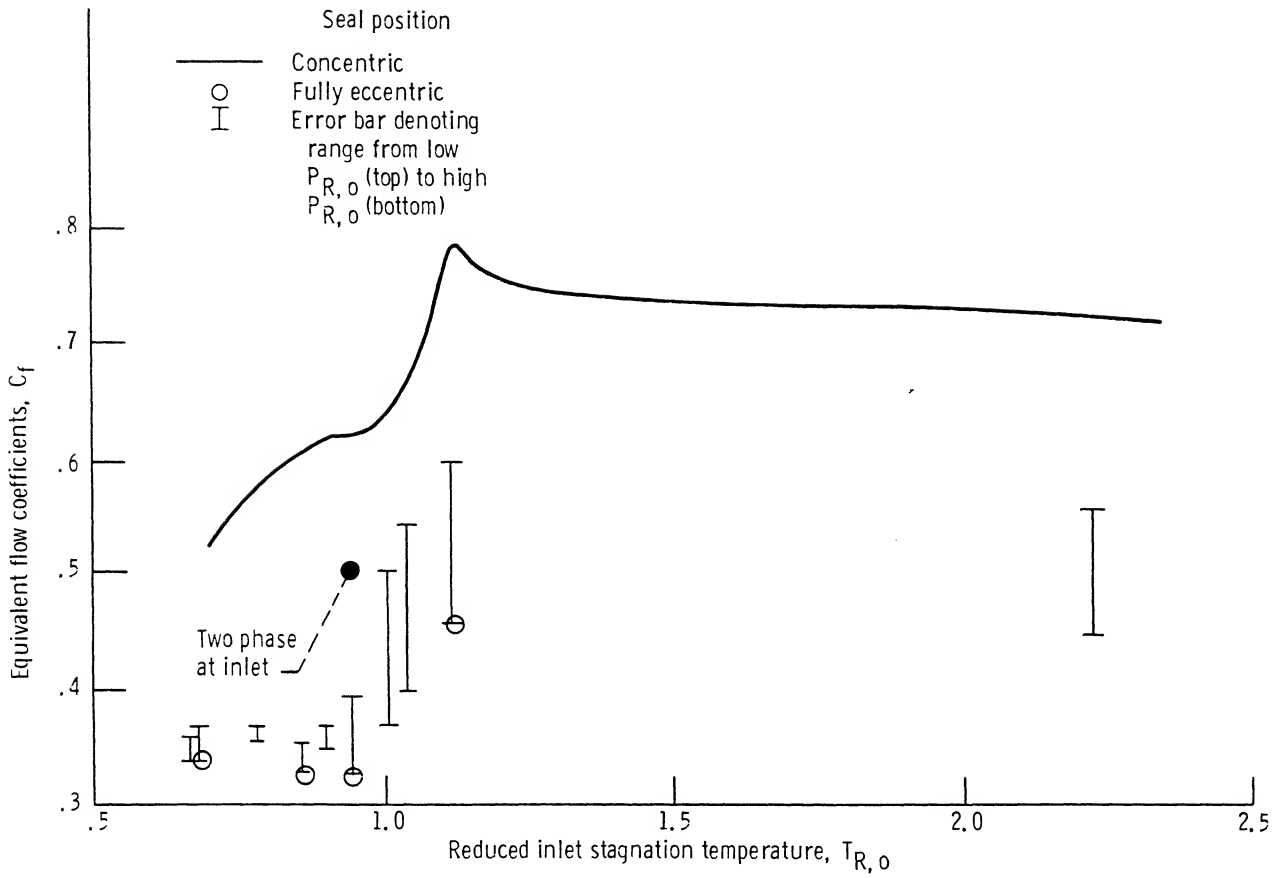

Figure 39.—Variation of flow coefficient for three-step cylindrical seal as function of reduced inlet stagnation temperature.

TABLE I.—FORMATS FOR DATA PRESENTATION AND VERIFICATION OF 180° PRESSURE JUMP PROFILE IN THIRD STEP BY INTERCHANGING OF PRESSURE TRANSDUCERS

[P_{tank} = AVD 85); T_{tank} = AVD 64 ; $\Delta P_{venturi}$ = AVD 88 − AVD 87 or AVD 76 ; T_{in} = AVD 65 .]

(a) Standard output

	Location of data set as presented in first row of each grouping in tables II, III, and V																	
	1	2	3	4	5	6	7	8	9	10	11	12	13	14	15	16	17	18
Data set parameter	Run	$\dot{w}$	P_o	T_o	P_0	$P_{1,1}$	$P_{2,1}$	$P_{3,1}$	$P_{4,1}$	$P_{5,1}$	$P_{6,1}$	$P_{7,1}$	$P_{8,1}$	$P_{9,1}$	$P_{90°}$	$P_{10,1}$	$P_{11,1}$	P_B
Data set name in data reduction program	IRDG	OUT (3) or OUT (1)	OUT (5)	OUT (4)	OUT (22)	OUT (6)	OUT (7)	OUT (8)	OUT (9)	OUT (10)	OUT (11)	OUT (12)	OUT (13)	OUTT (91)	OUTT (94)	OUTT (92)	OUTT (93)	OUT (23)
CADDE data system AVD number[a]	----	-----	86	47	89	30	31	32	33	34	35	36	37	91	94	92	93	90
	Location of data set as presented in second row of each grouping in tables II, III, and V																	
	(b)	(b)	(b)	(b)	(b)	19	20	21	22	23	24	25	26	27	28	29	30	(b)
Data set parameter	----	-----	----	----	----	$P_{1,2}$	$P_{2,2}$	$P_{3,2}$	$P_{4,2}$	$P_{5,2}$	$P_{6,2}$	$P_{7,2}$	$P_{8,2}$	$P_{9,2}$	$P_{270°}$	$P_{10,2}$	$P_{11,2}$	----
Data set name in data reduction program	----	-----	----	----	----	OUT (14)	OUT (15)	OUT (16)	OUT (17)	OUT (18)	OUT (19)	OUT (20)	OUT (21)	OUTT (95)	----	OUTT (96)	OUTT (97)	----
CADDE data system AVD number[a]	----	-----	----	----	----	38	39	40	41	42	43	44	45	95	----	96	97	----

(b) Modification 1 (runs 257 to 265)

	Location of data set as presented in first row of each grouping in tables II, III, and V																	
	1	2	3	4	5	6	7	8	9	10	11	12	13	14	15	16	17	18
Data set parameter	Run	$\dot{w}$	P_o	T_o	P_0	$P_{1,1}$	$P_{2,1}$	$P_{3,1}$	$P_{4,1}$	$P_{5,1}$	$P_{6,1}$	$P_{7,1}$	$P_{8,1}$	$P_{9,1}$	$P_{90°}$	$P_{10,1}$	$P_{11,1}$	P_B
Data set name in data reduction program	IRDG	OUT (3) or OUT (1)	OUT (5)	OUT (4)	OUT (22)	**OUT (12)[c]**	**OUT (13)**	**OUTT (91)**	OUT (9)	OUT (10)	OUT (11)	**OUT (6)**	**OUT (7)**	**OUT (8)**	OUT (94)	OUT (92)	OUT (93)	OUT (23)
CADDE data system AVD number[a]	----	-----	----	----	89	**36**	**37**	**91**	33	34	35	**30**	**31**	**32**	94	92	93	90
	Location of data set as presented in second row of each grouping in tables II, III, and V																	
	(b)	(b)	(b)	(b)	(b)	19	20	21	22	23	24	25	26	27	28	29	30	(b)
Data set parameter	----	-----	----	----	----	$P_{1,2}$	$P_{2,2}$	$P_{3,2}$	$P_{4,2}$	$P_{5,2}$	$P_{6,2}$	$P_{7,2}$	$P_{8,2}$	$P_{9,2}$	$P_{270°}$	$P_{10,2}$	$P_{11,2}$	----
Data set name in data reduction program	----	-----	----	----	----	**OUT (20)**	**OUT (21)**	**OUTT (95)**	OUT (17)	OUT (18)	OUT (19)	**OUT (14)**	**OUT (15)**	**OUT (16)**	----	OUTT (96)	OUTT (97)	----
CADDE data system AVD number[a]	----	-----	----	----	----	**44**	**45**	**95**	41	42	43	**38**	**39**	**40**	----	96	97	----

(c) Modification 2 (runs 276 to 295)

	Location of data set as presented in tables II, III, and V																	
	1	2	3	4	5	6	7	8	9	10	11	12	13	14	15	16	17	18
Data set parameter	Run	$\dot{w}$	P_o	T_o	P_0	$P_{1,1}$	$P_{2,1}$	$P_{3,1}$	$P_{4,1}$	$P_{5,1}$	$P_{6,1}$	$P_{7,1}$	$P_{8,1}$	$P_{9,1}$	$P_{90°}$	$P_{10,1}$	$P_{11,1}$	P_B
Data set name in data reduction program	IRDG	OUT (3) or OUT (1)	OUT (5)	OUT (4)	OUT (22)	OUT (12)	OUT (13)	OUTT (91)	**OUTT (92)[c]**	OUT (10)	OUT (11)	OUT (6)	OUT (7)	OUT (8)	OUTT (94)	**OUT (9)**	OUTT (93)	OUT (23)
CADDE data system AVD number[a]	----	-----	----	----	89	36	37	91	**92**	34	35	30	31	32	(94)	**(33)**	93	90
	Location of data set as presented in tables II, III, and V																	
	(b)	(b)	(b)	(b)	(b)	19	20	21	22	23	24	25	26	27	28	29	30	(b)
Data set parameter	----	-----	----	----	----	$P_{1,2}$	$P_{2,2}$	$P_{3,2}$	$P_{4,2}$	$P_{5,2}$	$P_{6,2}$	$P_{7,2}$	$P_{8,2}$	$P_{9,2}$	$P_{270°}$	$P_{10,2}$	$P_{11,2}$	----
Data set name in data reduction program	----	-----	----	----	----	OUT (20)	OUT (21)	OUTT (95)	**OUTT (96)**	OUT (18)	OUT (19)	OUT (14)	OUT (15)	OUT (16)	----	**OUT 17**	OUTT (97)	----
CADDE data system AVD number[a]	----	-----	----	----	----	44	45	95	**96**	42	43	38	39	40	----	**41**	97	----

[a]AVD—automatic voltage divider; CADDE—central automatic digital data encoder
[b]Not applicable
[c]Bolding denotes differences in the modification from previous part

TABLE II.—FLOW RATE AND PRESSURE DROP DATA FOR THREE-STEP CYLINDRICAL SEAL, CONCENTRIC POSITION

[Where two values are given, the top value is for 0° circumferential position and the bottom value is for 180° circumferential position; nominal clearance, 0.0125 cm (0.005 in.).]

(a) Fluid nitrogen

Run	$\dot{W}$, g/s	P_o, MPa	T_o, K	P_0, MPa	Pressure at pressure tap locations 1 to 11, MPa												P_B, MPa
					P_1	P_2	P_3	P_4	P_5	P_6	P_7	P_8	P_9	P_{9_f} (90°)	P_{10}	P_{11}	
10	174.	4.51	294.9	4.44	4.36	4.26	3.81	3.56	3.43	2.78	2.51	2.33	0.68	1.88	0.66	0.17	0.13
					4.16	4.08	3.76	3.48	3.39	3.05	2.42	2.33	2.03		1.09	0.13	
11	241.	6.18	296.0	6.09	6.05	5.90	5.32	4.97	4.78	3.82	3.44	3.16	0.88	2.51	0.91	0.23	0.15
					5.77	5.63	5.20	4.81	4.69	4.18	3.33	3.19	2.75		1.52	0.18	
12	94.	2.51	282.9	2.46	2.41	2.36	2.10	1.97	1.90	1.57	1.42	1.34	0.43	1.09	0.35	0.12	0.11
					2.30	2.26	2.08	1.92	1.88	1.70	1.34	1.30	1.14		0.59	0.08	
13	223.	5.61	291.2	5.53	5.44	5.31	4.77	4.45	4.29	3.44	3.10	2.87	2.12	2.29	0.83	0.21	0.15
					5.20	5.08	4.68	4.34	4.24	3.78	3.00	2.88	2.50		1.37	0.17	
14	154.	3.89	277.9	3.84	3.76	3.68	3.30	3.08	2.97	2.43	2.20	2.06	1.56	1.66	0.56	0.16	0.12
					3.59	3.53	3.26	3.01	2.94	2.65	2.11	2.03	1.77		0.94	0.11	
15	64.	1.74	277.1	1.71	1.66	1.64	1.46	1.37	1.32	1.11	1.01	0.96	0.76	0.80	0.22	0.11	0.11
					1.59	1.57	1.44	1.33	1.30	1.19	0.94	0.92	0.80		0.41	0.08	
16	96.	2.56	289.2	2.53	2.46	2.42	2.16	2.02	1.95	1.61	1.47	1.40	1.10	1.14	0.36	0.27	0.28
					2.36	2.32	2.14	1.98	1.94	1.74	1.41	1.33	1.16		0.61	0.16	
17	191.	4.83	288.6	4.77	4.69	4.58	4.11	3.85	3.70	3.01	2.74	2.56	1.95	2.05	0.71	0.48	0.48
					4.49	4.40	4.05	3.76	3.64	3.28	2.65	2.47	2.16		1.17	0.25	
44	276.	6.47	265.8	6.37	6.31	6.15	5.57	5.23	5.03	4.08	3.69	3.42	2.77	2.69	0.99	0.66	0.65
					6.05	5.87	5.45	5.05	4.92	4.39	3.55	3.31	2.89		1.44	0.37	
45	243.	5.65	260.7	5.57	5.48	5.35	4.85	4.56	4.39	3.59	3.27	3.04	2.48	2.41	0.87	0.57	0.57
					5.26	5.12	4.76	4.41	4.29	3.85	3.13	2.92	2.56		1.31	0.32	
46	196.	4.56	255.0	4.49	4.41	4.31	3.89	3.67	3.53	2.92	2.67	2.50	2.06	2.00	0.70	0.46	0.47
					4.23	4.13	3.84	3.56	3.46	3.12	2.54	2.37	2.08		1.11	0.26	
47	193.	4.59	261.9	4.52	4.45	4.35	3.93	3.70	3.57	2.95	2.70	2.53	2.07	2.03	0.70	0.46	0.46
					4.26	4.16	3.87	3.59	3.50	3.15	2.57	2.40	2.11		1.13	0.25	
48	155.	3.70	258.3	3.64	3.58	3.50	3.15	2.97	2.86	2.37	2.18	2.05	1.69	1.65	0.56	0.37	0.39
					3.42	3.35	3.11	2.88	2.80	2.54	2.07	1.93	1.70		0.93	0.21	
49	105.	2.61	261.4	2.56	2.51	2.47	2.21	2.08	2.01	1.68	1.54	1.47	1.20	1.19	0.38	0.28	0.30
					2.40	2.36	2.18	2.02	1.97	1.79	1.46	1.37	1.21		0.69	0.17	
50	104.	2.61	265.2	2.57	2.51	2.47	2.21	2.09	2.01	1.69	1.55	1.47	1.21	1.19	0.38	0.28	0.29
					2.40	2.36	2.19	2.03	1.97	1.80	1.46	1.38	1.21		0.69	0.17	
51	74.	1.91	258.3	1.87	1.82	1.80	1.60	1.52	1.46	1.22	1.12	1.07	0.89	0.87	0.27	0.23	0.24
					1.74	1.72	1.59	1.47	1.42	1.30	1.06	1.00	0.88		0.52	0.16	
52	1068.	5.69	93.6	5.51	5.27	4.99	4.09	3.58	3.33	2.26	1.82	1.53	1.05	1.07	0.47	0.47	0.50
					4.83	4.59	3.84	3.31	3.14	2.36	0.96	1.10	0.85		0.55	0.45	
53	994.	5.05	93.8	4.89	4.68	4.43	3.64	3.20	2.97	2.05	1.67	1.42	0.98	1.01	0.46	0.43	0.46
					4.29	4.08	3.43	2.96	2.81	2.14	0.98	1.03	0.81		0.54	0.42	
54	931.	4.53	94.2	4.38	4.17	3.95	3.25	2.86	2.67	1.87	1.53	1.32	0.93	0.95	0.46	0.40	0.43
					3.82	3.65	3.08	2.67	2.53	1.95	0.99	0.99	0.78		0.54	0.39	

TABLE II.—Continued.

(a) Continued.

Run	$\dot{w}_a$, g/s	P_o, MPa	T_o, K	P_0, MPa	Pressure at pressure tap locations 1 to 11, MPa												P_B, MPa
					P_1	P_2	P_3	P_4	P_5	P_6	P_7	P_8	P_9	P_{9j} (90°)	P_{10}	P_{11}	
55	1029.	5.00	85.6	4.82	4.60	4.34	3.50	3.03	2.80	1.82	1.45	1.19	0.76	0.76	0.25	0.36	0.39
					4.19	3.99	3.30	2.83	2.69	1.99	0.24	0.42	0.58		0.33	0.39	
56	942.	4.24	85.7	4.10	3.88	3.67	2.95	2.57	2.37	1.57	1.26	1.06	0.69	0.69	0.24	0.32	0.35
					3.55	3.39	2.82	2.41	2.28	1.72	0.23	0.51	0.53		0.33	0.33	
57	850.	3.54	85.9	3.43	3.23	3.07	2.47	2.16	1.99	1.35	1.09	0.93	0.61	0.63	0.24	0.30	0.33
					2.95	2.83	2.36	2.02	1.91	1.46	0.24	0.54	0.48		0.33	0.30	
58	743.	2.82	86.0	2.72	2.55	2.42	1.96	1.72	1.58	1.10	0.90	0.78	0.54	0.55	0.24	0.28	0.31
					2.33	2.24	1.88	1.61	1.53	1.19	0.25	0.53	0.43		0.32	0.28	
59	608	2.03	85.9	1.95	1.86	1.77	1.43	1.27	1.17	0.84	0.69	0.62	0.41	0.45	0.22	0.25	0.28
					1.69	1.64	1.38	1.19	1.13	0.89	0.30	0.46	0.36		0.31	0.26	
60	902.	3.90	84.9	3.76	3.55	3.36	2.69	2.33	2.16	1.43	1.14	0.96	0.62	0.63	0.23	0.32	0.35
					3.23	3.10	2.57	2.21	2.09	1.58	0.22	0.25	0.49		0.31	0.34	
61	805.	3.20	84.9	3.09	2.91	2.77	2.22	1.94	1.78	1.21	0.98	0.83	0.55	0.57	0.22	0.29	0.31
					2.67	2.56	2.13	1.82	1.73	1.33	0.22	0.39	0.44		0.31	0.30	
62	675.	2.40	85.2	2.32	2.18	2.08	1.67	1.47	1.36	0.94	0.77	0.68	0.47	0.48	0.22	0.26	0.29
					1.99	1.92	1.61	1.38	1.31	1.03	0.23	0.44	0.38		0.31	0.27	
63	565.	1.78	84.6	1.71	1.60	1.54	1.24	1.10	1.02	0.73	0.61	0.54	0.39	0.40	0.21	0.24	0.27
					1.47	1.43	1.20	1.03	0.98	0.78	0.23	0.40	0.32		0.29	0.25	
64	518.	1.55	84.8	1.49	1.39	1.34	1.08	0.97	0.89	0.65	0.55	0.50	0.36	0.38	0.21	0.24	0.26
					1.28	1.24	1.05	0.91	0.86	0.69	0.29	0.37	0.30		0.29	0.25	
65	430.	1.15	85.5	1.11	1.03	1.01	0.82	0.74	0.69	0.52	0.45	0.41	0.32	0.33	0.21	0.22	0.25
					0.95	0.93	0.79	0.69	0.65	0.54	0.32	0.33	0.28		0.29	0.23	
66	1113.	5.77	85.5	5.57	5.38	5.08	4.10	3.55	3.28	2.12	1.67	1.36	0.85	0.85	0.26	0.38	0.41
					4.91	4.66	3.84	3.28	3.11	2.27	0.24	0.78	0.64		0.35	0.41	
67	1111.	5.73	85.8	5.54	5.26	4.96	4.01	3.48	3.21	2.08	1.65	1.35	0.85	0.85	0.26	0.35	0.37
					4.80	4.56	3.77	3.22	3.04	2.24	0.25	0.79	0.65		0.35	0.35	
68	1052.	5.25	86.2	5.07	4.85	4.58	3.70	3.22	2.97	1.95	1.55	1.28	0.82	0.82	0.26	0.34	0.36
					4.42	4.20	3.48	2.97	2.81	2.08	0.26	0.79	0.62		0.35	0.34	
69	1013.	4.90	86.4	4.74	4.50	4.25	3.43	2.99	2.75	1.82	1.46	1.21	0.78	0.79	0.26	0.33	0.36
					4.11	3.91	3.25	2.78	2.62	1.96	0.26	0.78	0.60		0.35	0.33	
70	935.	4.22	86.5	4.07	3.86	3.65	2.95	2.57	2.37	1.59	1.29	1.08	0.64	0.72	0.26	0.31	0.34
					3.53	3.37	2.81	2.41	2.28	1.72	0.26	0.73	0.56		0.35	0.31	
71	831.	3.43	87.2	3.31	3.13	2.97	2.40	2.10	1.94	1.33	1.09	0.93	0.64	0.64	0.27	0.30	0.33
					2.86	2.74	2.29	1.97	1.87	1.43	0.32	0.67	0.51		0.35	0.30	
76	103.	2.59	255.3	2.55	2.47	2.42	2.17	2.03	1.96	1.65	1 49	1.40	1.17	1.14	0.42	0.28	0.29
					2.38	2.34	2.15	1.99	1.93	1.75	1.44	1.35	1.18		0.60	0.19	
77	166.	4.02	262.4	3.97	3.87	3.77	3.40	3.18	3.07	2.56	2.31	2.16	1.79	1.73	0.68	0.40	0.41
					3.72	3.66	3.36	3.12	3.04	2.72	2.24	2.09	1.83		0.95	0.24	
78	227.	5.39	265.6	5.32	5.22	5.07	4.59	4.29	4.14	3.42	3.08	2.86	2.35	2.28	0.91	0.53	0.52
					5.02	4.91	4.52	4.20	4.10	3.65	3.00	2.80	2.44		1.29	0.30	
79	1002.	5.28	97.1	5.12	4.86	4.61	3.84	3.39	3.18	2.27	1.85	1.60	1.17	1.18	0.59	0.57	0.60
					4.47	4.29	3.62	3.12	2.90	2.29	1.30	1.20	0.96		0.59	0.56	
80	940.	4.74	97.2	4.60	4.40	4.17	3.49	3.09	2.89	2.09	1.73	1.50	1.11	1.11	0.56	0.48	0.50
					4.05	3.89	3.29	2.84	2.63	2.10	1.27	1.14	0.92		0.56	0.47	

TABLE II.—Continued.

(a) Continued.

Run	$\dot{w}_o$, g/s	P_o, MPa	T_o, K	P_0, MPa	Pressure at pressure tap locations 1 to 11, MPa												P_B, MPa
					P_1	P_2	P_3	P_4	P_5	P_6	P_7	P_8	P_9	P_{9j} (90°)	P_{10}	P_{11}	
81	858.	4.09	97.2	3.98	3.78	3.59	3.00	2.67	2.51	1.84	1.53	1.35	3.58	1.01	0.53	0.41	0.44
					3.48	3.35	2.84	2.47	2.29	1.85	1.18	1.05	0.86		0.54	0.42	
82	758.	3.43	99.0	3.33	3.16	3.02	2.55	2.27	2.15	1.62	1.38	1.24	0.88	0.97	0.55	0.38	0.40
					2.93	2.83	2.43	2.13	1.99	1.65	1.15	1.02	0.87		0.57	0.39	
83	613.	2.56	100.2	2.49	2.36	2.28	1.94	1.76	1.67	1.32	1.15	1.06	0.87	0.87	0.53	0.33	0.35
					2.21	2.15	1.88	1.67	1.57	1.36	1.03	0.94	0.82		0.57	0.35	
84	518.	2.04	99.9	1.98	1.90	1.84	1.58	1.45	1.38	1.11	0.99	0.92	0.51	0.77	0.48	0.30	0.32
					1.78	1.74	1.54	1.38	1.31	1.16	0.91	0.85	0.76		0.53	0.30	
85	904.	5.69	113.3	5.55	5.33	5.07	4.35	3.92	3.73	2.87	2.48	2.27	1.86	1.85	1.12	0.57	0.60
					5.00	4.78	4.16	3.68	3.47	2.94	2.25	2.03	1.78		1.21	0.54	
86	852.	5.27	113.4	5.14	4.96	4.73	4.07	3.68	3.50	2.74	2.39	2.20	1.82	1.81	1.10	0.55	0.58
					4.66	4.47	3.91	3.48	3.28	2.81	2.18	1.99	1.76		1.20	0.51	
87	776.	4.61	113.1	4.51	4.33	4.14	3.59	3.27	3.12	2.49	2.20	2.05	1.73	1.72	1.05	0.50	0.53
					4.08	3.93	3.47	3.11	2.94	2.56	2.04	1.88	1.69		1.16	0.49	
88	731.	4.48	115.1	4.38	4.19	4.02	3.52	3.23	3.09	2.52	2.26	2.12	1.84	1.82	1.09	0.49	0.52
					3.97	3.83	3.43	3.10	2.95	2.60	2.13	1.98	1.82		1.26	0.49	
89	658.	4.01	115.5	3.92	3.78	3.64	3.21	2.97	2.86	2.38	2.16	2.05	1.80	1.79	1.04	0.45	0.49
					3.59	3.49	3.15	2.88	2.75	2.47	2.08	1.95	1.81		1.25	0.46	
90	533.	3.36	116.5	3.30	3.19	3.09	2.78	2.61	2.53	2.19	2.04	1.96	1.79	1.76	0.89	0.39	0.43
					3.06	2.99	2.75	2.57	2.48	2.30	2.03	1.95	1.85		1.23	0.40	
91	675.	6.13	131.6	6.03	5.88	5.67	5.06	4.71	4.55	3.84	3.53	3.34	2.92	2.74	1.32	0.61	0.64
					5.64	5.47	5.02	4.66	4.57	4.10	3.55	3.39	3.19		2.03	0.58	
92	589.	5.48	131.8	5.40	5.26	5.08	4.58	4.29	4.16	3.57	3.30	3.13	2.63	2.47	1.18	0.55	0.58
					5.07	4.95	4.58	4.29	4.22	3.83	3.39	3.26	2.90		1.79	0.50	
93	466.	4.74	132.9	4.67	4.56	4.43	4.01	3.77	3.66	3.12	2.81	2.64	2.26	2.22	1.03	0.49	0.52
					4.43	4.33	4.04	3.79	3.74	3.41	2.84	2.69	2.40		1.49	0.33	
94	311.	3.68	129.5	3.63	3.54	3.45	3.11	2.92	2.84	2.47	2.22	2.10	1.81	1.78	0.80	0.38	0.41
					3.44	3.37	3.14	2.92	2.87	2.61	2.12	2.02	1.82		1.10	0.25	
95	191.	2.77	130.9	2.73	2.65	2.58	2.33	2.18	2.12	1.83	1.66	1.56	1.33	1.33	0.59	0.29	0.31
					2.56	2.51	2.31	2.15	2.10	1.90	1.57	1.49	1.31		0.80	0.17	
96	98.	1.73	138.1	1.69	1.64	1.61	1.42	1.34	1.30	1.12	1.02	0.97	0.82	0.81	0.31	0.21	0.22
					1.58	1.55	1.42	1.32	1.29	1.17	0.97	0.92	0.81		0.46	0.16	
97	74.	1.34	140.7	1.31	1.26	1.24	1.10	1.03	1.00	0.86	0.79	0.75	0.63	0.63	0.23	0.19	0.20
					1.21	1.20	1.10	1.02	0.99	0.90	0.75	0.71	0.63		0.35	0.16	
102	1143.	6.12	85.9	5.94	5.71	5.39	4.43	3.81	3.58	2.38	1.88	1.54	0.92	0.96	0.28	0.44	0.45
					5.21	5.00	4.10	3.48	3.15	2.40	0.84	0.98	0.69		0.29	0.47	
103	1123.	5.90	86.0	5.73	5.42	5.11	4.21	3.63	3.41	2.27	1.80	1.48	0.90	0.94	0.27	0.40	0.41
					4.95	4.75	3.91	3.32	2.99	2.30	0.85	0.96	0.68		0.29	0.41	
104	1055.	5.21	85.6	5.04	4.78	4.51	3.67	3.15	2.96	1.97	1.56	1.29	0.79	0.80	0.24	0.37	0.39
					4.38	4.20	3.44	2.92	2.66	2.03	0.63	0.84	0.59		0.25	0.39	
105	1007.	4.77	85.7	4.62	4.35	4.11	3.35	2.88	2.70	1.81	1.45	1.20	0.75	0.76	0.24	0.34	0.35
					3.98	3.83	3.15	2.67	2.42	1.87	0.64	0.79	0.57		0.25	0.35	
106	914.	4.00	85.8	3.88	3.65	3.45	2.81	2.43	2.27	1.56	1.24	1.04	0.67	0.68	0.23	0.31	0.33
					3.34	3.21	2.65	2.26	2.05	1.60	0.62	0.71	0.52		0.25	0.32	

TABLE II.—Continued.

(a) Concluded.

Run	$\dot{w}$, g/s	P_o, MPa	T_o, K	P_0, MPa	Pressure at pressure tap locations 1 to 11, MPa												P_B, MPa
					P_1	P_2	P_3	P_4	P_5	P_6	P_7	P_8	P_9	P_{9j} (90°)	P_{10}	P_{11}	
107	804.	3.21	85.9	3.11	2.92 2.68	2.77 2.59	2.26 2.15	1.96 1.83	1.83 1.66	1.28 1.32	1.03 0.59	0.88 0.62	0.58 0.46	0.59	0.23 0.24	0.29 0.29	0.31
108	686.	2.47	86.5	2.40	2.24 2.07	2.14 1.99	1.75 1.67	1.52 1.43	1.43 1.30	1.02 1.05	0.84 0.57	0.72 0.54	0.50 0.42	0.51	0.23 0.24	0.27 0.27	0.29
109	929.	4.09	84.9	3.96	3.68 3.41	3.52 3.28	2.85 2.69	2.47 2.29	2.29 2.08	1.55 1.62	1.23 0.27	1.00 0.70	0.64 0.50	0.65	0.22 0.23	0.31 0.33	0.33
110	800.	3.15	84.9	3.05	2.85 2.61	2.70 2.52	2.19 2.09	1.90 1.77	1.77 1.60	1.22 1.28	0.99 0.44	0.82 0.58	0.54 0.43	0.56	0.21 0.22	0.28 0.30	0.30
111	665.	2.32	84.9	2.25	2.10 1.94	2.00 1.86	1.62 1.56	1.42 1.33	1.33 1.20	0.94 0.97	0.77 0.45	0.66 0.48	0.45 0.37	0.47	0.21 0.21	0.26 0.26	0.28
112	600.	1.95	84.5	1.89	1.77 1.63	1.68 1.57	1.37 1.32	1.20 1.12	1.12 1.02	0.81 0.83	0.66 0.42	0.57 0.43	0.40 0.33	0.42	0.20 0.20	0.24 0.25	0.26
113	518.	1.53	84.6	1.48	1.38 1.27	1.32 1.23	1.08 1.04	0.95 0.89	0.90 0.81	0.66 0.68	0.55 0.40	0.48 0.38	0.35 0.30	0.37	0.20 0.20	0.23 0.24	0.25
114	428.	1.13	84.9	1.09	1.02 0.95	0.99 0.92	0.82 0.78	0.72 0.67	0.68 0.62	0.52 0.53	0.44 0.35	0.40 0.33	0.31 0.27	0.32	0.20 0.20	0.22 0.22	0.24
115	385.	0.97	85.5	0.94	0.87 0.81	0.85 0.79	0.71 0.68	0.63 0.59	0.60 0.55	0.46 0.47	0.40 0.33	0.37 0.31	0.29 0.26	0.30	0.20 0.20	0.21 0.21	0.23
116	730.	5.99	127.6	5.89	5.74 5.48	5.51 5.31	4.91 4.82	4.56 4.45	4.41 4.36	3.69 3.85	3.36 3.29	3.16 3.11	2.79 2.89	2.74	1.38 2.12	0.61 0.58	0.64
117	707.	5.82	127.7	5.73	5.55 5.32	5.33 5.16	4.77 4.71	4.44 4.36	4.30 4.27	3.62 3.80	3.31 3.28	3.13 3.11	2.78 2.90	2.71	1.34 2.07	0.59 0.58	0.63
118	669.	5.49	127.4	5.41	5.25 5.05	5.06 4.91	4.55 4.50	4.24 4.18	4.11 4.11	3.50 3.67	3.22 3.20	3.05 3.05	2.71 2.87	2.61	1.28 1.94	0.56 0.56	0.60
119	619.	5.05	126.8	4.97	4.83 4.66	4.67 4.53	4.21 4.19	3.95 3.91	3.84 3.86	3.31 3.48	3.06 3.07	2.92 2.94	2.56 2.77	2.46	1.19 1.77	0.53 0.52	0.56
120	575.	4.69	126.3	4.62	4.50 4.35	4.35 4.24	3.95 3.93	3.71 3.70	3.61 3.66	3.15 3.32	2.93 2.96	2.80 2.85	2.40 2.61	2.33	1.12 1.63	0.49 0.49	0.53
121	517.	4.36	127.0	4.30	4.19 4.07	4.07 3.98	3.71 3.72	3.51 3.52	3.43 3.49	3.02 3.20	2.81 2.81	2.64 2.68	2.22 2.38	2.17	1.03 1.46	0.46 0.44	0.50
122	457.	3.90	126.6	3.86	3.76 3.67	3.66 3.59	3.36 3.38	3.19 3.21	3.11 3.19	2.72 2.93	2.48 2.48	2.32 2.36	1.96 2.10	1.91	0.92 1.28	0.42 0.40	0.46
123	294.	3.21	125.5	3.17	3.09 3.00	3.01 2.95	2.78 2.78	2.59 2.56	2.53 2.53	2.27 2.33	2.02 1.86	1.90 1.78	1.63 1.61	1.66	0.75 0.95	0.35 0.26	0.39

(b) Fluid hydrogen

Run	$\dot{w}$, g/s	P_o, MPa	T_o, K	P_0, MPa	Pressure at pressure tap locations 1 to 11, MPa												P_B, MPa
					P_1	P_2	P_3	P_4	P_5	P_6	P_7	P_8	P_9	P_{9j} (90°)	P_{10}	P_{11}	
18	25.	2.57	290.2	2.53	2.46 2.37	2.42 2.33	2.15 2.12	2.03 1.98	1.95 1.93	1.61 1.73	1.46 1.41	1.39 1.33	1.10 1.15	1.13	0.33 0.59	0.26 0.16	0.29
19	56.	5.47	291.1	5.41	5.32 5.10	5.20 4.99	4.66 4.56	4.39 4.24	4.22 4.11	3.38 3.67	3.07 2.99	2.87 2.79	2.27 2.42	2.25	0.76 1.30	0.53 0.29	0.55

TABLE II.—Continued.

(b) Continued.

Run	$\dot{w}$, g/s	P_0, MPa	T_0, K	P_0, MPa	Pressure at pressure tap locations 1 to 11, MPa												P_B, MPa
					P_1	P_2	P_3	P_4	P_5	P_6	P_7	P_8	P_9	P_{9j} (90°)	P_{10}	P_{11}	
20	49.	4.73	285.0	4.68	4.58	4.49	4.01	3.79	3.64	2.93	2.67	2.51	1.99	1.99	0.63	0.45	0.48
					4.39	4.31	3.95	3.67	3.55	3.18	2.60	2.43	2.11		1.12	0.25	
21	49.	4.75	285.7	4.71	4.61	4.51	4.04	3.82	3.66	2.96	2.70	2.53	2.01	2.00	0.64	0.46	0.48
					4.43	4.34	3.97	3.69	3.58	3.20	2.62	2.45	2.13		0.05	0.25	
22	41.	3.92	277.4	3.88	3.78	3.71	3.31	3.13	3.00	2.43	2.22	2.09	1.67	1.67	0.51	0.38	0.41
					3.63	3.57	3.27	3.03	2.94	2.63	2.15	2.02	1.75		-0.09	0.22	
23	33.	3.28	278.8	3.25	3.17	3.11	2.77	2.63	2.52	2.06	1.88	1.78	1.42	1.43	0.42	0.32	0.36
					3.04	2.99	2.74	2.55	2.47	2.22	1.82	1.71	1.48		0.29	0.19	
24	24.	2.39	270.3	2.36	2.29	2.26	2.00	1.90	1.82	1.50	1.36	1.30	1.03	1.06	0.30	0.25	0.29
					2.20	2.17	1.98	1.84	1.79	1.60	1.32	1.24	1.07		0.48	0.17	
25	17.	1.78	271.3	1.76	1.70	1.68	1.48	1.43	1.36	1.12	1.02	0.97	0.77	0.80	0.22	0.21	0.24
					1.64	1.62	1.47	1.37	1.33	1.19	0.99	0.93	0.80		0.39	0.15	
26	13.	1.35	270.9	1.33	1.27	1.27	1.11	1.08	1.02	0.85	0.77	0.73	0.57	0.61	0.18	0.18	0.21
					1.23	1.21	1.10	1.02	1.00	0.89	0.75	0.70	0.60		-0.14	0.15	
27	10.	1.09	276.0	1.07	1.02	1.02	0.88	0.86	0.81	0.68	0.62	0.58	0.45	0.49	0.16	0.16	0.20
					0.99	0.97	0.87	0.82	0.80	0.71	0.60	0.57	0.48		-0.77	0.15	
28	224.	3.09	25.7	2.99	2.83	2.74	2.20	2.01	1.86	1.37	1.17	1.04	0.79	0.82	0.40	0.36	0.42
					2.60	2.49	2.14	1.87	1.78	1.45	0.81	0.79	0.69		0.41	0.36	
29	222.	3.09	25.9	2.99	2.83	2.73	2.20	2.02	1.87	1.37	1.18	1.05	0.80	0.82	0.39	0.34	0.40
					2.60	2.49	2.14	1.87	1.78	1.46	0.85	0.81	0.70		0.42	0.33	
30	210.	2.70	25.0	2.61	2.47	2.39	1.91	1.75	1.61	1.19	1.02	0.91	0.69	0.73	0.37	0.36	0.42
					2.27	2.18	1.87	1.63	1.55	1.27	0.67	0.70	0.60		0.37	0.36	
31	190.	2.28	24.3	2.20	2.06	2.01	1.59	1.48	1.36	1.02	0.88	0.79	0.61	0.64	0.34	0.33	0.39
					1.91	1.83	1.57	1.38	1.31	1.08	0.62	0.62	0.54		0.33	0.33	
32	172.	1.95	24.4	1.89	1.76	1.72	1.36	1.28	1.17	0.90	0.79	0.71	0.56	0.59	0.31	0.30	0.36
					1.64	1.57	1.34	1.17	1.11	0.93	0.64	0.58	0.50		0.31	0.30	
33	151.	1.59	23.8	1.53	1.41	1.40	1.09	1.05	0.96	0.74	0.66	0.60	0.48	0.52	0.29	0.29	0.34
					1.33	1.27	1.08	0.96	0.91	0.77	0.56	0.51	0.45		0.29	0.30	
34	127.	1.19	23.4	1.14	1.04	1.05	0.82	0.81	0.73	0.58	0.54	0.49	0.41	0.44	0.25	0.24	0.30
					0.98	0.95	0.81	0.73	0.70	0.61	0.47	0.43	0.39		0.25	0.26	
35	240.	3.49	26.1	3.38	3.21	3.08	2.48	2.26	2.07	1.51	1.28	1.14	0.85	0.88	0.41	0.37	0.43
					2.96	2.83	2.41	2.06	1.94	1.59	0.91	0.88	0.74		0.42	0.36	
36	197.	2.48	25.1	2.40	2.25	2.19	1.74	1.62	1.48	1.11	0.97	0.87	0.67	0.70	0.35	0.34	0.40
					2.09	2.01	1.70	1.48	1.40	1.16	0.76	0.69	0.59		0.35	0.34	
37	182.	2.11	24.1	2.03	1.89	1.85	1.45	1.37	1.24	0.93	0.82	0.73	0.56	0.60	0.31	0.30	0.37
					1.76	1.69	1.43	1.24	1.18	0.98	0.63	0.58	0.50		0.30	0.31	
38	182.	2.11	24.3	2.03	1.89	1.85	1.46	1.38	1.25	0.94	0.83	0.74	0.56	0.60	0.30	0.28	0.34
					1.76	1.69	1.43	1.25	1.18	0.98	0.64	0.59	0.51		0.30	0.29	
39	162.	1.70	23.4	1.64	1.52	1.50	1.16	1.12	1.00	0.76	0.68	0.60	0.47	0.51	0.28	0.27	0.33
					1.42	1.36	1.15	1.01	0.96	0.80	0.54	0.49	0.43		0.27	0.28	
40	141.	1.36	23.2	1.30	1.19	1.20	0.92	0.91	0.81	0.63	0.57	0.51	0.40	0.44	0.25	0.23	0.29
					1.13	1.09	0.91	0.81	0.77	0.65	0.48	0.43	0.38		0.24	0.25	
41	255.	3.90	26.5	3.78	3.59	3.45	2.78	2.54	2.33	1.68	1.43	1.25	0.92	0.96	0.44	0.37	0.44
					3.31	3.16	2.69	2.30	2.17	1.77	1.02	0.96	0.80		0.46	0.36	
42	154.	1.89	27.3	1.83	1.70	1.69	1.35	1.30	1.20	0.96	0.87	0.80	0.67	0.72	0.36	0.28	0.34
					1.60	1.55	1.34	1.20	1.15	1.01	0.80	0.73	0.66		0.42	0.28	

TABLE II.—Continued.

(b) Continued.

Run	$\dot{w}$, g/s	P_o, MPa	T_o, K	P_0, MPa	Pressure at pressure tap locations 1 to 11, MPa												P_B, MPa
					P_1	P_2	P_3	P_4	P_5	P_6	P_7	P_8	P_9	P_{9j} (90°)	P_{10}	P_{11}	
124	45.	4.43	285.6	4.36	4.28 4.13	4.16 4.06	3.78 3.71	3.53 3.44	3.42 3.34	2.84 2.97	2.58 2.47	2.42 2.32	1.96 2.01	1.91	0.75 1.03	0.41 0.25	0.43
125	35.	3.48	284.5	3.43	3.35 3.24	3.26 3.19	2.97 2.91	2.77 2.70	2.69 2.62	2.25 2.35	2.04 1.95	1.92 1.84	1.57 1.60	1.53	0.57 0.80	0.33 0.20	0.35
126	25.	2.59	284.8	2.55	2.48 2.39	2.42 2.36	2.20 2.16	2.06 2.01	2.00 1.94	1.68 1.75	1.52 1.46	1.44 1.38	1.18 1.20	1.16	0.41 0.59	0.26 0.17	0.28
127	19.	2.00	274.5	1.97	1.91 1.84	1.87 1.81	1.69 1.66	1.58 1.54	1.53 1.48	1.29 1.34	1.17 1.11	1.10 1.05	0.91 0.91	0.89	0.31 0.44	0.22 0.16	0.24
128	56.	5.56	291.5	5.49	5.39 5.21	5.24 5.12	4.76 4.67	4.45 4.32	4.31 4.20	3.55 3.71	3.21 3.09	3.00 2.89	2.43 2.49	2.32	0.96 1.30	0.52 0.32	0.53
129	283.	4.98	28.7	4.83	4.69 4.36	4.41 4.14	3.73 3.57	3.30 3.07	3.10 2.95	2.29 2.34	1.89 1.60	1.66 1.38	1.23 1.11	1.27	0.61 0.62	0.49 0.46	0.52
130	280.	4.76	28.0	4.61	4.45 4.14	4.18 3.94	3.54 3.39	3.14 2.91	2.95 2.80	2.19 2.21	1.81 1.50	1.59 1.30	1.18 1.04	1.20	0.58 0.58	0.46 0.44	0.50
132	274.	4.44	27.6	4.30	4.14 3.85	3.88 3.67	3.29 3.15	2.91 2.70	2.74 2.60	2.05 2.06	1.68 1.39	1.48 1.20	1.10 0.97	1.13	0.54 0.55	0.45 0.43	0.49
133	265.	4.16	27.3	4.01	3.85 3.59	3.62 3.41	3.05 2.93	2.70 2.51	2.54 2.41	1.90 1.92	1.57 1.29	1.37 1.12	1.03 0.91	1.06	0.51 0.51	0.40 0.38	0.44
134	241.	3.44	26.1	3.34	3.15 2.94	2.96 2.80	2.50 2.41	2.21 2.07	2.07 2.00	1.57 1.59	1.30 1.07	1.14 0.93	0.87 0.77	0.89	0.44 0.44	0.38 0.37	0.42
135	212.	2.70	25.1	2.61	2.47 2.30	2.33 2.19	1.96 1.89	1.73 1.62	1.62 1.57	1.24 1.27	1.04 0.86	0.92 0.75	0.71 0.63	0.73	0.37 0.37	0.33 0.33	0.37
136	202.	2.48	24.8	2.40	2.26 2.11	2.14 2.01	1.79 1.73	1.59 1.49	1.49 1.45	1.15 1.17	0.96 0.80	0.85 0.70	0.67 0.59	0.68	0.35 0.35	0.32 0.31	0.35
137	183.	2.10	24.6	2.03	1.92 1.79	1.82 1.71	1.52 1.47	1.36 1.28	1.27 1.24	0.99 1.01	0.85 0.71	0.75 0.63	0.60 0.54	0.61	0.32 0.32	0.28 0.28	0.32
138	160.	1.68	23.6	1.62	1.52 1.42	1.45 1.35	1.21 1.17	1.08 1.02	1.02 0.99	0.80 0.82	0.69 0.59	0.61 0.52	0.49 0.45	0.51	0.29 0.29	0.28 0.28	0.32
139	141.	1.35	23.5	1.30	1.21 1.14	1.17 1.09	0.98 0.95	0.88 0.84	0.83 0.80	0.67 0.68	0.58 0.50	0.52 0.45	0.44 0.40	0.45	0.26 0.26	0.24 0.24	0.27
140	123.	1.12	23.3	1.08	1.01 0.94	0.98 0.90	0.82 0.79	0.75 0.71	0.70 0.68	0.58 0.59	0.51 0.45	0.46 0.41	0.40 0.37	0.41	0.24 0.24	0.22 0.23	0.25
141	196.	4.00	37.8	3.91	3.78 3.60	3.61 3.47	3.18 3.12	2.92 2.82	2.80 2.76	2.31 2.39	2.06 1.90	1.90 1.76	1.61 1.57	1.59	0.77 1.01	0.45 0.34	0.48
142	180.	3.68	37.9	3.60	3.46 3.32	3.32 3.20	2.95 2.90	2.72 2.63	2.60 2.57	2.18 2.26	1.96 1.83	1.81 1.71	1.56 1.54	1.54	0.72 0.97	0.40 0.30	0.44
143	151.	2.97	36.8	2.90	2.78 2.67	2.68 2.59	2.39 2.37	2.22 2.17	2.14 2.14	1.83 1.91	1.67 1.61	1.56 1.52	1.37 1.41	1.36	0.59 0.80	0.34 0.27	0.38
144	194.	3.66	36.3	3.57	3.35 3.21	3.21 3.09	2.83 2.79	2.60 2.52	2.49 2.47	2.07 2.15	1.86 1.72	1.71 1.61	1.50 1.47	1.49	0.72 0.95	0.41 0.33	0.45
145	190.	3.73	37.2	3.64	3.51 3.34	3.35 3.22	2.96 2.91	2.72 2.63	2.60 2.57	2.17 2.24	1.94 1.80	1.79 1.67	1.54 1.51	1.52	0.73 0.97	0.41 0.31	0.44
146	156.	2.95	36.2	2.88	2.76 2.65	2.66 2.56	2.36 2.34	2.19 2.15	2.11 2.11	1.80 1.88	1.64 1.58	1.53 1.49	1.36 1.39	1.34	0.59 0.80	0.33 0.26	0.37
147	114.	2.10	34.6	2.05	1.96 1.90	1.91 1.84	1.71 1.71	1.61 1.60	1.55 1.57	1.37 1.45	1.26 1.23	1.18 1.17	1.01 1.04	1.00	0.43 0.56	0.27 0.24	0.31

TABLE II.—Concluded.

(b) Concluded.

Run	$\dot{w}$, g/s	P_o, MPa	T_o, K	P_0, MPa	Pressure at pressure tap locations 1 to 11, MPa												P_B, MPa
					P_1	P_2	P_3	P_4	P_5	P_6	P_7	P_8	P_9	$P_{9'}$ (90°)	P_{10}	P_{11}	
148	217.	3.37	30.6	3.28	3.13 2.94	2.97 2.81	2.52 2.45	2.27 2.16	2.15 2.10	1.71 1.75	1.48 1.29	1.33 1.17	1.10 1.02	1.12	0.60 0.64	0.12 0.14	0.41
149	180.	2.58	30.0	2.50	2.37 2.24	2.26 2.15	1.93 1.90	1.76 1.69	1.67 1.65	1.37 1.41	1.22 1.10	1.11 1.01	0.96 0.91	0.97	0.51 0.58	0.15 0.26	0.34
150	137.	1.78	29.1	1.72	1.63 1.56	1.58 1.50	1.36 1.35	1.26 1.23	1.21 1.20	1.03 1.07	0.94 0.88	0.87 0.83	0.79 0.78	0.79	0.38 0.48	0.20 0.24	0.28
151	109.	1.39	28.9	1.35	1.28 1.24	1.25 1.19	1.09 1.09	1.03 1.01	0.99 0.99	0.87 0.91	0.81 0.79	0.76 0.76	0.70 0.70	0.70	0.30 0.41	0.22 0.22	0.25
152	223.	3.14	27.8	3.04	2.90 2.70	2.73 2.57	2.30 2.23	2.05 1.94	1.94 1.88	1.50 1.53	1.27 1.08	1.12 0.95	0.90 0.81	0.92	0.47 0.48	0.34 0.33	0.38
153	184.	2.25	26.8	2.18	2.05 1.93	1.95 1.83	1.65 1.60	1.48 1.41	1.40 1.37	1.12 1.14	0.97 0.84	0.86 0.76	0.72 0.66	0.74	0.38 0.40	0.27 0.27	0.31
154	145.	1.57	26.1	1.52	1.42 1.35	1.37 1.28	1.17 1.13	1.06 1.02	1.01 0.99	0.83 0.85	0.74 0.66	0.67 0.61	0.58 0.55	0.60	0.32 0.34	0.23 0.23	0.26
155	198.	3.16	31.8	3.06	2.93 2.77	2.80 2.65	2.40 2.34	2.18 2.09	2.07 2.04	1.68 1.73	1.49 1.33	1.35 1.22	1.16 1.10	1.17	0.62 0.73	0.36 0.32	0.41
156	141.	2.02	31.0	1.96	1.88 1.79	1.81 1.72	1.58 1.56	1.47 1.43	1.41 1.40	1.21 1.26	1.11 1.06	1.04 1.00	0.94 0.94	0.94	0.42 0.57	0.27 0.25	0.31
157	104.	1.47	30.6	1.43	1.37 1.32	1.34 1.27	1.19 1.18	1.13 1.12	1.08 1.10	0.97 1.02	0.91 0.89	0.85 0.84	0.74 0.75	0.7[illegible]	0.31 0.42	0.22 0.21	0.26
158	192.	3.02	31.9	2.94	2.80 2.65	2.67 2.54	2.30 2.25	2.09 2.01	2.00 1.97	1.64 1.68	1.45 1.31	1.33 1.20	1.1[illegible] 1.09	1.14	0.61 0.73	0.35 0.31	0.40
159	141.	2.01	30.9	1.96	1.86 1.78	1.80 1.71	1.57 1.55	1.46 1.43	1.40 1.40	1.21 1.25	1.11 1.05	1.03 1.00	0.94 0.94	0.94	0.42 0.57	0.27 0.25	0.30
160	106.	1.47	30.4	1.43	1.37 1.33	1.34 1.28	1.18 1.18	1.12 1.11	1.08 1.10	0.97 1.02	0.91 0.89	0.85 0.85	0.74 0.76	0.74	0.31 0.42	0.22 0.21	0.26
161	88.	1.25	30.4	1.22	1.16 1.13	1.15 1.09	1.02 1.02	0.98 0.97	0.95 0.96	0.84 0.90	0.77 0.75	0.71 0.71	0.62 0.63	0.63	0.27 0.35	0.21 0.20	0.24

TABLE III.—FLOW RATE AND PRESSURE DROP DATA FOR THREE-STEP CYLINDRICAL SEAL, FULLY ECCENTRIC POSITION

[Where two values are given, the top value is for 0° circumferential position (maximum clearance) and the bottom is for the 180° circumferential position (minimum clearance).]

(a) Fluid nitrogen

Run	$\dot{w}$, g/s	P_o, MPa	T_o, K	P_0, MPa	Pressure at pressure tap locations 1 to 11, MPa												P_B, MPa
					P_1	P_2	P_3	P_4	P_5	P_6	P_7	P_8	P_9	P_{9j} (90°)	P_{10}	P_{11}	
162	108.	2.86	292.2	2.81	2.80	2.76	2.43	2.28	2.20	1.76	1.62	1.52	1.17	1.28	0.27	0.30	0.30
					2.63	2.58	2.42	2.20	2.15	1.98	1.51	1.44	1.27		0.71	0.15	
163	163.	4.15	293.7	4.10	4.09	4.03	3.58	3.37	3.25	2.57	2.37	2.23	1.67	1.84	0.37	0.41	0.41
					3.85	3.77	3.53	3.22	3.16	2.88	2.20	2.09	1.84		1.05	0.18	
164	198.	4.97	292.2	4.90	4.89	4.84	4.32	4.08	3.95	3.09	2.85	2.67	1.97	2.18	0.43	0.48	0.48
					4.60	4.51	4.22	3.85	3.78	3.44	2.63	2.49	2.20		1.27	0.21	
165	226.	5.60	290.5	5.52	5.53	5.47	4.92	4.67	4.53	3.53	3.27	3.07	2.23	2.45	0.49	0.54	0.54
					5.20	5.09	4.76	4.36	4.27	3.88	2.97	2.81	2.48		1.44	0.23	
166	186.	4.53	280.2	4.46	4.45	4.41	3.94	3.73	3.62	2.85	2.66	2.51	1.89	2.00	0.40	0.44	0.45
					4.19	4.11	3.84	3.52	3.44	3.14	2.41	2.28	2.01		1.16	0.19	
167	142.	3.51	274.5	3.46	3.44	3.41	3.04	2.87	2.78	2.23	2.09	1.98	1.54	1.58	0.32	0.35	0.36
					3.24	3.18	2.98	2.72	2.66	2.45	1.87	1.78	1.57		0.89	0.16	
168	72.	1.86	264.9	1.83	1.81	1.80	1.60	1.50	1.45	1.20	1.13	1.08	0.88	0.86	0.20	0.22	0.23
					1.70	1.68	1.57	1.44	1.40	1.30	0.99	0.95	0.84		0.46	0.13	
169	53.	1.39	270.4	1.37	1.35	1.34	1.19	1.12	1.09	0.90	0.87	0.83	0.67	0.66	0.18	0.19	0.20
					1.27	1.25	1.17	1.07	1.04	0.97	0.74	0.71	0.63		0.34	0.14	
170	79.	2.10	284.4	2.06	2.04	2.02	1.79	1.67	1.62	1.33	1.23	1.16	0.94	0.96	0.21	0.23	0.24
					1.92	1.89	1.77	1.62	1.58	1.46	1.11	1.06	0.94		0.22	0.13	
171	172.	4.31	288.4	4.24	4.25	4.19	3.74	3.53	3.42	2.71	2.51	2.35	0.97	1.92	0.38	0.42	0.42
					3.99	3.90	3.67	3.36	3.28	3.00	2.30	2.18	1.92		0.26	0.18	
172	255.	6.19	286.1	6.10	6.13	6.05	5.49	5.21	5.07	3.91	3.62	3.36	2.41	2.69	0.54	0.60	0.60
					5.77	5.62	5.28	4.83	4.73	4.30	3.29	3.10	2.74		0.46	0.26	
173	1098.	5.80	77.8	5.62	5.57	5.42	4.65	4.28	4.08	2.69	2.43	2.21	1.43	0.84	0.43	0.45	0.47
					4.92	4.71	4.10	3.48	3.33	2.72	0.26	0.28	0.30		0.20	0.50	
174	1027.	5.14	77.8	4.98	4.94	4.80	4.06	3.71	3.52	2.31	2.09	1.90	1.25	0.79	0.35	0.37	0.40
					4.33	4.17	3.63	3.09	2.96	2.43	0.26	0.28	0.30		0.20	0.39	
175	891.	3.95	77.8	3.82	3.77	3.67	3.04	2.76	2.62	1.75	1.58	1.46	1.00	0.68	0.30	0.33	0.35
					3.31	3.19	2.79	2.38	2.29	1.90	0.26	0.28	0.30		0.19	0.31	
176	738.	2.91	77.8	2.81	2.76	2.70	2.21	2.01	1.91	1.32	1.20	1.12	0.81	0.59	0.29	0.30	0.31
					2.44	2.36	2.08	1.79	1.71	1.44	0.30	0.32	0.34		0.21	0.29	
177	914.	4.14	77.8	4.01	3.96	3.86	3.14	2.81	2.63	1.67	1.47	1.32	0.86	0.63	0.32	0.33	0.35
					3.45	3.32	2.90	2.45	2.35	1.96	0 23	0 25	0.27		0.35	0.35	
178	779.	3.11	77.8	3.01	2.98	2.90	2.34	2.09	1.95	1.29	1.15	1.04	0.71	0.54	0.28	0.29	0.31
					2.59	2.50	2.19	1.86	1.78	1.50	0.23	0.25	0.26		0.35	0.28	
179	589.	1.96	77.8	1.89	1.85	1.82	1.45	1.30	1.22	0.86	0.78	0.72	0.53	0.41	0.24	0.24	0.26
					1.62	1.58	1.39	1.19	1.14	0.98	0.23	0.24	0.26		0.33	0.24	
180	471.	1.38	77.8	1.33	1.29	1.27	1.03	0.92	0.87	0.64	0.59	0.55	0.44	0.35	0.22	0.23	0.24
					1.15	1.12	0.99	0.86	0.82	0.72	0.25	0.26	0.27		0.32	0.23	
181	1121.	5.93	85.7	5.73	5.69	5.53	4.63	4.20	3.96	2.42	2.12	1.87	0.87	0.77	0.34	0.36	0.38
					4.97	4.76	4.13	3.50	3.34	2.74	0.22	0.23	0.25		0.10	0.39	
182	1043.	5.18	85.7	5.02	4.98	4.84	4.00	3.61	3.40	2.11	1.84	1.64	-2.87	0.72	0.30	0.32	0.34
					4.35	4.17	3.62	3.07	2.94	2.42	0.21	0.23	0.25		0.07	0.33	
183	896.	3.90	85.6	3.78	3.73	3.63	2.94	2.65	2.49	1.60	1.41	1.27	0.82	0.60	0.28	0.29	0.31
					3.25	3.13	2.74	2.32	2.22	1.85	0.21	0.23	0.25		-0.01	0.29	

TABLE III.—Continued.

(a) Continued.

Run	$\dot{w}$, g/s	P_o, MPa	T_o, K	P_0, MPa	Pressure at pressure tap locations 1 to 11, MPa												P_B, MPa
					P_1	P_2	P_3	P_4	P_5	P_6	P_7	P_8	P_9	P_{9j} (90°)	P_{10}	P_{11}	
184	704.	2.59	86.0	2.51	2.47	2.41	1.93	1.73	1.63	1.10	0.98	0.90	0.58	0.47	0.25	0.26	0.28
					2.15	2.09	1.83	1.56	1.49	1.27	0.22	0.24	0.25		-0.02	0.26	
185	519.	1.58	86.0	1.53	1.49	1.46	1.18	1.06	1.00	0.72	0.65	0.61	0.37	0.36	0.23	0.23	0.24
					1.32	1.28	1.13	0.97	0.93	0.81	0.23	0.24	0.26		-0.02	0.23	
186	964.	5.83	108.7	5.67	5.62	5.48	4.67	4.31	4.09	2.83	2.55	2.31	1.61	1.59	0.66	0.57	0.57
					5.04	4.80	4.29	3.71	3.58	3.05	1.11	1.16	1.24		-0.06	0.54	
187	907.	5.35	108.9	5.20	5.18	5.06	4.30	3.97	3.77	2.66	2.42	2.21	1.58	1.57	0.64	0.55	0.55
					4.65	4.44	3.98	3.46	3.34	2.87	1.15	1.19	1.29		-0.06	0.53	
188	827.	4.66	109.0	4.54	4.52	4.42	3.75	3.46	3.30	2.41	2.20	2.03	1.50	1.51	0.59	0.51	0.51
					4.07	3.91	3.52	3.08	2.98	2.58	1.17	1.22	1.38		-0.07	0.49	
189	770.	4.24	109.2	4.13	4.07	3.98	3.38	3.13	2.99	2.23	2.05	1.91	1.36	1.48	0.55	0.48	0.48
					3.68	3.54	3.20	2.82	2.73	2.39	1.21	1.27	1.43		-0.06	0.47	
190	703.	3.76	109.4	3.67	3.65	3.58	3.04	2.82	2.71	2.08	1.92	1.79	1.40	1.44	0.52	0.45	0.46
					3.31	3.20	2.91	2.57	2.50	2.21	1.31	1.48	1.41		-0.07	0.44	
191	615.	3.29	110.2	3.21	3.18	3.13	2.68	2.50	2.41	1.91	1.79	1.68	1.35	1.44	0.48	0.41	0.42
					2.91	2.83	2.60	2.34	2.28	2.05	1.53	1.53	1.44		1.23	0.39	
192	804.	6.31	125.1	6.17	6.22	6.12	5.33	5.07	4.88	3.64	3.40	3.15	2.25	2.74	0.68	0.68	0.68
					5.68	5.48	5.05	4.52	4.41	3.94	2.98	2.89	2.69		2.34	0.60	
193	725.	5.57	124.5	5.45	5.47	5.38	4.70	4.47	4.31	3.35	3.14	2.94	2.17	2.65	0.62	0.62	0.61
					5.04	4.89	4.54	4.11	4.02	3.65	2.88	2.80	2.63		2.26	0.54	
194	583.	4.39	123.0	4.31	4.32	4.26	3.75	3.58	3.47	2.87	2.72	2.58	2.01	2.36	0.51	0.51	0.51
					4.04	3.94	3.72	3.44	3.38	3.15	2.63	2.58	2.41		1.89	0.43	
195	513.	3.89	122.5	3.82	3.83	3.79	3.36	3.21	3.12	2.65	2.52	2.41	1.92	2.10	0.46	0.45	0.46
					3.61	3.54	3.36	3.14	3.09	2.91	2.45	2.38	2.16		1.66	0.42	
196	475.	3.61	122.3	3.56	3.56	3.52	3.14	3.01	2.93	2.52	2.40	2.31	1.88	1.96	0.44	0.43	0.43
					3.37	3.31	3.16	2.96	2.92	2.77	2.31	2.22	2.01		1.54	0.41	
197	450.	3.44	122.2	3.38	3.39	3.35	3.00	2.88	2.80	2.44	2.32	2.24	1.84	1.87	0.42	0.41	0.41
					3.22	3.16	3.02	2.85	2.81	2.67	2.19	2.10	1.90		1.46	0.39	
198	391.	3.05	122.0	3.01	3.01	2.98	2.69	2.58	2.51	2.18	2.09	2.02	65	1.61	0.38	0.37	0.37
					2.88	2.84	2.73	2.57	2.53	2.37	1.79	1.78	1.63		1.26	0.36	
199	188.	2.43	119.3	2.39	2.38	2.35	2.13	2.03	1.96	1.71	1.63	1.57	1.27	1.23	0.28	0.28	0.29
					2.25	2.21	2.12	1.92	1.89	1.80	1.30	1.27	1.18		0.85	0.15	
200	109.	1.71	126.7	1.67	1.67	1.65	1.45	1.39	1.32	1.14	1.10	1.06	0.90	0.83	0.20	0.21	0.22
					1.56	1.54	1.46	1.33	1.30	1.21	0.93	0.89	0.80		0.58	0.13	
201	566.	6.33	141.0	6.22	6.30	6.23	5.54	5.34	5.21	4.06	3.83	3.66	2.22	3.09	0.70	0.70	0.70
					5.89	5.75	5.44	4.99	4.91	4.55	3.66	3.56	3.25		2.37	0.47	
202	498.	5.49	137.8	5.41	5.44	5.38	4.78	4.62	4.48	3.60	3.45	3.32	2.20	2.69	0.59	0.60	0.59
					5.12	5.00	4.75	4.38	4.32	4.03	3.17	3.07	2.76		2.07	0.41	
203	357.	4.65	139.9	4.58	4.61	4.55	4.03	3.88	3.76	3.05	2.96	2.87	2.11	2.25	0.47	0.48	0.48
					4.33	4.24	4.01	3.67	3.61	3.34	2.57	2.48	2.24		1.68	0.26	
204	267.	3.83	140.7	3.77	3.78	3.73	3.30	3.17	3.10	2.55	2.47	2.41	1.96	1.80	0.38	0.39	0.39
					3.55	3.48	3.28	2.98	2.93	2.69	2.04	1.95	1.74		1.31	0.20	
205	191.	3.01	142.8	2.96	2.96	2.93	2.56	2.46	2.38	1.97	1.92	1.88	1.58	1.41	0.30	0.31	0.32
					2.78	2.73	2.57	2.34	2.30	2.12	1.61	1.54	1.38		0.97	0.15	
206	115.	1.94	142.9	1.91	1.90	1.88	1.63	1.57	1.52	1.28	1.25	1.23	1.08	0.92	0.22	0.23	0.23
					1.78	1.76	1.65	1.50	1.47	1.36	1.04	0.99	0.89		0.64	0.13	

TABLE III.—Continued.

(a) Continued.

Run	$\dot{w}$, g/s	P_o, MPa	T_o, K	P_0, MPa	Pressure at pressure tap locations 1 to 11, MPa												P_B, MPa
					P_1	P_2	P_3	P_4	P_5	P_6	P_7	P_8	P_9	P_{9j} (90°)	P_{10}	P_{11}	
207	79.	1.43	141.5	1.40	1.39	1.38	1.20	1.15	1.10	0.95	0.93	0.91	0.81	0.68	0.19	0.19	0.20
					1.30	1.29	1.21	1.10	1.08	1.00	0.76	0.73	0.65		0.49	0.14	
257	984.	4.99	86.5	4.85	3.83	3.64	2.71	2.10	1.95	1.53	0.78	0.80	0.59	0.70	0.37	0.37	0.40
					4.15	3.98	3.49	3.00	2.89	2.48	0.23	0.23	0.26		-0.28	0.41	
258	897.	4.19	86.5	4.06	3.11	2.98	2.23	1.84	1.66	1.33	0.94	0.92	0.61	0.63	0.32	0.32	0.35
					3.45	3.33	2.94	2.51	2.41	2.09	0.23	0.23	0.26		-0.14	0.32	
259	820.	3.59	86.6	3.49	2.63	2.52	1.91	1.65	1.49	1.18	0.87	0.86	0.60	0.58	0.29	0.29	0.32
					2.95	2.84	2.52	2.15	2.07	1.79	0.23	0.24	0.26		-0.26	0.28	
260	648.	2.41	86.7	2.34	1.72	1.65	1.27	1.21	1.06	0.85	0.72	0.72	0.54	0.45	0.26	0.26	0.28
					1.98	1.92	1.70	1.46	1.40	1.23	0.23	0.24	0.26		-0.39	0.25	
261	539.	1.77	86.4	1.71	1.27	1.22	0.93	1.06	0.84	0.68	0.64	0.65	0.49	0.38	0.24	0.24	0.26
					1.47	1.43	1.25	1.09	1.05	0.93	0.23	0.23	0.25		-0.27	0.24	
262	746.	4.45	112.1	4.35	3.89	3.58	2.90	2.59	2.45	2.15	1.52	1.50	1.14	1.65	0.50	0.50	0.52
					3.85	3.70	3.40	3.00	2.92	2.63	1.33	1.38	1.52		0.31	0.49	
263	642.	3.71	112.1	3.62	3.23	2.98	2.51	2.33	2.16	1.95	1.60	1.54	1.17	1.58	0.44	0.44	0.46
					3.24	3.14	2.90	2.60	2.53	2.31	1.44	1.55	1.56		0.39	0.43	
264	537.	3.06	111.9	3.00	2.70	2.53	2.18	2.09	1.96	1.78	1.55	1.50	1.16	1.52	0.39	0.39	0.41
					2.74	2.66	2.48	2.27	2.21	2.06	1.55	1.57	1.51		0.63	0.37	
265	386.	2.23	111.3	2.19	2.01	1.90	-0.24	1.67	1.60	1.50	1.36	1.33	1.07	1.29	0.30	0.30	0.31
					2.04	2.01	1.92	1.80	1.76	1.69	1.43	1.38	1.27		0.69	0.27	
266	1061.	5.64	87.9	5.46	5.41	5.27	4.28	4.07	3.87	2.60	2.31	2.07	1.33	0.87	0.31	0.36	0.38
					4.72	4.54	3.94	3.37	3.24	2.68	0.26	0.27	0.30		0.30	0.34	
267	1071.	5.68	87.1	5.49	5.44	5.30	4.40	3.98	3.78	2.44	2.13	1.87	1.18	0.82	0.29	0.34	0.37
					4.75	4.58	3.95	3.38	3.24	2.67	0.24	0.25	0.28		0.28	0.32	
268	1085.	5.77	86.1	5.58	5.53	5.38	4.44	4.00	3.81	2.42	2.08	1.84	1.15	0.80	0.34	0.36	0.39
					4.83	4.64	4.00	3.41	3.28	2.70	0.22	0.23	0.26		0.26	0.39	
269	762.	3.09	85.8	2.99	2.92	2.84	2.27	2.03	1.91	1.28	1.12	1.04	0.70	0.53	0.25	0.27	0.29
					2.57	2.49	2.17	1.86	1.77	1.50	0.22	0.23	0.25		0.24	0.27	
270	495.	1.52	85.6	1.47	1.41	1.37	1.12	1.00	0.94	0.69	0.62	0.59	0.45	0.35	0.22	0.23	0.25
					1.26	1.23	1.10	0.95	0.89	0.78	0.22	0.23	0.24		0.23	0.23	
271	488.	4.27	128.7	4.20	4.18	4.12	3.60	3.42	3.32	2.77	2.50	2.33	1.94	2.16	0.55	0.48	0.49
					3.98	3.91	3.72	3.49	3.44	3.24	2.52	2.47	2.23		1.42	0.44	
272	1082.	5.73	84.6	5.53	5.48	5.33	4.38	3.95	3.74	2.34	2.02	1.77	1.12	0.76	0.37	0.38	0.41
					4.79	4.61	3.98	3.38	3.25	2.69	0.20	0.21	0.23		0.23	0.44	
273	1070.	5.62	85.2	5.43	5.40	5.25	4.25	3.84	3.66	2.28	1.94	1.72	1.07	0.76	0.26	0.31	0.33
					4.71	4.53	3.89	3.32	3.20	2.64	0.21	0.22	0.24		0.23	0.31	
274	935.	5.82	110.6	5.66	5.61	5.49	4.56	4.15	3.96	2.84	2.54	2.30	1.74	1.72	0.73	0.58	0.59
					4.95	4.81	4.28	3.73	3.61	3.10	1.23	1.28	1.39		1.20	0.56	
275	176.	5.80	97.3	5.64	5.52	5.41	5.41	4.19	4.04	2.91	2.64	2.41	1.72	1.19	0.71	0.71	0.74
					4.92	4.73	4.14	3.51	3.38	2.81	0.63	0.65	0.67		0.68	0.71	
276	121.	3.11	95.3	3.02	2.92	2.87	3.26	2.17	2.06	1.53	1.39	1.32	0.98	0.80	0.42	0.37	0.40
					2.20	2.28	2.21	1.94	1.85	1.56	0.52	0.55	0.59		0.51	0.38	
277	133.	6.14	116.3	6.01	5.91	5.82	4.94	4.54	4.35	3.27	2.98	2.74	2.16	2.12	0.91	0.65	0.67
					4.55	4.71	4.57	4.07	3.92	3.35	2.41	2.27	2.03		1.45	0.60	
278	72.	3.46	115.1	3.41	3.33	3.29	2.90	2.70	2.61	2.19	2.07	1.98	1.69	1.80	0.57	0.43	0.45
					2.81	2.86	2.83	2.62	2.55	2.34	1.96	1.89	1.78		1.25	0.40	

TABLE III.—Continued.

(a) Concluded.

Run	$\dot{w}$, g/s	P_o, MPa	T_o, K	P_0, MPa	Pressure at pressure tap locations 1 to 11, MPa												P_B, MPa
					P_1	P_2	P_3	P_4	P_5	P_6	P_7	P_8	P_9	P_{9j} (90°)	P_{10}	P_{11}	
279	76.	3.53	116.8	3.46	3.40	3.36	2.95	2.78	2.70	2.29	2.16	2.07	1.78	1.93	0.57	0.43	0.45
					2.90	2.95	2.92	2.73	2.65	2.45	2.09	2.02	1.91		1.32	0.40	
280	1122.	6.03	85.5	5.84	5.77	5.66	4.77	4.40	4.23	2.86	2.57	2.34	1.54	0.86	0.43	0.46	0.49
					5.12	4.90	4.20	3.57	3.44	2.81	0.23	0.25	0.26		0.27	0.53	
281	770.	3.04	85.5	2.95	2.88	2.83	2.30	2.10	2.01	1.38	1.25	1.17	0.83	0.55	0.29	0.30	0.32
					2.56	2.46	2.14	1.83	1.75	1.47	0.22	0.24	0.25		0.24	0.31	
282	1072.	6.07	97.9	5.90	5.84	5.64	4.80	4.41	4.23	2.86	2.52	2.26	1.54	1.16	0.57	0.52	0.53
					5.16	4.93	4.28	3.67	3.54	2.93	0.57	0.61	0.64		0.62	0.50	
283	724.	3.13	96.9	3.05	2.98	2.91	2.40	2.21	2.11	1.52	1.38	1.29	0.96	0.82	0.39	0.35	0.37
					2.68	2.57	2.28	1.98	1.91	1.64	0.56	0.59	0.62		0.55	0.35	
284	988.	6.07	107.8	5.91	5.87	5.72	4.82	4.43	4.28	2.96	2.66	2.40	1.78	1.61	0.77	0.58	0.59
					5.24	5.03	4.41	3.83	3.71	3.14	1.04	1.07	1.18		1.06	0.55	
285	644.	3.28	107.4	3.20	3.16	3.10	2.60	2.42	2.34	1.82	1.68	1.59	1.29	1.29	0.53	0.41	0.43
					2.88	2.78	2.52	2.25	2.19	1.95	1.20	1.36	1.27		0.90	0.40	
286	777.	6.74	129.2	6.61	6.61	6.48	5.60	5.26	5.12	3.97	3.65	3.38	2.71	3.12	0.77	0.71	0.71
					6.09	5.92	5.43	4.94	4.84	4.35	3.47	3.32	3.09		2.35	0.58	
287	347.	3.66	127.3	3.61	3.59	3.53	3.09	2.93	2.88	2.50	2.30	2.18	1.88	1.84	0.50	0.42	0.43
					3.44	3.38	3.19	2.93	2.90	2.71	2.01	1.98	1.82		1.14	0.30	
288	1027.	5.89	101.0	5.73	5.69	5.55	4.73	4.39	4.23	2.89	2.58	2.39	1.72	1.27	0.63	0.57	0.59
					5.02	4.79	4.20	3.61	3.48	2.93	0.71	0.75	0.79		0.75	0.55	
289	696.	3.23	101.3	3.15	3.11	3.04	2.53	2.35	2.25	1.65	1.51	1.44	1.12	1.01	0.43	0.39	0.41
					2.77	2.67	2.39	2.10	2.02	1.77	0.77	0.81	0.87		0.70	0.39	
290	909.	6.07	115.1	5.93	5.92	5.79	4.95	4.63	4.51	3.28	2.95	2.78	2.15	2.03	0.77	0.63	0.64
					5.31	5.11	4.54	3.99	3.88	3.36	1.56	1.64	1.93		1.39	0.59	
291	575.	3.53	115.2	3.46	3.42	3.38	2.92	2.77	2.70	2.23	2.09	2.01	1.69	1.82	0.50	0.43	0.45
					3.18	3.10	2.89	2.66	2.60	2.39	1.96	1.92	1.81		1.27	0.39	
292	869.	6.29	119.8	6.14	6.16	6.04	5.12	4.79	4.68	3.50	3.14	2.97	2.35	2.36	0.77	0.66	0.66
					5.56	5.36	4.79	4.25	4.15	3.63	2.61	2.53	2.30		1.66	0.60	
293	524.	3.71	119.9	3.65	3.62	3.58	3.12	2.98	2.91	2.48	2.32	2.24	1.91	2.05	0.50	0.44	0.45
					3.41	3.34	3.14	2.94	2.89	2.71	2.32	2.27	2.08		1.38	0.40	
294	588.	6.72	141.6	6.61	6.64	6.56	5.71	5.41	5.31	4.22	3.80	3.51	2.67	3.28	0.72	0.68	0.68
					6.21	6.08	5.66	5.22	5.15	4.73	3.89	3.75	3.49		2.13	0.50	
295	249.	3.70	139.8	3.64	3.63	3.57	3.10	2.94	2.86	2.39	2.22	2.14	1.77	1.70	0.41	0.37	0.39
					3.41	3.35	3.12	2.85	2.79	2.56	2.00	1.90	1.68		1.00	0.19	

(b) Fluid hydrogen

Run	$\dot{w}$, g/s	P_o, MPa	T_o, K	P_0, MPa	Pressure at pressure tap locations 1 to 11, MPa												P_B, MPa
					P_1	P_2	P_3	P_4	P_5	P_6	P_7	P_8	P_9	P_{9j} (90°)	P_{10}	P_{11}	
209	49.	4.75	294.8	4.69	4.71	4.65	4.21	3.98	3.87	3.02	2.81	2.62	1.85	2.09	0.45	0.45	0.46
					4.41	4.33	4.03	3.70	3.62	3.30	2.53	2.41	2.11		1.29	0.19	
210	42.	4.02	284.6	3.97	3.97	3.92	3.54	3.33	3.23	2.53	2.38	2.23	1.65	1.75	0.38	0.40	0.40
					3.72	3.66	3.40	3.11	3.04	2.77	2.11	2.01	1.77		1.06	0.18	
211	35.	3.40	283.5	3.36	3.36	3.32	2.98	2.82	2.74	2.16	2.04	1.93	1.45	1.51	0.33	0.34	0.35
					3.15	3.10	2.89	2.64	2.58	2.36	1.80	1.72	1.52		0.89	0.16	

TABLE III.—Continued.

(b) Continued.

Run	$\dot{w}$, g/s	P_o, MPa	T_o, K	P_0, MPa	Pressure at pressure tap locations 1 to 11, MPa												P_B, MPa
					P_1	P_2	P_3	P_4	P_5	P_6	P_7	P_8	P_9	P_{9j} (90°)	P_{10}	P_{11}	
212	323.	6.24	30.4	6.09	6.13 5.46	5.99 5.18	5.14 4.61	4.76 3.94	4.54 3.78	2.96 3.18	2.68 0.57	2.45 0.61	1.62 0.65	1.43	0.56 0.80	0.60 0.53	0.61
213	308.	5.69	29.9	5.55	5.54 4.92	5.42 4.67	4.59 4.18	4.24 3.57	4.04 3.43	2.64 2.90	2.40 0.54	2.19 0.58	1.49 0.62	1.31	0.52 0.75	0.54 0.48	0.56
214	288.	4.97	29.1	4.84	4.82 4.27	4.71 4.06	3.94 3.64	3.62 3.11	3.44 2.98	2.28 2.53	2.09 0.49	1.92 0.53	1.36 0.57	1.16	0.46 0.68	0.48 0.43	0.50
215	257.	3.98	27.9	3.86	3.84 3.40	3.75 3.24	3.08 2.90	2.82 2.48	2.67 2.38	1.82 2.04	1.73 0.43	1.48 0.46	1.12 0.50	0.95	0.41 0.57	0.42 0.38	0.44
216	227.	3.18	26.9	3.09	3.07 2.71	3.00 2.60	2.44 2.33	2.23 1.99	2.12 1.91	1.48 1.65	1.42 0.39	1.24 0.42	0.96 0.45	0.80	0.38 0.45	0.38 0.36	0.41
217	201.	2.55	26.3	2.48	2.45 2.16	2.40 2.08	1.94 1.86	1.77 1.60	1.69 1.53	1.21 1.34	1.16 0.36	1.04 0.38	0.83 0.42	0.68	0.31 0.40	0.32 0.30	0.34
218	172.	1.91	26.0	1.86	1.84 1.63	1.81 1.57	1.45 1.41	1.34 1.22	1.26 1.17	0.94 1.03	0.91 0.35	0.82 0.37	0.68 0.41	0.57	0.29 0.36	0.30 0.29	0.32
219	135.	1.35	25.9	1.31	1.29 1.15	1.27 1.11	1.03 1.01	0.96 0.88	0.92 0.85	0.72 0.77	0.70 0.37	0.64 0.42	0.55 0.46	0.49	0.24 0.31	0.25 0.24	0.27
220	112.	0.98	23.9	0.95	0.93 0.83	0.92 0.80	0.74 0.72	0.70 0.64	0.66 0.61	0.52 0.55	0.51 0.27	0.47 0.29	0.41 0.32	0.35	0.23 0.24	0.23 0.23	0.25
221	258.	5.90	40.7	5.78	5.80 5.27	5.68 5.06	4.94 4.61	4.62 4.06	4.43 3.92	3.19 3.42	2.96 2.30	2.67 2.13	1.92 1.82	1.95	0.51 1.29	0.57 0.34	0.59
222	237.	5.31	40.4	5.20	5.18 4.72	5.08 4.54	4.40 4.15	4.12 3.67	3.95 3.55	2.91 3.13	2.71 2.16	2.48 2.01	1.82 1.75	1.87	0.46 1.28	0.52 0.30	0.53
223	203.	6.13	52.8	6.04	6.00 5.56	5.90 5.40	5.24 5.02	4.97 4.53	4.79 4.41	3.67 3.95	3.53 2.87	2.93 2.69	2.35 2.34	2.40	0.61 1.33	0.64 0.40	0.65
224	154.	5.29	60.4	5.22	5.21 4.86	5.12 4.73	4.56 4.43	4.34 4.02	4.20 3.92	3.31 3.56	3.19 2.65	2.68 2.49	2.15 2.17	2.23	0.49 1.25	0.54 0.34	0.56
225	120.	4.42	60.0	4.36	4.35 4.07	4.28 3.97	3.81 3.72	3.64 3.39	3.51 3.31	2.82 3.01	2.73 2.25	2.34 2.12	1.91 1.85	1.91	0.41 1.07	0.46 0.29	0.48
226	87.	3.31	57.9	3.26	3.24 3.04	3.20 2.97	2.84 2.79	2.71 2.54	2.62 2.48	2.15 2.27	2.08 1.70	1.83 1.61	1.54 1.41	1.47	0.32 0.82	0.36 0.23	0.38
227	244.	5.15	38.6	5.03	5.04 4.57	4.92 4.39	4.25 3.99	3.99 3.51	3.78 3.40	2.77 2.97	2.68 1.94	2.16 1.86	1.74 1.63	1.76	0.45 1.24	0.50 0.31	0.52
228	188.	3.61	37.0	3.53	3.50 3.20	3.43 3.09	2.95 2.85	2.78 2.55	2.66 2.48	2.07 2.23	2.01 1.64	1.71 1.56	1.43 1.43	1.50	0.35 1.09	0.39 0.24	0.41
229	93.	2.41	40.1	2.37	2.34 2.18	2.30 2.14	2.02 2.01	1.93 1.84	1.87 1.80	1.55 1.67	1.52 1.32	1.36 1.27	1.19 1.12	1.16	0.27 0.68	0.29 0.19	0.31
230	185.	4.03	40.6	3.95	3.92 3.60	3.84 3.49	3.32 3.23	3.13 2.89	2.99 2.82	2.33 2.54	2.25 1.85	1.89 1.75	1.67 1.58	1.65	0.39 1.18	0.42 0.24	0.43
231	145.	3.15	39.7	3.10	3.08 2.85	3.03 2.78	2.63 2.59	2.51 2.35	2.38 2.29	1.93 2.11	1.90 1.62	1.55 1.55	1.34 1.43	1.45	0.33 0.98	0.35 0.19	0.37
232	126.	2.82	39.7	2.77	2.75 2.55	2.70 2.50	2.36 2.34	2.25 2.13	2.15 2.08	1.77 1.92	1.74 1.50	1.47 1.44	1.22 1.33	1.33	0.32 0.83	0.33 0.19	0.35
233	74.	2.02	39.7	1.99	1.97 1.85	1.95 1.82	1.74 1.71	1.69 1.58	1.64 1.54	1.44 1.44	1.44 1.15	1.36 1.10	1.36 0.97	1.12	0.25 0.63	0.25 0.16	0.28
234	41.	1.29	39.6	1.26	1.24 1.16	1.24 1.14	1.08 1.07	1.05 0.98	1.02 0.96	0.88 0.90	0.87 0.69	0.81 0.66	0.75 0.60	0.66	0.19 0.29	0.20 0.17	0.21

TABLE III.—Concluded.

(b) Concluded.

Run	$\dot{w}$, g/s	P_o, MPa	T_o, K	P_0, MPa	Pressure at pressure tap locations 1 to 11, MPa												P_B, MPa
					P_1	P_2	P_3	P_4	P_5	P_6	P_7	P_8	P_9	P_{9j} (90°)	P_{10}	P_{11}	
235	25.	0.87	40.9	0.85	0.82 0.77	0.83 0.76	0.71 0.71	0.69 0.65	0.67 0.63	0.56 0.59	0.56 0.44	0.52 0.42	0.47 0.36	0.40	0.16 0.07	0.17 0.17	0.19
236	217.	3.66	33.9	3.57	3.54 3.18	3.46 3.07	2.92 2.79	2.73 2.45	2.60 2.37	1.94 2.11	1.88 0.77	1.51 0.82	1.26 1.00	1.29	0.35 0.50	0.37 0.29	0.38
237	144.	2.20	33.0	2.15	2.12 1.95	2.08 1.90	1.78 1.76	1.69 1.60	1.62 1.56	1.34 1.44	1.32 1.12	1.12 1.11	0.99 1.05	1.07	0.26 0.29	0.27 0.26	0.29
238	103.	1.67	33.4	1.64	1.61 1.51	1.59 1.49	1.39 1.40	1.34 1.31	1.30 1.28	1.11 1.22	1.10 0.93	0.96 0.91	0.84 0.82	0.84	0.23 0.31	0.24 0.19	0.25
239	203.	3.44	34.7	3.36	3.33 3.00	3.25 2.90	2.74 2.66	2.58 2.35	2.46 2.28	1.90 2.06	1.85 0.81	1.53 0.85	1.28 1.24	1.33	0.34 1.02	0.36 0.27	0.38
240	164.	2.71	34.5	2.65	2.62 2.39	2.57 2.33	2.20 2.15	2.07 1.94	1.99 1.89	1.61 1.73	1.57 1.31	1.33 1.27	1.41 1.21	1.24	0.29 0.91	0.31 0.23	0.33
241	82.	1.93	220.0	1.89	1.87 1.74	1.85 1.72	1.62 1.61	1.51 1.44	1.45 1.40	1.15 1.30	1.06 0.95	1.02 0.90	0.79 0.30	0.82	0.23 0.44	0.24 0.17	0.26
242	128.	2.81	211.6	2.76	2.73 2.54	2.67 2.50	2.36 2.36	2.22 2.13	2.13 2.08	1.68 1.92	1.55 1.42	1.48 1.33	1.15 1.19	1.20	0.31 0.65	0.32 0.20	0.34
243	167.	4.51	218.9	4.47	3.26 3.99	3.24 3.81	2.79 3.51	2.60 3.13	2.50 3.04	2.13 2.67	1.37 1.97	1.28 1.84	0.84 1.58	1.58	0.40 0.83	0.40 0.21	0.41

TABLE IV.—DEPENDENCE OF COINCIDENT DIP AND INLET STAGNATION TEMPERATURE ON ADIABATIC COMPRESSION FROM APPROXIMATELY 20 K

[Thermodynamic critical pressure, P_c, 1.295 MPa (187.5 psia); thermodynamic critical temperature, T_c, 33 K (59.4 °R).]

Run	Inlet temperature, T_{in}		Inlet pressure, P_{in}		Reduced inlet stagnation temperature, $T_{R,o}$	Reduced inlet stagnation pressure, $P_{R,o}$
	K	°R	MPa	psia		
220	23.8	42.8	0.92	134	0.72	0.72
217	26.4	47.5	2.46	356	.80	1.90
215	28.0	50.4	4.06	558	.85	2.97
212	30.4	54.7	6.13	889	.92	4.74
209	Gas	Gas	---	---	---	---

TABLE V.—FLOW RATE AND PRESSURE DROP DATA FOR THREE-STEP CYLINDRICAL SEAL, WITH BACKPRESSURE CONTROL

(a) Fluid nitrogen, fully eccentric postion[a]

Run	$\dot{w}$, g/s	P_o, MPa	T_o, K	P_0, MPa	Pressure at pressure tap locations 1 to 11, MPa												P_B, MPa
					P_1	P_2	P_3	P_4	P_5	P_6	P_7	P_8	P_9	P_{9j} (90°)	P_{10}	P_{11}	
296	119.	2.92	278.5	2.86	2.86 2.67	2.84 2.64	2.46 2.47	2.28 2.25	2.20 2.20	1.81 2.03	1.65 1.55	1.55 1.47	1.15 1.30	1.30	0.31 0.70	0.32 0.17	0.32
297	119.	2.95	279.8	2.90	2.89 2.70	2.87 2.67	2.49 2.50	2.30 2.28	2.23 2.23	1.85 2.06	1.70 1.58	1.61 1.50	1.21 1.32	1.33	0.47 0.72	0.47 0.41	0.49
298	120	2.97	280.3	2.91	2.91 2.72	2.89 2.69	2.51 2.52	2.32 2.29	2.25 2.25	1.87 2.07	1.72 1.59	1.63 1.51	1.25 1.33	1.34	0.62 0.72	0.62 0.60	0.64
299	120.	2.99	280.8	2.94	2.93 2.74	2.91 2.71	2.53 2.54	2.33 2.31	2.26 2.27	1.89 2.09	1.75 1.60	1.66 1.52	1.31 1.34	1.36	0.79 0.74	0.79 0.80	0.81
300	120.	3.03	281.3	2.97	2.97 2.78	2.94 2.74	2.56 2.57	2.36 2.34	2.29 2.30	1.92 2.11	1.79 1.62	1.71 1.54	1.40 1.36	1.38	0.96 0.81	0.96 0.98	0.97
301	122.	3.09	282.0	3.04	3.04 2.84	3.01 2.80	2.62 2.63	2.43 2.39	2.35 2.35	1.98 2.17	1.87 1.66	1.80 1.57	1.51 1.39	1.44	1.14 0.95	1.14 1.16	1.15
302	116.	3.03	281.4	2.98	2.98 2.79	2.96 2.75	2.59 2.58	2.41 2.36	2.34 2.32	2.00 2.14	1.90 1.66	1.85 1.59	1.61 1.43	1.51	1.31 1.15	1.31 1.32	1.32
304	1026.	5.03	86.2	4.87	4.88 4.28	4.79 4.07	3.88 3.56	**3.52** 3.03	3.33 2.91	2.18 2.43	2.00 0.23	1.86 0.24	1.35 0.27	1.01	0.75 0.26	0.75 0.82	0.77
305	882.	4.13	86.9	4.00	4.01 3.52	3.95 3.39	3.23 3.00	2.94 2.58	2.80 2.48	2.04 2.12	1.94 1.32	1.85 1.23	1.52 1.07	1.24	1.05 0.78	1.05 1.07	1.07
306	727.	3.48	88.4	3.39	3.42 3.05	3.37 2.97	2.83 2.69	2.61 2.38	2.52 2.32	2.02 2.07	1.95 1.56	1.89 1.44	1.67 1.33	1.45	1.32 1.06	1.31 1.32	1.32
307	1017.	4.78	86.1	4.61	4.60 4.02	4.52 3.83	3.52 3.34	3.09 2.85	2.89 2.74	1.72 2.29	1.47 0.22	1.30 0.24	0.79 0.26	0.69	0.35 0.19	0.35 0.38	0.37
308	969.	4.49	87.1	4.34	4.32 3.78	4.24 3.60	3.32 3.15	2.94 2.68	2.75 2.59	1.74 2.17	1.55 0.24	1.41 0.26	0.98 0.28	0.78	0.57 0.24	0.57 0.63	0.59
309	949.	4.46	87.9	4.31	4.29 3.75	4.22 3.58	3.33 3.14	2.97 2.67	2.80 2.58	1.84 2.17	1.66 0.26	1.54 0.28	1.13 0.30	0.93	0.73 0.32	0.73 0.79	0.75
310	898.	4.22	90.2	4.09	4.09 3.59	4.03 3.42	3.21 3.02	2.88 2.57	2.73 2.49	1.90 2.11	1.75 0.31	1.65 0.34	1.29 0.55	1.10	0.92 0.64	0.92 0.94	0.94
311	811.	3.88	97.8	3.76	3.76 3.33	3.71 3.17	2.96 2.83	2.66 2.44	2.53 2.37	1.86 2.05	1.74 0.56	1.66 0.60	1.36 0.92	1.19	1.03 0.78	1.03 1.05	1.05
312	492.	4.10	124.3	4.02	4.00 3.75	3.97 3.66	3.43 3.48	3.15 3.23	3.07 3.19	2.66 2.99	2.46 2.39	2.35 2.35	1.94 2.18	2.12	1.14 1.29	1.13 1.06	1.15
313	1003.	4.82	87.1	4.65	4.66 4.07	4.58 3.87	3.62 3.39	3.24 2.88	3.06 2.78	1.96 2.33	1.74 0.24	1.60 0.26	1.16 0.28	0.97	0.76 0.31	0.76 0.81	0.78
314	941.	4.44	87.5	4.29	4.30 3.76	4.24 3.59	3.36 3.15	3.02 2.68	2.87 2.58	1.94 2.17	1.77 0.25	1.65 0.27	1.27 0.29	1.09	0.90 0.62	0.90 0.92	0.92
315	866.	3.97	88.4	3.83	3.85 3.36	3.79 3.22	3.01 2.84	2.72 2.43	2.58 2.34	1.83 1.98	1.70 0.62	1.61 1.08	1.30 0.97	1.13	0.96 0.73	0.95 0.97	0.97
316	827.	3.75	89.2	3.63	3.64 **3.19**	3.59 **3.07**	2.86 **2.72**	2.59 **2.33**	2.47 2.25	1.80 1.93	1.68 1.18	1.60 1.14	1.32 1.00	1.15	0.99 0.78	0.99 1.01	1.01
317	1014.	4.96	86.8	4.80	4.84 4.23	4.76 4.01	3.78 3.51	3.41 2.98	3.21 2.87	2.10 2.40	1.88 0.24	1.74 0.26	1.30 0.28	1.07	0.86 0.45	0.85 0.90	0.87
318	924.	4.33	87.1	4.18	4.20 3.66	4.13 3.50	3.29 3.07	2.97 2.62	2.80 2.52	1.94 2.12	1.79 0.24	1.68 0.26	1.33 0.94	1.12	0.93 0.65	0.93 0.95	0.95

[a]Where two values are given, the top value is for minimum clearance (0° circumferential position) and the bottom value is for maximum clearance (180° circumferential position).

TABLE V.—Continued.

(a) Continued.

Run	$\dot{w}$, g/s	P_o, MPa	T_o, K	P_0, MPa	Pressure at pressure tap locations 1 to 11, MPa												P_B, MPa
					P_1	P_2	P_3	P_4	P_5	P_6	P_7	P_8	P_9	P_{9j} (90°)	P_{10}	P_{11}	
319	861.	3.94	87.6	3.82	3.82 3.34	3.77 3.21	3.01 2.83	2.72 2.42	2.58 2.34	1.85 1.98	1.73 1.13	1.64 1.14	1.34 0.99	1.14	0.97 0.73	0.97 0.99	0.99
320	740.	3.40	88.1	3.30	3.33 2.95	3.28 2.87	2.68 2.57	2.46 2.25	2.36 2.19	1.84 1.93	1.75 1.41	1.69 1.29	1.47 1.18	1.30	1.17 0.93	1.17 1.18	1.18
321	871.	3.61	85.3	3.48	3.47 3.00	3.41 2.90	2.59 2.53	2.28 2.15	2.10 2.08	1.33 1.76	1.20 0.21	1.08 0.22	0.73 0.24	0.57	0.33 0.17	0.33 0.35	0.35
322	851.	3.63	85.7	3.50	3.50 3.03	3.44 2.92	2.69 2.56	2.40 2.17	2.26 2.10	1.56 1.77	1.45 0.21	1.36 0.23	1.07 0.25	0.86	0.70 0.45	0.70 0.72	0.72
323	811.	3.49	86.4	3.38	3.39 2.94	3.33 2.84	2.64 2.50	2.37 2.14	2.24 2.05	1.62 1.75	1.52 0.92	1.44 0.99	1.19 0.86	1.00	0.85 0.62	0.85 0.87	0.87
324	776.	3.36	90.9	3.24	3.24 2.83	3.20 2.73	2.52 2.41	2.26 2.07	2.13 1.99	1.56 1.71	1.47 0.33	1.40 0.59	1.16 0.84	0.97	0.83 0.61	0.83 0.85	0.85
389	960.	5.12	85.6	4.98	4.08 5.04	4.16 4.37	3.58 3.63	2.87 2.78	2.81 2.71	2.37 2.24	0.39 1.43	1.10 1.34	4.35 1.21	1.30	0.99	1.14 1.14	1.16
390	1001.	5.43	86.4	5.28	4.60 5.32	4.28 4.99	3.78 3.92	3.03 3.43	2.96 3.25	2.50 2.35	0.23 1.83	0.25 1.55	1.12 1.30	1.31	0.99	1.15 1.15	1.17
391	895.	4.61	87.0	4.50	3.90 4.51	3.65 4.12	3.25 3.29	2.63 2.64	2.57 2.56	2.20 2.07	1.13 1.50	1.26 1.32	1.11 1.21	1.26	0.99	1.13 1.12	1.15
392	926.	4.80	84.9	4.67	4.08 4.70	3.80 4.47	3.38 3.27	2.72 2.79	2.66 2.68	2.26 2.04	0.96 1.75	1.27 1.54	1.11 1.29	1.26	1.00	1.13 1.13	1.15
393	852.	4.27	85.2	4.16	3.60 4.14	3.37 3.86	3.01 2.86	2.45 2.39	2.40 2.31	2.06 1.87	1.25 1.60	1.20 1.44	1.08 1.25	1.22	0.98	1.11 1.10	1.12
394	649	3.32	85.9	3.25	2.93 3.27	2.80 3.07	2.58 2.46	2.23 2.22	2.20 2.16	1.99 1.90	1.55 1.79	1.46 1.71	1.40 1.56	1.47	1.33	1.40 1.41	1.43
395	822.	3.55	86.2	3.46	2.89 3.37	2.71 3.06	2.41 2.15	1.96 1.54	1.91 1.49	1.65 1.16	0.22 0.88	0.24 0.70	0.26 0.46	0.53	0.26	0.26 0.29	0.30
396	1119.	6.04	84.2	5.87	4.95 5.89	4.70 5.69	4.15 0.24	3.34 3.78	3.25 3.56	2.73 2.05	0.20 1.68	0.20 1.30	0.25 0.83	0.76	0.25	0.62 0.57	0.59
397	1017.	5.19	84.3	5.04	4.26 5.06	4.05 4.87	3.59 0.43	2.90 3.22	2.83 3.05	2.38 1.98	0.19 1.69	0.20 1.44	0.24 1.05	0.96	0.34	0.84 0.79	0.81
398	925.	4.53	84.6	4.41	3.72 4.41	3.56 4.25	3.16 0.58	2.55 2.82	2.49 2.68	2.11 1.91	0.20 1.69	0.20 1.51	0.88 1.19	1.09	0.81	0.95 0.95	0.97
399	832.	4.03	84.9	3.92	3.35 3.93	3.22 3.78	2.89 0.76	2.38 2.58	2.32 2.46	2.00 1.88	1.30 1.74	1.20 1.61	1.08 1.34	1.21	0.98	1.10 1.09	1.11
400	1024.	5.49	86.0	5.33	4.71 5.45	4.36 5.28	3.88 1.19	3.13 3.72	3.06 3.49	2.57 2.36	0.22 2.13	0.45 1.90	0.94 1.47	1.33	1.01	1.18 1.17	1.19
401	975.	5.27	86.4	5.12	4.56 5.24	4.26 5.11	3.80 4.00	3.11 3.73	3.03 3.44	2.58 2.45	1.56 2.29	1.49 2.10	1.33 1.69	1.50	1.21	1.36 1.35	1.37
402	15.	1.44	305.0	1.42	1.32 1.40	1.29 1.39	1.22 1.19	1.10 1.09	1.09 1.08	0.99 0.91	0.75 0.88	0.72 0.84	0.64 0.63	0.66	0.37	0.16 0.20	0.20
403	25.	2.67	303.9	2.63	2.46 2.63	2.39 2.61	2.27 2.26	2.05 2.10	2.02 2.06	1.85 1.68	1.38 1.59	1.32 1.49	1.16 1.00	1.21	0.71	0.19 0.32	0.32
404	36.	3.52	303.9	3.46	3.23 3.47	3.14 3.45	2.97 2.99	2.70 2.79	2.64 2.72	2.42 2.18	1.81 2.06	1.72 1.87	1.52 1.18	1.56	0.94	0.24 0.40	0.40
405	341.	6.51	28.8	6.31	5.58 6.33	5.21 6.25	4.70 5.09	4.05 4.67	3.88 4.44	3.28 2.71	0.46 2.46	0.48 2.10	0.51 1.19	1.35	0.59	0.65 0.67	0.68

TABLE V.—Continued.

(a) Continued.

Run	$\dot{w}$, g/s	P_o, MPa	T_o, K	P_0, MPa	Pressure at pressure tap locations 1 to 11, MPa												P_B, MPa
					P_1	P_2	P_3	P_4	P_5	P_6	P_7	P_8	P_9	P_{9j} (90°)	P_{10}	P_{11}	
406	336.	6.37	28.6	6.17	5.48 6.18	5.10 6.11	4.61 4.98	3.97 4.58	3.79 4.36	3.23 2.80	0.44 2.61	0.46 2.34	0.49 1.62	1.43	0.76	1.25 1.20	1.23
407	334.	6.37	28.0	6.17	5.48 6.17	5.08 6.10	4.61 4.99	3.96 4.61	3.78 4.39	3.23 2.90	0.41 2.71	0.42 2.45	0.49 1.84	1.63	1.24	1.44 1.44	1.46
408	325.	6.13	27.8	5.95	5.33 6.00	4.96 5.92	4.50 4.85	3.88 4.48	3.70 4.27	3.17 2.88	1.72 2.70	1.72 2.47	1.48 1.91	1.68	1.32	1.51 1.50	1.52
409	351.	7.04	28.9	6.82	6.11 6.86	5.66 6.76	5.11 5.62	4.40 5.23	4.19 4.99	3.55 3.26	0.46 3.04	0.47 2.77	0.72 2.06	1.74	1.31	1.54 1.53	1.55
410	350.	7.02	28.3	6.81	6.12 6.85	5.68 6.75	5.13 5.64	4.44 5.24	4.23 5.00	3.60 3.35	2.15 3.14	1.94 2.89	1.66 2.20	1.88	1.46	1.69 1.67	1.70
411	346.	6.79	28.5	6.57	5.92 6.63	5.49 6.53	4.97 5.44	4.29 5.07	4.09 4.84	3.49 3.24	2.05 3.05	1.89 2.80	1.62 2.14	1.83	1.43	1.66 1.64	1.67
412	341.	6.63	28.3	6.42	5.79 6.48	5.37 6.38	4.86 5.31	4.21 4.92	4.01 4.71	3.43 3.19	2.05 3.00	1.87 2.76	1.63 2.12	1.84	1.44	1.67 1.65	1.68
413	337.	6.34	28.0	6.14	5.52 6.20	5.11 6.10	4.63 5.04	3.99 4.65	3.80 4.43	3.25 2.97	0.42 2.77	0.84 2.54	1.42 1.94	1.66	1.27	1.50 1.48	1.51
414	326.	5.96	27.8	5.76	5.17 5.80	4.78 5.71	4.33 4.69	3.75 4.30	3.56 4.11	3.06 2.79	0.66 2.61	1.02 2.40	1.41 1.85	1.60	1.24	1.45 1.43	1.46
415	322.	5.82	27.6	5.63	5.06 5.68	4.69 5.59	4.25 4.58	3.67 4.21	3.50 4.01	3.01 2.73	0.87 2.57	1.24 2.35	1.40 1.83	1.58	1.24	1.44 1.43	1.45
416	40.	3.78	293.0	3.72	3.49 3.73	3.38 3.69	3.20 3.24	2.91 3.06	2.84 2.97	2.59 2.33	1.96 2.18	1.87 2.00	1.63 1.36	1.65	1.01	0.29 0.45	0.45
417	344.	6.57	29.0	6.40	5.69 6.41	5.25 6.28	4.76 5.17	4.11 4.75	3.92 4.50	3.30 2.74	0.47 2.47	0.50 2.14	0.52 1.27	1.36	0.60	0.68 0.70	0.71
[b] 418	364.	7.48	29.2	7.28	6.48 7.27	5.99 7.13	5.42 5.99	4.65 5.56	4.44 5.30	3.71 3.40	0.49 3.11	0.52 2.80	0.60 2.02	1.72	1.02	1.52 1.48	1.50
[b,c] 419	366.	7.62	29.0	7.42	6.63 7.42	6.11 7.27	5.53 6.17	4.76 5.74	4.53 5.48	3.84 3.59	0.48 3.31	0.51 3.01	1.68 2.24	1.92	1.45	1.70 1.68	1.70
[b,d] 420	366.	7.83	29.2	7.64	6.87 7.67	6.34 7.52	5.76 6.39	4.97 5.94	4.74 5.68	4.06 3.77	2.47 3.48	2.21 3.17	1.93 2.44	2.17	1.70	1.96 1.93	1.95
[b,e] 421	364.	7.58	28.7	7.39	6.68 7.47	6.17 7.32	5.62 6.24	4.85 5.75	4.61 5.48	3.93 3.63	1.63 3.33	2.04 3.02	1.79 2.31	2.04	1.57	1.83 1.80	1.82
[b,f] 422	371.	7.97	29.5	7.77	6.97 7.76	6.40 7.59	5.83 6.58	5.02 6.14	4.77 5.87	4.04 3.89	0.51 3.56	0.55 3.25	1.75 2.42	2.02	1.50	1.76 1.74	1.76
[b,g] 423	382.	8.37	29.5	8.17	7.36 8.21	6.76 8.03	6.16 6.91	5.30 6.40	5.04 6.10	4.26 3.95	0.51 3.56	1.15 3.21	1.85 2.42	2.15	1.62	1.90 1.88	1.89
[b,g] 424	364.	7.55	29.0	7.36	6.60 7.37	6.07 7.20	5.54 6.09	4.78 5.59	4.54 5.31	3.89 3.47	0.47 3.16	1.81 2.79	1.76 2.18	2.01	1.56	1.81 1.79	1.80

[b]Choke swallowing is very abrupt at these pressures, less so at lower pressures. Large quantities of hydrogen are being injected downstream, but flow rate changes only a little. Backpressure established with trickle flow through test section; flow valve closed, then reopened followed by valve open wide.

[c]Choke was established by driving the pressure front out in a transient manner (i.e., like a superimposed flow out of the nozzle rather than in to it.)

[d]Insufficient stagnation pressure to drive it out.

[e]Choke was established by driving out gas; as run progressed the shock was driven back and high pressure reestablished.

[f]Started at 350 and dropped to 325 and then to 310 and shock became well established.

[g]Definite choke; very sharp drop and rapid recovery.

TABLE V.—Continued.

(a) Concluded.

Run	$\dot{w}$, g/s	P_o, MPa	T_o, K	P_0, MPa	Pressure at pressure tap locations 1 to 11, MPa												P_B, MPa
					P_1	P_2	P_3	P_4	P_5	P_6	P_7	P_8	P_9	P_{9j} (90°)	P_{10}	P_{11}	
425	314.	7.45	40.4	7.29	6.64 7.33	6.16 7.20	5.70 6.12	4.99 5.67	4.77 5.40	4.17 3.48	1.75 3.04	2.30 2.60	1.95 1.76	2.12	1.33	1.29 1.28	1.30
426	347.	7.48	33.8	7.29	6.57 7.33	6.04 7.19	5.57 5.88	4.80 4.62	4.57 4.33	3.94 3.14	0.74 2.19	0.76 1.64	0.81 1.47	1.74	0.98	1.42 1.39	1.41
427	329.	7.62	39.2	7.44	6.76 7.45	6.25 7.23	5.81 5.90	5.06 4.41	4.84 4.25	4.22 3.32	1.01 2.19	1.04 1.11	1.88 0.95	2.05	1.30	0.71 0.88	0.89
428	305.	7.18	40.5	7.02	6.39 6.63	5.95 6.49	5.54 5.49	4.84 4.07	4.64 3.97	4.06 3.19	1.51 2.23	2.25 1.11	1.92 0.88	2.06	1.33	0.57 0.79	0.80

(b) Fluid hydrogen, fully eccentric postion[a]

Run	$\dot{w}$, g/s	P_o, MPa	T_o, K	P_0, MPa	Pressure at pressure tap locations 1 to 11, MPa												P_B, MPa
					P_1	P_2	P_3	P_4	P_5	P_6	P_7	P_8	P_9	P_{9j} (90°)	P_{10}	P_{11}	
326	34.	3.26	291.7	3.21	3.21 2.99	3.19 2.95	2.77 2.75	2.60 2.52	2.52 2.46	2.04 2.25	1.88 1.73	1.77 1.65	1.76 1.44	1.45	0.34	0.34 0.18	0.35
327	34.	3.27	293.1	3.22	3.22 3.01	3.20 2.97	2.78 2.76	2.61 2.53	2.53 2.48	2.05 2.26	1.89 1.74	1.77 1.66	1.27 1.45	1.46	0.34	0.34 0.18	0.36
328	34.	3.29	293.6	3.24	3.24 3.02	3.22 2.98	2.79 2.78	2.61 2.54	2.53 2.49	2.06 2.28	1.91 1.76	1.79 1.67	1.29 1.47	1.47	0.51	0.51 0.44	0.54
329	34.	3.33	294.1	3.28	3.28 3.06	3.26 3.02	2.82 2.81	2.64 2.58	2.56 2.53	2.09 2.31	1.94 1.78	1.83 1.70	1.35 1.49	1.49	0.68	0.68 0.66	0.71
330	35.	3.40	293.8	3.35	3.35 3.12	3.34 3.08	2.88 2.87	2.70 2.63	2.62 2.58	2.14 2.36	2.00 1.82	1.89 1.73	1.44 1.52	1.53	0.87	0.87 0.88	0.90
333	319.	5.63	28.2	5.46	5.46 4.80	5.38 4.57	4.29 4.06	3.86 3.47	3.63 3.33	2.33 2.79	2.02 0.43	1.79 0.47	1.09 0.51	1.22	0.59	0.60 0.59	0.63
335	323.	5.76	28.1	5.59	5.59 4.93	5.52 4.69	4.45 4.18	4.02 3.58	3.79 3.43	2.40 2.89	2.07 0.43	1.87 0.47	1.23 0.51	1.24	0.85	0.85 0.91	0.89
336	313.	5.94	28.3	5.78	5.83 5.20	5.77 4.97	4.72 4.48	4.22 3.89	3.98 3.75	2.93 3.23	2.59 2.06	2.47 1.90	2.00 1.65	1.87	1.61	1.61 1.64	1.64
337	327.	5.78	27.9	5.61	5.60 4.94	5.52 4.68	4.46 4.16	4.06 3.56	3.80 3.41	2.36 2.87	2.08 0.41	1.78 0.45	1.12 0.48	1.21	0.62	0.63 0.64	0.67
338	321.	5.67	27.7	5.50	5.51 4.86	5.43 4.62	4.40 4.11	4.02 3.52	3.79 3.37	2.46 2.84	2.27 0.41	2.00 0.44	1.51 0.47	1.36	1.12	1.12 1.19	1.16
339	309.	5.43	27.3	5.28	5.32 4.70	5.26 4.47	4.25 4.00	3.82 3.44	3.61 3.30	2.52 2.81	2.34 1.63	2.09 1.57	1.68 1.38	1.58	1.37	1.37 1.40	1.41
340	224.	3.88	26.0	3.78	4.02 3.62	3.98 3.49	3.30 3.22	2.99 2.88	2.80 2.80	2.37 2.54	2.30 1.96	2.18 1.84	1.95 1.71	1.82	1.70	1.70 1.71	1.73
341	333.	5.87	27.7	5.70	5.69 5.02	5.60 4.75	4.55 4.22	4.18 3.62	3.88 3.47	2.39 2.91	2.18 0.41	1.76 0.44	1.13 0.47	1.20	0.56	0.57 0.55	0.60
342	327.	5.67	27.7	5.50	5.50 4.85	5.41 4.60	4.38 4.08	3.96 3.50	3.71 3.35	2.30 2.82	2.09 0.40	1.64 0.43	1.08 0.46	1.16	0.53	0.53 0.51	0.57
343	5.	3.33	288.9	3.28	3.29 3.06	3.26 3.01	2.83 2.81	2.64 2.56	2.55 2.51	2.03 2.29	1.87 1.76	1.75 1.67	1.25 1.47	1.46	0.36	0.36 0.21	0.38

[a]Where two values are given, the top value is for minimum clearance (0° circumferential position) and the bottom value is for maximum clearance (180° circumferential position).

TABLE V.—Continued.

(b) Concluded.

Run	$\dot{w}$, g s	P_o, MPa	T_o, K	P_0, MPa	Pressure at pressure tap locations 1 to 11, MPa												P_B, MPa
					P_1	P_2	P_3	P_4	P_5	P_6	P_7	P_8	P_9	P_{9j} (90°)	P_{10}	P_{11}	
344	6.	3.35	288.3	3.30	3.31 3.08	3.27 3.03	2.83 2.83	2.65 2.58	2.56 2.52	2.05 2.30	1.89 1.78	1.77 1.68	1.28 1.49	1.47	0.53	0.53 0.47	0.56
345	6.	3.41	287.5	3.36	3.36 3.13	3.33 3.08	2.88 2.88	2.69 2.63	2.60 2.57	2.10 2.35	1.96 1.81	1.85 1.72	1.42 1.52	1.51	0.88	0.88 0.90	0.91
346	3.	2.51	274.6	2.46	2.50 2.33	2.49 2.30	2.19 2.16	2.09 1.98	2.03 1.93	1.71 1.79	1.66 1.42	1.61 1.36	1.43 1.24	1.32	1.17	1.17 1.19	1.19
347	38.	3.57	295.2	3.52	3.53 3.29	3.50 3.23	3.02 3.02	2.81 2.78	2.72 2.72	2.22 2.48	2.04 1.93	1.90 1.84	1.34 1.62	1.60	0.38	0.38 0.20	0.40
348	38.	3.58	289.2	3.53	3.53 3.29	3.50 3.23	3.03 3.01	2.83 2.76	2.74 2.70	2.20 2.46	2.03 1.91	1.89 1.81	1.35 1.60	1.58	0.55	0.56 0.48	0.59
349	36.	3.44	285.4	3.39	3.41 3.17	3.38 3.12	2.92 2.91	2.73 2.66	2.64 2.60	2.13 2.38	2.00 1.84	1.88 1.74	1.45 1.53	1.52	0.92	0.92 0.94	0.95
350	316.	5.52	28.1	5.36	5.42 4.74	5.32 4.49	4.22 4.01	3.72 3.42	3.49 3.28	2.24 2.75	1.91 0.44	1.69 0.47	1.03 0.51	1.19	0.59	0.59 0.59	0.63
351	304.	5.62	27.7	5.47	5.55 4.91	5.46 4.67	4.41 4.24	3.89 3.67	3.70 3.53	2.72 3.05	2.49 2.05	2.32 1.85	1.90 1.64	1.83	1.62	1.62 1.65	1.65
352	265.	4.78	27.2	4.65	4.79 4.27	4.73 4.09	3.85 3.77	3.35 3.31	3.18 3.21	2 60 2.86	2 45 2.08	2.31 1.93	2.09 1.78	1.93	1.76	1.76 1.78	1.79
353	266.	4.38	26.1	4.26	4.26 3.77	4.19 3.59	3.36 3.28	2.92 2.85	2.71 2.75	2.16 2.42	2.05 1.67	1.84 1.52	1.61 1.39	1.53	1.38	1.37 1.40	1.41
354	232.	3.73	28.3	3.62	3.61 3.22	3.57 3.09	2.87 2.83	2.54 2.49	2.34 2.41	1.95 2.15	1.91 1.55	1.69 1.43	1.52 1.32	1.43	1.30	1.30 1.33	1.34
355	188.	2.80	27.5	2.72	2.70 2.45	2.68 2.37	2.21 2.21	1.98 1.99	1.90 1.93	1.66 1.78	1.64 1.41	1.53 1.33	1.62 1.27	1.35	1.26	1.26 1.28	1.30
356	253.	4.08	28.0	3.97	3.99 3.53	3.94 3.37	3.15 3.08	2.69 2.69	2.55 2.59	2.06 2.30	1.99 1.58	1.75 1.45	1.57 1.34	1.46	1.34	1.34 1.37	1.38
357	216.	3.36	28.0	3.26	3.25 2.92	3.21 2.79	2.61 2.59	2.31 2.30	2.19 2.23	1.86 2.03	1.83 1.52	1.65 1.42	1.53 1.34	1.44	1.34	1.34 1.37	1.38
358	168.	2.49	26.5	2.42	2.39 2.19	2.38 2.12	1.99 1.99	1.85 1.82	1.76 1.78	1.57 1.66	1.56 1.37	1.46 1.30	1.41 1.27	1.33	1.27	1.26 1.29	1.30
359	147.	2.31	26.7	2.25	2.26 2.09	2.25 2.03	1.91 1.92	1.79 1.77	1.71 1.73	1.56 1.63	1.55 1.39	1.47 1.33	1.41 1.29	1.34	1.29	1.29 1.31	1.33
360	208.	3.10	25.0	3.01	3.11 2.79	3.08 2.67	2.51 2.47	2.25 2.21	2.16 2.14	1.82 1.95	1.79 1.50	1.66 1.40	1.52 1.32	1.41	1.33	1.32 1.35	1.37
361	318.	5.12	27.3	4.95	5.00 4.36	4.90 4.10	3.86 3.70	3.35 3.17	3.14 3.04	2.06 2.62	1.94 0.38	1.41 0.41	1.00 0.44	1.06	0.54	0.54 0.55	0.59

(c) Fluid hydrogen, fully eccentric postion[b]

Run	$\dot{w}$, g s	P_o, MPa	T_o, K	P_0, MPa	Pressure at pressure tap locations 1 to 11, MPa												P_B, MPa
					P_1	P_2	P_3	P_4	P_5	P_6	P_7	P_8	P_9	P_{9j} (90°)	P_{10}	P_{11}	
363	35.	3.37	287.0	3.32	3.10 3.31	3.02 3.29	2.83 2.84	2.58 2.66	2.51 2.54	2.30 2.02	1.70 1.83	1.63 1.66	1.43 1.17	1.47	0.88	0.23 0.38	0.39
364	35.	3.48	287.4	3.43	3.22 3.44	3.13 3.42	2.95 2.95	2.68 2.76	2.62 2.63	2.40 2.14	1.78 1.99	1.70 1.84	1.49 1.43	1.54	0.95	1.07 1.07	1.08

[a]Where two values are given, the top value is for maximum clearance (0° circumferential position) and the bottom value is for minimum clearance (180° circumferential position).

TABLE V.—Continued.

(c) Fluid hydrogen, fully eccentric postion[b]

Run	$\dot{w}$, g/s	P_o, MPa	T_o, K	P_0, MPa	Pressure at pressure tap locations 1 to 11, MPa												P_B, MPa
					P_1	P_2	P_3	P_4	P_5	P_6	P_7	P_8	P_9	P_{9j} (90°)	P_{10}	P_{11}	
365	331.	6.41	28.4	6.23	5.55 6.21	5.09 6.11	4.57 4.99	3.93 4.53	3.73 4.21	3.13 2.65	0.43 2.28	0.46 1.97	0.49 1.21	1.29	0.57	0.66 0.67	0.69
366	334.	6.40	28.0	6.22	5.52 6.22	5.03 6.11	4.55 5.02	3.92 4.60	3.73 4.31	3.14 2.68	0.40 2.35	0.44 2.03	0.46 1.25	1.27	0.53	0.63 0.65	0.66
367	334.	6.44	28.0	6.26	5.58 6.28	5.10 6.16	4.62 5.10	3.97 4.67	3.78 4.42	3.19 2.75	0.40 2.46	0.43 2.17	0.53 1.44	1.28	0.57	1.01 0.95	0.98
368	317	5.85	27.3	5.68	5.09 5.73	4.66 5.63	4.23 4.62	3.64 4.24	3.46 4.01	2.93 2.64	0.36 2.39	0.39 2.17	0.41 1.60	1.37	0.75	1.21 1.18	1.20
369	286.	5.15	27.4	5.01	4.55 5.08	4.20 5.00	3.84 4.10	3.35 3.77	3.19 3.57	2.76 2.54	1.73 2.38	1.59 2.19	1.42 1.75	1.56	1.26	1.42 1.42	1.44
370	236.	4.15	27.4	4.04	3.79 4.17	3.55 4.11	3.29 3.39	2.94 3.15	2.83 3.00	2.53 2.35	1.86 2.25	1.69 2.13	2.04 1.83	1.69	1.48	1.58 1.59	1.61
371	245.	4.13	27.8	4.02	3.65 4.05	3.40 3.99	3.13 3.27	2.77 3.02	2.66 2.87	2.36 2.18	1.65 2.07	1.49 1.95	1.36 1.65	1.49	1.26	1.38 0.18	1.40
372	211.	3.39	26.2	3.30	3.03 3.33	2.85 3.28	2.64 2.70	2.38 2.51	2.29 2.40	2.07 1.94	1.57 1.87	1.44 1.78	1.36 1.56	1.44	1.27	1.36 1.37	1.39
373	178.	2.80	27.4	2.73	2.53 2.75	2.41 2.72	2.25 2.27	2.06 2.13	2.00 2.05	1.83 1.73	0.19 1.68	1.36 0.18	1.30 1.46	0.20	1.24	0.20 0.32	1.33
374	126.	1.93	24.8	1.89	1.77 1.89	1.74 1.87	1.64 1.63	1.56 1.56	1.52 1.52	1.44 1.39	1.26 1.37	0.43 0.30	1.17 1.27	1.22	1.15	1.18 1.19	1.21
375	115.	1.76	26.6	1.72	1.60 1.70	1.58 1.69	1.49 1.48	1.42 1.42	1.39 1.38	1.32 1.27	1.16 1.25	1.12 0.50	1.09 1.17	1.13	1.07	1.10 1.11	1.13
376	244.	3.55	28.7	3.45	2.99 3.37	2.75 3.32	2.52 2.58	2.21 2.32	2.11 2.18	1.86 1.50	0.45 1.38	0.46 0.51	0.51 0.88	0.90	0.53	0.42 0.96	0.48
377	39.	3.30	246.0	3.25	2.99 3.25	2.99 3.22	2.80 2.84	2.52 2.69	2.48 2.61	2.27 2.08	1.67 1.96	1.59 1.80	1.40 1.21	1.47	0.86	0.24 0.38	0.39
378	41.	3.34	234.1	3.28	3.02 3.29	3.02 3.25	2.82 2.87	2.55 2.72	2.50 2.64	2.29 2.09	1.68 1.98	1.60 1.83	1.50 1.26	1.46	0.87	0.25 0.39	0.41
379	305.	5.86	28.4	5.72	4.94 5.05	5.04 4.71	4.49 3.63	3.91 3.11	3.77 3.05	3.33 2.82	2.23 2.04	2.03 1.99	1.87 1.92	2.03	1.75	1.91 1.90	1.92
380	310.	5.70	28.0	5.55	4.79 4.89	4.86 4.77	4.34 3.74	3.78 2.99	3.64 2.95	3.21 2.73	2.09 1.95	1.92 1.88	1.76 1.81	1.92	1.64	1.79 1.78	1.81
381	327.	5.82	27.9	5.65	4.85 5.05	4.90 4.97	4.32 4.10	3.72 3.10	3.58 3.03	3.10 2.66	1.81 1.79	1.72 1.66	1.54 1.60	1.71	1.40	1.57 1.56	1.59
382	329.	5.66	27.6	5.50	4.66 4.99	4.74 4.80	4.15 3.95	3.57 2.94	3.42 2.87	2.95 2.48	0.37 1.64	0.38 1.50	1.12 1.41	1.52	1.19	1.38 1.37	1.40
383	352.	6.35	28.2	6.17	5.21 5.57	5.25 5.32	4.61 4.41	3.97 3.09	3.80 3.02	3.27 2.62	0.40 1.63	0.41 1.45	0.44 1.36	1.50	0.83	1.38 1.34	1.36
384	338.	5.95	28.3	5.78	4.84 5.41	4.92 5.04	4.34 4.10	3.74 2.87	0.24 0.12	0.66 2.48	0.31 1.52	0.12 0.18	0.71 0.14	1.45	0.37	0.34 0.24	1.31
385	329.	5.69	28.3	5.52	4.62 4.86	4.70 4.80	4.19 4.05	3.61 2.86	3.46 2.79	3.01 2.46	0.41 1.54	0.43 1.44	0.45 1.35	1.47	0.93	1.33 1.30	1.33
386	311.	5.21	27.7	5.05	4.25 4.59	4.33 4.51	3.86 3.80	3.33 2.62	3.19 2.57	2.78 2.38	0.79 1.57	1.11 1.48	1.32 1.38	1.49	1.18	1.34 1.35	1.37

[b]Where two values are given, the top value is for maximum clearance (0° circumferential position) and the bottom value is for minimum clearance (180° circumferential position).

TABLE V.—Continued.

(c) Fluid hydrogen, fully eccentric postion[b]

Run	$\dot{w}$, g/s	P_o, MPa	T_o, K	P_0, MPa	Pressure at pressure tap locations 1 to 11, MPa												P_B, MPa
					P_1	P_2	P_3	P_4	P_5	P_6	P_7	P_8	P_9	P_{9j} (90°)	P_{10}	P_{11}	
387	295.	4.93	27.0	4.79	4.09 4.64	4.18 4.36	3.74 3.69	3.26 2.59	3.13 2.56	2.75 2.39	1.72 1.69	1.59 1.60	1.47 1.52	1.60	1.34	1.48 1.47	1.50
388	276.	4.65	30.1	4.52	3.87 4.32	3.95 4.15	3.55 3.52	3.10 2.50	2.98 2.47	2.62 2.31	1.67 1.64	1.53 1.55	1.42 1.48	1.55	1.30	1.43 1.42	1.45

(d) Fluid hydrogen, concentric postion[c]

Run	$\dot{w}$, g/s	P_o, MPa	T_o, K	P_0, MPa	Pressure at pressure tap locations 1 to 11, MPa												P_B, MPa
					P_1	P_2	P_3	P_4	P_5	P_6	P_7	P_8	P_9	P_{9j} (90°)	P_{10}	P_{11}	
429	293.	7.12	41.8	6.98	6.29 6.49	5.88 6.36	5.48 5.42	4.80 4.05	4.62 3.97	4.05 3.27	2.55 2.34	2.33 1.58	1.99 1.48	2.12	1.35	1.48 1.42	1.44
430	42	3.56	194.5	3.52	3.40 3.29	3.32 3.25	2.99 2.97	2.80 2.76	2.71 2.69	2.26 2.39	2.03 2.00	1.90 1.88	1.58 1.62	1.62	0.58	0.37 0.28	0.38
431	17.	1.78	194.5	1.75	1.68 1.63	1.66 1.61	1.49 1.47	1.39 1.37	1.35 1.33	1.13 1.19	1.01 0.99	0.96 0.94	0.80 0.80	0.81	0.27	0.22 0.19	0.23
432	53.	4.93	194.5	4.88	4.77 4.62	4.64 4.53	4.21 4.15	3.95 3.86	3.83 3.78	3.19 3.33	2.88 2.82	2.68 2.64	2.21 2.26	2.25	0.87	0.48 0.33	0.48
433	49.	4.72	292.6	4.67	4.67 4.51	4.54 4.43	4.11 4.04	3.86 3.76	3.73 3.68	3.11 3.24	2.80 2.74	2.61 2.56	4.87 2.15	2.13	0.83	0.47 0.33	0.48
434	39.	3.70	274.1	3.66	3.55 3.43	3.47 3.38	3.11 3.07	2.91 2.85	2.81 2.78	2.33 2.45	2.10 2.06	1.97 1.93	1.77 1.65	1.63	0.62	0.39 0.30	0.40
435	18.	1.82	251.7	1.79	1.72 1.67	1.69 1.64	1.51 1.49	1.42 1.39	1.37 1.35	1.15 1.20	1.03 1.00	0.97 0.94	0.81 0.81	0.81	0.28	0.23 0.19	0.24
436	329.	6.39	28.7	6.23	5.86 5.58	5.53 5.24	4.66 4.46	4.12 3.81	3.88 3.62	2.70 2.77	2.19 1.87	1.89 1.59	1.36 1.22	1.33	0.65	0.64 0.62	0.66
437	354.	7.30	28.9	7.12	6.81 6.43	6.43 6.02	5.40 5.13	4.77 4.40	4.50 4.18	3.11 3.18	2.50 2.13	2.13 1.80	1.52 1.35	1.49	0.99	1.15 1.19	1.19
438	349.	7.17	29.0	7.00	6.50 6.34	6.29 5.94	5.34 5.10	4.74 4.39	4.46 4.18	3.20 3.24	2.62 2.23	2.27 1.91	1.72 1.50	1.64	1.26	1.40 1.44	1.44
439	345.	7.23	29.1	7.06	6.76 6.46	6.40 6.08	5.46 5.26	4.87 4.58	4.60 4.38	3.41 3.47	2.82 2.49	2.49 2.16	1.95 1.75	1.89	1.51	1.66 1.69	1.69
440	338.	7.12	28.7	6.96	6.67 6.36	6.30 5.99	5.40 5.22	4.82 4.56	4.57 4.36	3.45 3.54	2.90 2.61	2.60 2.30	2.13 1.94	2.06	1.74	1.87 1.90	1.90
441	333.	7.08	28.6	6.93	6.64 6.35	6.29 6.00	5.43 5.28	4.87 4.62	4.63 4.44	3.57 3.67	3.04 2.76	2.76 2.46	2.30 2.12	2.25	1.94	2.06 2.09	2.08
442	275.	7.16	44.6	7.02	6.66 6.54	6.28 6.16	5.55 5.46	5.02 4.89	4.81 4.72	3.76 3.96	3.16 2.99	2.84 2.68	2.23 2.22	2.31	1.18	1.24 1.23	1.25
443	288.	6.81	41.1	6.67	6.23 6.16	5.82 5.77	5.13 5.09	4.63 4.50	4.42 4.34	3.42 3.61	2.85 2.67	2.55 2.37	2.03 1.98	2.09	1.22	1.22 1.22	1.24
444	289.	6.63	40.0	6.50	5.90 5.91	5.50 5.50	4.89 4.90	4.38 4.32	4.17 4.16	3.23 3.48	2.69 2.54	2.41 2.25	1.93 1.89	1.97	1.25	1.36 1.38	1.38
445	302.	6.41	36.8	6.27	5.68 5.67	5.29 5.28	4.66 4.68	4.17 4.08	3.96 3.91	3.03 3.23	2.49 2.31	2.23 2.02	1.78 1.69	1.81	1.21	1.36 1.38	1.38

[b]Where two values are given, the top value is for maximum clearance (0° circumferential position) and the bottom value is for minimum clearance (180° circumferential position).
[c]Where two values are given, the top value is for 0° circumferential position and the bottom value is for 180° circumferential position; nominal clearance, 0.0125 cm (0.005 in.).

TABLE V.—Concluded.

(d) Fluid hydrogen, concentric postion[c]

Run	$\dot{w}$, g/s	P_o, MPa	T_o, K	P_0, MPa	Pressure at pressure tap locations 1 to 11, MPa												P_B, MPa
					P_1	P_2	P_3	P_4	P_5	P_6	P_7	P_8	P_9	P_{9j} (90°)	P_{10}	P_{11}	
446	310.	6.29	34.0	6.14	5.42 5.30	5.04 5.08	4.46 4.48	3.97 3.90	3.74 3.73	2.82 3.03	2 31 2.13	2.04 1.83	1.60 1.5	1.64	1.20	1.33 1.36	1.36
447	317.	6.18	31.5	6.03	5.33 5.14	5.03 4.97	4.38 4.36	3.88 3.75	3.65 3.58	2.73 2.87	2.21 1.97	1.95 1.67	1.52 1.36	1.51	1.22	1.31 1.35	1.35
448	318.	5.95	28.5	5.80	5.24 5.10	4.92 4.84	4.21 4.21	3.75 3.62	3.53 3.45	2.66 2.79	2.18 1.93	1.94 1.65	1.55 1.36	1.52	1.26	1.34 1.38	1.38

[c]Where two values are given, the top value is for 0° circumferential position and the bottom value is for 180° circumferential position; nominal clearance, 0.0125 cm (0.005 in.).

1. Report No.	2. Government Accession No.	3. Recipient's Catalog No.
NASA TP-1849		

4. Title and Subtitle	5. Report Date
Three-Step Cylindrical Seal for High-Performance Turbomachines	June 1987
	6. Performing Organization Code

7. Author(s)	8. Performing Organization Report No.
Robert C. Hendricks	E-3185
	10. Work Unit No.

9. Performing Organization Name and Address	11. Contract or Grant No.
National Aeronautics and Space Administration Lewis Research Center Cleveland, Ohio 44135	13. Type of Report and Period Covered Technical Paper

12. Sponsoring Agency Name and Address	14. Sponsoring Agency Code
National Aeronautics and Space Administration Washington, D.C. 20546	

15. Supplementary Notes

Data and information contained herein were released for general use in May 1977.

16. Abstract

A three-step cylindrical seal configuration representing the seal for a high-performance turbopump (e.g., the space shuttle main engine fuel pump) was tested under *static* (*nonrotating*) conditions. The test data included critical mass flux and pressure profiles over a wide range of inlet temperatures and pressures for fluid nitrogen and fluid hydrogen with the seal in concentric and fully eccentric positions. The critical mass flux (leakage rate) was 70 percent that of an equivalent straight cylindrical seal with a correspondingly higher pressure drop based on the same flow areas of 0.3569 cm^2 (0.05531 $in.^2$) but 85 percent that of the straight seal based on the third-step flow area of 0.3044 cm^2 (0.04718 $in.^2$). The mass flow rates for the three-step cylindrical seal in the fully eccentric and concentric positions were essentially the same, and the trends in flow coefficient followed those of a simple axisymmetric inlet configuration. However, for inlet stagnation temperatures less than the thermodynamic critical temperature the pressure profiles exhibited a flat region throughout the third step of the seal, with the pressure magnitude dependent on the inlet stagnation temperature. Such profiles represent an extreme positive direct stiffness. These conditions engendered a crossover in the pressure profile upstream of the postulated choke that resulted in a local negative stiffness. Flat and crossover pressure profiles resulting from choking within the seal are practically unknown to the seal designer. However, they are of critical importance to the stability of a turbomachine, and must be properly integrated into any dynamic analysis of a seal of this configuration. Turbomachine dynamics are also quite sensitive to the inlet configuration and the fluid conditions. Further, in seal designs it has been assumed that choking cannot occur within the seal if the backpressure is above the thermodynamic critical pressure. This is shown to be an invalid assumption. Choking is highly dependent on geometry, inlet-to-backpressure ratio, and inlet temperature and can occur within the seal even though the backpressure is above the thermodynamic critical pressure.

17. Key Words (Suggested by Author(s))	18. Distribution Statement
Seals; Turbomachines: Fluid mechanics; Space shuttle main engine; Dynamics; Instability	Unclassified – unlimited STAR Category 34

19. Security Classif. (of this report)	20. Security Classif. (of this page)	21. No of pages	22. Price*
Unclassified	Unclassified	78	A05

*For sale by the National Technical Information Service, Springfield, Virginia 22161

NASA-Langley, 1987